Master's thesis

NTNU
Norwegian University of Science and Technology
Faculty of Information Technology and Electrical Engineering
Department of Electric Power Engineering

Einar Boman Rinde

# TIMES-LYR – a long-term deterministic scenario analysis of the future energy system in Longyearbyen

Master's thesis in Energy and Environmental Engineering
Supervisor: Karen Byskov Linberg
June 2020

NTNU
Kunnskap for en bedre verden

Einar Boman Rinde

# TIMES-LYR – a long-term deterministic scenario analysis of the future energy system in Longyearbyen

Master's thesis in Energy and Environmental Engineering
Supervisor: Karen Byskov Linberg
June 2020

Norwegian University of Science and Technology
Faculty of Information Technology and Electrical Engineering
Department of Electric Power Engineering

NTNU
Norwegian University of
Science and Technology

# Summary

In this thesis, a model is developed in VEDA-TIMES to analyze the transition of the coal-based energy system in Longyearbyen to a renewable one towards 2050. As the local coal mine supplying the power plant is due to shut down within ten years, it is urgent to investigate an alternative energy supply. In this thesis, it is assumed that the existing power plant is shut down along with the coal mine. Technical and economical parameters for the existing system and potential investment decisions are obtained, evaluated and implemented in the model.

Five different scenarios representing political decisions are created and investigated. The base scenario (B) chooses freely among the technologies in the model without any restrictions. In the base scenario with no $CO_2$ (BNC), $CO_2$ emissions are restricted to zero in all periods from 2030. Import of diesel and hydrogen is restricted to zero throughout the modeling horizon in the isolated scenario (ISO). In the no wind scenario (NWI) and the no wind scenario with no $CO_2$ (NWC), investments in wind turbines are not allowed and $CO_2$ emissions are restricted to zero in all periods from 2030 in NWC.

B, BNC and ISO have similar solutions with a large investment of about 28 MW wind power and a 13 MWh (8 MWh in B) battery in 2030. Solar power contributes to electricity production towards the end of the modelling horizon, but more than 97% of the electricity is produced from wind. Heat is mainly produced by a centralized heat pump, utilizing electricity from the wind turbines and by electric radiators distributed in the buildings.

When wind turbines are restricted (NWI), the lowest costs are obtained by a solar-diesel system where spring and summer are 100% powered by renewable solar energy in 2050, with about 70 MWp installed solar photovoltaic. However, the total discounted costs is increased with 24% and the $CO_2$ emissions related to this solution is significantly larger than when allowing wind. NWC is the only scenario including hydrogen, importing more than 100 GWh of hydrogen annually to cover the demand. No investments are made in renewable energy sources, emphasizing that the current costs and performance of a hydrogen storage system make curtailment of renewable energy more beneficial than seasonal energy storage. Cars and snowmobiles powered by diesel are replaced with electric vehicles in all scenarios.

The main challenge in this thesis has been to properly model the renewable energy sources and thermal load in the chosen time-slices. To represent three different data-sets containing 8760 data points, considering consistency of the chosen data sample and representing seasonal and daily variations proved to be difficult. Consistency of data sources regarding the economical and technical performance of all technologies in the model is also a challenge, and all results in this report are dependent and sensitive to the assumptions and cost projections utilized in the model. The developed model is based upon Ringkjøb, Haugan, and Nybø's TIMES-Longyearbyen [1], and further improved. For instance, is the district heating system modeled with increased detail and the transport sector included, along with different production and demand profiles and additional investment decisions.

# Sammendrag

Denne masteroppgaven utvikler en modell i VEDA-TIMES for å analysere overgangen fra dagens kullbaserte energisystem i Longyearbyen til et fornybart system fram mot 2050. Den lokale kullgruva som forsyner kraftverket stenges i løpet av ti år, så det haster å undersøke alternative energikilder. I denne oppgaven antas det at det eksisterende kullkraftverket stenges samtidig som kullgruva. Tekniske og økonomiske parametere som beskriver det eksisterende systemet samt potensielle investeringsbeslutninger har blitt evaluert og implementert i modellen.

Ulike politiske beslutninger er representert av fem ulike scenarier. Basisscenarioet (B) velger fritt blant teknologiene i modellen. I basisscenarioet uten $CO_2$ (BNC) er utslippene begrenset til null i alle perioder fra og med 2030. Import av diesel og hydrogen er ikke tillatt i noen perioder i det isolerte scenarioet (ISO). Ikke-vind scenarioet (NWI) og ikke-vind uten $CO_2$ scenarioet (NWC) tillates ikke investeringer i vindkraft, og i NWC er heller ikke $CO_2$ utlipp tillatt fra 2030.

B, BNC og ISO har lignende løsninger med store investeringer i rundt 28 MW vindkraft og 13 MWh (8 MWh i B) batterilagring i 2030. Solkraft bidrar til strømproduksjon mot slutten av modelleringshorisonten, men mer enn 97% av strømmen er produsert i vindturbinene. Varme blir hovedsakelig produsert i en sentralisert varmepumpe med elektrisitet fra vindturbinene i tillegg til elektriske panelovner fordelt i byggene.

Når vindmøller ikke er tillatt (NWI), gir et sol-diesel-system med 70 MWp installert i en solpark i 2050 de laveste kostnadene. Hele energibehovet gjennom sommeren og våren kan da dekkes med solenergi. De totale diskonterte kostnadene øker med 24% og $CO_2$ utslippene knyttet til denne løsningen er betydelig større enn løsningene som tillater vind. NWC er det eneste scenariet som inkluderer hydrogen. Her importeres over 100 GWh hydrogen årlig for å dekke energibehovet, og det investeres ikke i noe fornybar kraftproduksjon i Longyearbyen. Dette understreker at kostnadene og de tekniske parameterne knyttet til hydrogensystemer må forbedres for å være konkurransedyktig i energisystemet. Biler og snøscootere blir elektrifisert i alle scenariene.

Den største utfordringen i denne oppgaven har vært å representere produksjonsprofilene fra sol- og vindkraft samt forbruksprofilene for varme på en god måte. Og samtidig representere variasjonen i tre ulike datasett med 8760 punkter i de 192 definerte tidsenhetene på en konsistent måte viste seg å være utfordrende. Å finne konsistente kilder med tekniske og økonomiske parametere for de ulike teknologiene i modellen var også utfordrende, og alle resultater i denne rapporten er avhengige av antakelsene som er gjort. Modellen i denne oppgaven er en videreutvikling av TIMES-Longyearbyen utviklet av Ringkjøb, Haugan og Nybø [1]. Modellen er utvidet til å inkludere transportsektoren og modelleringen av fjernvarmenettet er forbedret. Det er også gjort andre antakelser knyttet til produksjon- og forbruksprofiler og flere investeringsbeslutninger er lagt til.

# Preface

This report is written as a master thesis at the Department of Electric Power Engineering at the Norwegian University of Science and Technology during the spring semester 2020. The master thesis finalizes the five-year MSc Energy and Environmental Engineering and is valued 30 credits.

First and foremost, thank you to my supervisor Karen Byskov Lindberg for creating this exciting, relevant and challenging task. For understanding my frustration, motivating me and for your excellent feedback and sincere interest in my work.

Thank you to Alexandra Roos and NVE for allowing me to use your licence for VEDA, allowing me to solve this task with TIMES. A special appreciation is directed to PdD candidate Hans-Kristian Ringkjøb, for allowing me to base my work upon TIMES-Longyearbyen [1] developed at the University of Bergen, Mohammadreza Ahang, for helping me get started with the modelling and answering my questions. Bjørn Thorud, for your extensive knowledge of solar power and for sharing your production profiles. Arne Aalberg and Rasmus Bøckman, for providing me with additional information and insight of Longyearbyen. My fellow student Emil Risvik Buseth, for your insight in the task, discussions and collaboration.

Thank you, Linnea Espevik, for allowing me to live in your apartment for more than a month, making it easier to return to Trondheim. To all my other friends, for shared experiences, frustrations and laughs throughout these five years. Thank you for the endless digital lunches, and thank you all so much, for creating some kind of illusion that the world is normalized once more.

# Contents

# Abbreviations

**B** base scenario.

**B-BiPV** base scenario with bi-facial solar PV modules.

**B-CF** base scenario with reduced CF of wind turbines.

**B-COST** base scenario with increased costs of wind turbines.

**B-G** base scenario with population growth.

**BNC** base scenario with no $CO_2$.

**CAPEX** capital expenditures.

**CF** capacity factor.

**CHP** combined heat and power.

**$CO_2$** carbon dioxide.

**COP** coefficient of performance.

**DHS** district heating system.

**EC** European Commission.

**ETSAP** Energy Technology Systems Analysis Program.

**EV** electric vehicle.

**FOM** fixed operating and maintenance costs.

**GHG** greenhouse gas.

**ICE** internal combustion engine.

**IEA** International Energy Agency.

**ISO** isolated scenario.

**KSAT** Kongsberg Satellite Services.

**LCOE** Levelized Cost Of Energy.

**NOK** Norwegian kroner.

**NPV** net present value.

**NWC** no wind scenario with no $CO_2$.

**NWI** no wind scenario.

**OPEX** operating expenditure.

**PV** photovoltaic.

**RES** renewable energy sources.

**SNSK** Store Norske Spitsbergen Kulkompani.

**TIMES** The Integrated MARKAL-EFOM System.

**UNIS** The University Centre in Svalbard.

**USD** US dollar.

**V2G** vehicle-to-grid.

**Vkm** vehicle-kilometres.

**VOM** variable operating and maintenance costs.

**WLPT** Worldwide Harmonised Light Vehicle Test Procedure.

# List of Tables

# List of Figures

Chapter 1

# Introduction

## 1.1 Problem definition

The objective of this thesis is to use an existing energy system modelling tool to investigate a transition from the fossil-based energy system in Longyearbyen to a renewable one. This is done by developing a TIMES-model from scratch of the Longyearbyen energy system, described in detail in the section 3.1. The development of the model has been an ongoing project until mid-May, and there is still potential to improve the model further. Alongside working with the model itself, decisions about modelling time horizon and assumed development of Longyearbyen affecting the energy situation were made at the start of the semester. Relevant sources for technical and economical parameters were obtained and evaluated by a literature search and considered implemented in the model during completion.

There are various technologies that could have been a part of the future solution that is omitted from the model, and some are briefly mentioned here. Fossil alternatives, like a gas power plant or a new coal power plant are not included in the model, as the main motivation behind this thesis is to investigate a transition into renewable energy sources. Other potential thermal alternatives include combustion of biomass and nuclear power that could cover the demand in Longyearbyen. Solar irradiance could be used for heating purposes in solar collectors but are found to be less efficient than PV modules [2], and hence excluded. Pumped hydro energy storage was investigated in [3], but not modeled due to the large uncertainties related to costs and suitable locations. The transport sector included in the model is limited to land based personal transport.

## 1.2 Structure

This thesis is structured with chapters presenting different aspects of the task. Chapter 1 presents the objective of the thesis and a brief introduction to the city of Longyearbyen and Svalbard including the existing energy system. This was presented in specialisation project preceding this thesis [3], and a slightly revised version is included below in sections 1.3 and 1.4. In chapter 2 the concept of energy system modelling is briefly explained, and a sample of energy system modelling tools are presented. Chapter 3 describes the development of the model in detail,

and the input data are accounted for in chapter 4. The investigated scenarios are presented in chapter 5, and the results are presented and discussed in chapter 6. General observations from all scenarios are presented, before investigating scenario specific results. Chapter 7 contains the sensitivity analysis performed at the base scenario. Some additional discussion is found in chapter 8 before concluding the thesis in chapter 9. Some suggestions for further work is presented in chapter 10. Model input parameters as well as detailed results are found in appendix A and B.

## 1.3 The exiting energy system

The main component in the existing energy system in Longyearbyen is a coal-fired combined heat and power (CHP) plant. The power plant, built in 1982, is one of three similar power plants in operation, which makes spare parts expensive and the delivery time is long. The coal supplied to the power plant is mined locally by Store Norske Spitsbergen Kulkompani (SNSK) in "Gruve 7." Close to 30 000 tons of coal are used annually to provide the city with heat and electricity, emitting about 60 000 tons of carbon dioxide ($CO_2$) [2].

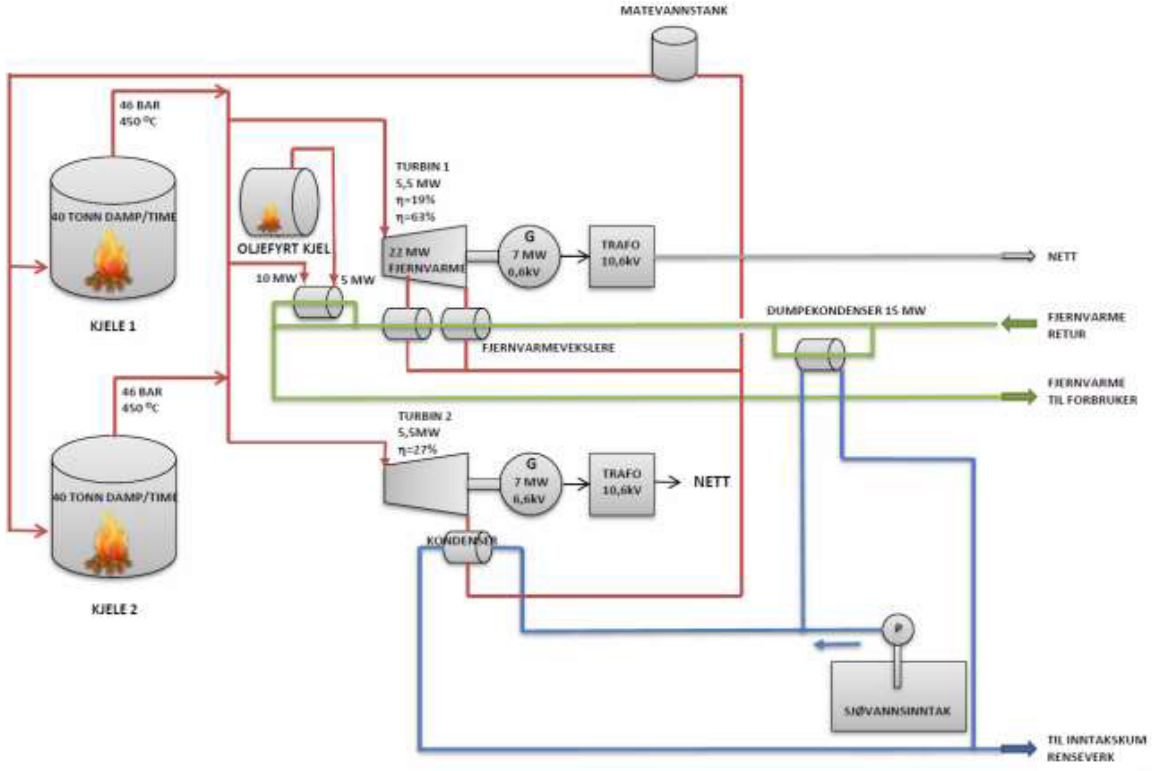


**Figure 1.1:** Flow scheme of the existing power plant

Figure 1.1 shows an overview of the existing power plant. The two coal-fired boilers are operated alternately and $NO_X$, $SO_2$ and dust are removed from the flue gases by a scrubber. The scrubber is only dimensioned to cleanse one boiler at the time. The steam is led into two turbines, where turbine 1 (top of the figure) produces both heat and electricity. Turbine 1 is governed by the thermal demand and deliverers the entire heat demand. Supplying both heat and power, turbine 1 has high total efficiency. However, the lowest possible thermal generation in turbine 1 is 5 MW and the optimal electricity to heat ratio is 1:3.6. Whenever this ratio is not fulfilled the efficiency

of the system drops. If the thermal demand is less than 5 MW (including transfer losses), surplus heat is curtailed in the dump condenser to maintain sufficient cooling of turbine 1 [4].

Turbine 2 is providing electricity and is governed by the electricity demand and produce most of the electricity. As turbine 1 is governed by the thermal demand, turbine 2 must react to changes in the electricity demand. This leads to a low efficiency due to partial load, as well as high wear and tear due to rapid changes [2]. Turbine 2 is as shown cooled by seawater.

The power plant also includes a diesel boiler for backup steam production, and the possibility to deliver heat to the district heating system (DHS) directly by a heat-exchanger. Not included in the figure is a short-term steam storage providing some flexibility to the turbines. Due to the limitations of being able to operate only one coal boiler at the time, the power plant cannot supply the full capacity of its generators simultaneously.

In addition to the coal boilers in the power plant, a diesel back up power plant and diesel boilers are located decentralized in the DHS for backup and peak power. There is also a small amount of grid-connected solar photovoltaic (PV), mainly at the airport, and private backup generators supplying industry like Kongsberg Satellite Services (KSAT) and Gruve 7. Table 1.1 shows an overview energy-producing units in the existing system, with the actual power capacity due to the mentioned restrictions [2].

**Table 1.1:** Producing units in the existing energy system

| | | Power [MW] | Heat [MW] | Fuel |
|---|---|---|---|---|
| Power plant | T1 | - | 22 | Coal |
| | T1 + T2 | 7.5 | - | Coal |
| | Boiler | - | 5 | Diesel |
| | Heat-Ex | - | 10 | Coal |
| Backup power plant | | 8.8 | - | Diesel |
| Boiler houses | | - | 15.7 | Diesel |
| Airport | | 138 $kW_p$ | - | Solar |
| Elvesletta | | 27.81 $kW_p$ | - | Solar |

Since the power plant was built in 1982, the energy demand in Longyearbyen has increased. This leads to deficit production capacity and the backup generators are used more frequently, leading to higher costs. In addition to the overloaded system, the age of the power plant is an increasing problem and can only be operated until 2038 [2]. However, SNSK remaining coal production in ”Gruve 7” is expected to last for no more than 2030 [4], and after this coal is likely to be imported to maintain the energy supply.

### 1.3.1 Production profiles

Longyear Energiverk produces about 70 GWh heat and 44 GWh electricity annually through the coal-fired CHP. In addition to this, an unknown amount of electricity and heat is produced by diesel generators and boilers. Large amounts of heat are curtailed in the dump exchanger mentioned above, especially during summer, but the amount in unknown. The end-user heat consumption is also unknown, as the majority of buildings does not measure their consumption. Therefore, fig. 1.2 shows the production profile of the power plant. It is evident that the

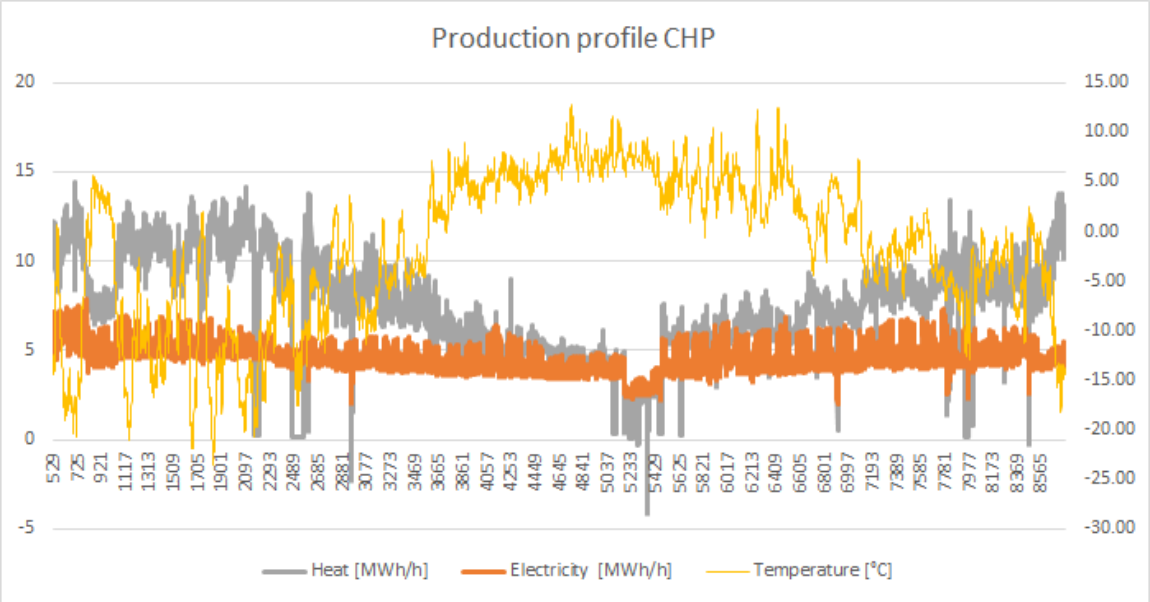


**Figure 1.2:** Hourly production profiles for heat and power from Longyear Energiverk in 2017 [5]

heat production is dependent on the temperature, while electricity production is rather stable throughout the year. Also, the challenge of the optimal power-to-heat ratio of turbine 1 is evident, as the heat and power production is roughly equal in size during summer.

The scrubber installed in the power plant has a large energy demand. In 2017, the power plant consumed 17% of the produced electricity shown in fig. 1.2 while Gruve 7 consumed 13%. Generally, electricity is utilized by businesses, and most of the heat is delivered to households [2].

### 1.3.2 Transmission systems

The city of Longyearbyen has two energy transmission systems, a district heating system and an electric power grid. Like any other system, losses are related to the operation, and for any other infrastructure in Longyearbyen, special concerns regarding the permafrost must be taken, and therefore most of the systems are above ground level.

#### District heating system

The district heating system that almost exclusively supplies Longyearbyen with heat consists of a primary grid supplying the six decentralized boiler houses. The secondary grid supplies approximately 240 substations. An overview of the system is provided in table 1.2 [5].

**Table 1.2:** Overview of the district heating grid

| | Supply temperature [°C] | Return temperature [°C] | Pressure [kPa] | Distance [km] |
|---|---|---|---|---|
| Primary | 120 | 90 | 1600 | 3 |
| Secondary | 90 | 70 | 600 | 21.4 |

As previously stated, the loss in the system is unknown. Bøckman [5] estimates the losses to be between 10 and 15%. However, this figure might be too low compared to numbers from the mainland. The total loss in the distribution grid at the mainland has been roughly 11% the last decade according to numbers from SSB [6] and the losses are assumed to be higher in Svalbard, due to the structure with different temperature levels and the pipes placed above ground in boxes. However, some of these losses make sure that other critical infrastructure like the water supply does not freeze- and thus these losses can be seen as "useful". The state of the substations is also varying leading to unknown losses in the grid. The high temperatures in the DHS, combined with a low outside temperature will also increase losses compered to modern systems operating with lower temperatures [7].

#### Electrical power grid

The electric power in Longyearbyen is distributed from the power plant to the consumers by overhead lines and cables. Parts of the transmission system are old, and reinvestments are needed. For instance, there are existing plans to change the overhead lines to Adventdalen [2]. If the central power production is to be moved, additional investments might be necessary to handle the new situation. Table 1.3 gives an overview of the existing transmission system. In general, the equipment is owned by Lokalstyre, but some transformers are owned by SNSK and KSAT.

**Table 1.3:** Overview of the electric power grid [4]

| | Cable [km] | Line [km] | Transformer [kVA] | Comment |
|---|---|---|---|---|
| 11/22 kV | 29.5 | 16.3 | - | Mostly 11 kV, 22 kV in Adventdalen |
| 230/400 V | 9 | - | - | IT/TN |
| HV | - | - | 21050 | 5 main transformers |
| LV | - | - | 17110 | 41 transformers |

## 1.4 Background information affecting the future energy system in Longyearbyen

### 1.4.1 Population

The population of about 2300 [8] people in Longyearbyen is highly depended on the job market, and generally, people move to Longyearbyen to work. The number of registered adults was identical to the number of full-time equivalents in 2017 (0,8 in the mainland 2014). The dominant industry has traditionally been mining, but in 2015 tourism became the largest industry. Even though the mining industry has been reduced, the number of inhabitants has increased because of growth in other fields, such as tourism and research [9].

As Longyearbyen is becoming more and more dependent on tourism, there are large variations in the number of people staying in the city. This is true both for tourists and for employees in the tourism industry since this includes a lot of seasonal workers. Tourism is mostly happening between March and August [8].

The population in Longyearbyen is in addition to being controlled by the job market, a political question. The official policy from the Norwegian government is among other things to maintain

the Norwegian settlements and sovereignty of Svalbard [10]. However, political decisions made in Stortinget could both decrease and increase the population. The reduced mining activity is a political decision, and the Svea mines were decided closed by Stortinget. As the sole owner in SNSK, this could happen with Gruve 7 as well, and thus reducing the need for labour in SNSK drastically. Following the logic above, shutting down the mine would automatically reduce the population by about 100 people working in Gruve 7 [8].

On the other hand, Svalbard Folkehøgskole opened in September 2019 with 45 students, after rapid political processing. The school is planned to have 25 employees and up to 125 students when it is fully operational [11]. In a city with roughly 2250 inhabitants [12], this represents ”an overnight growth” of almost 7%. The share of Norwegians will increase from 65 to 73 % [13].

Similar decisions could be made for instance regarding the number of research positions at The University Centre in Svalbard (UNIS) or other governmental capacity or state-owned companies. The number of inhabitants will of course affect the total energy demand.

### 1.4.2 Climate

Located 78° north, Longyearbyen has a special climate. Among many things, the most evident characteristic of Longyearbyen is the differences from summer to winter. From April 20. to August 23., the sun never sets and Longyearbyen is embossed by midnight sun. However, the long summer period with constant sunlight has its price, and from October 26. until February 15., the polar night leaves the city in darkness [14].

The location far into the arctic region also affects the temperatures. The annual mean temperature in Longyearbyen was -5.9 °C from 1971-2000, the mean winter temperature -14.0 °C and the mean summer temperature was not more than 4.5 °C [15]. Most of Svalbard, and thus Longyearbyen is covered by permafrost, that means that the ground is frozen throughout the summer. As the ground is frozen, special measures must be taken during construction work, and it is common to place buildings on poles. This way, the building is not in direct contact with the ground and heat is removed by natural ventilation, reducing the impact on the permafrost. Keeping the soil frozen is important to maintain stability of buildings and the landscape. The mean annual precipitation in Longyearbyen from 1971-2000 was 196 mm [15], locating the city in an arctic desert.

#### Climate change

The climate is changing rapidly at Svalbard. As of November 2019, every single month the last nine years has been warmer than the average temperature of a mean month (1961-1990). The amount of precipitation is increasing, and rainfalls occur more often during the winter. The climate change happens faster in the arctic regions, and the mean temperature has increased by 5.6 °C in Longyearbyen compared to the global average of 0.9 °C since 1961 [16]. The warmer climate increases the active layer of the permafrost, making old buildings unstable. The active layer is the top of the soil, thawing during summer and freezing during winter. Traditionally, the buildings were built on wooden poles, but the increased active layer demand steel poles, which are secured even deeper in the ground than before. More rain and a deeper active layer in the permafrost increase the risk of avalanches and landslides, and the coastline is experiencing more erosion [16]. The rapid changes of the landscape are important considerations regarding new infrastructure discussed in this thesis.

### 1.4.3 Special concerns at Svalbard

There are several other concerns regarding operation in Longyearbyen and Svalbard in general. For instance are all traces of human activity predating 1946 protected as cultural monuments and other structures, like some of the newer ropeways crossing the city, including ”Taubanesentralen” has statutory protection [17].

About 65% of the archipelago is a protected area, and access to some areas are limited. The arctic nature is generally vulnerable and plucking of flowers are for instance prohibited [18]. Intervention in nature and landscape is likely to affect areas for longer periods because of the low temperature and short growing season [2]. Movement outside the settlements is associated with a considerable risk of encountering polar bears, which require security measures related to any activity outside the city.

Norway has sovereignty of Svalbard but not all laws regulating the mainland are valid at Svalbard. For instance, was the opening of Svalbard Folkehøgskole delayed while ”folkehøyskoleloven” was changed to include Svalbard [13]. Of greater importance to this thesis, the energy legislation is among the laws not valid at Svalbard [19].

Located about 900 km north of the Norwegian mainland, goods are transported by ship or plane to Longyearbyen. Transportation by ship from Tromsø to Longyearbyen is estimated to last for 2-4 days [20], affecting the delivery time of any spare parts or construction material.

Chapter 2

# Literature Review

## 2.1 Energy system analysis tools

Energy system modeling tools are frequently used to make decisions upon investments to ensure a future energy supply. With an increasing share of renewable energy sources (RES) the operation of the energy system is getting more complex, and analysis of the entire energy system is needed to secure energy of supply as well as reduce the socio-economic costs. There exists a vast number of energy system analysis tools that are frequently used in research communities to investigate these questions, documented in several publications [21, 22]. A sample of tools are briefly presented in this chapter.

## 2.2 TIMES

TIMES (The Integrated MARKAL-EFOM System) is an open source model developed as a part of the International Energy Agency (IEA) Energy Technology Systems Analysis Program (ETSAP). 20 countries and the European Commission (EC) contributes to ETSAP and TIMES can be used in long-term energy scenarios for global, national and local scale. The model is demand driven, and makes investments to cover the future energy demand while minimizing the net present value (NPV). Several models exists, for instance TIMES-Norway developed by IFE, representing the Norwegian energy system in seven different regions [23]. TIMES-Oslo was developed to guide decision-makers on how to reach Oslo's climate goals and Ringkjøb, Haugan, and Nybø [1] developed a stochastic TIMES-Longyearbyen. On the other hand, TIMES-North Europe represents a larger model, emphasizing the flexibility in use of the model framework.

TIMES models energy supply (power plants, import and resource extraction), transmission and demand technologies with costs, efficiency and other relevant properties like greenhouse gas (GHG) emissions. Demand is for instance heating, specific electricity consumption and transportation. TIMES assumes perfect foresight and offers the user to choose the modeling horizon, dividing the year into time-slices. Different loads can be modeled individually on an annual, seasonal, weekly or hourly basis. Technologies are defined by the user, allowing all types of production, storage and demand technologies to be modeled. This makes the model flexible and possible to apply for various analysis purposes. Detailed documentation of TIMES is found

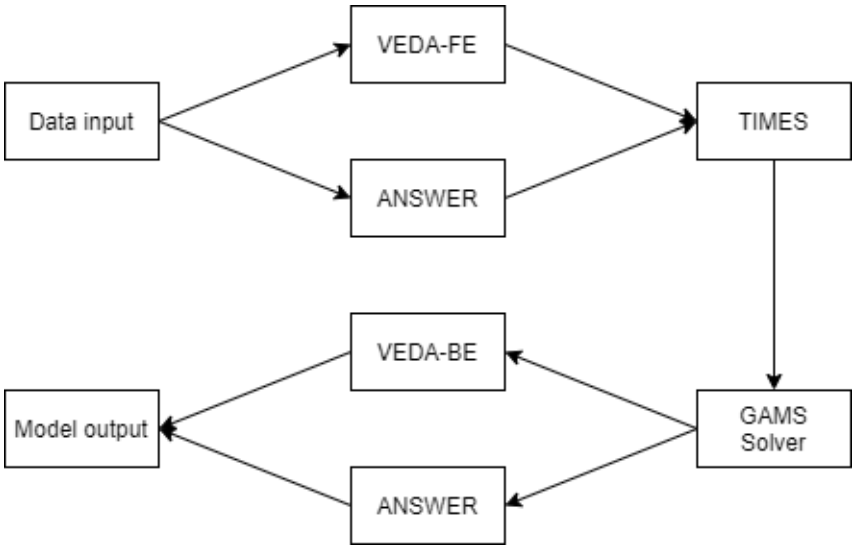


**Figure 2.1:** Structure of the TIMES model adapted from [26]

in [24].

Although the TIMES model it self is open source, the model is written in the commercial modelling language GAMS [25] and use data handle tools requiring licenses to operate. Two different data handling shells exists, and fig. 2.1 shows how the different parts interact.

### 2.2.1 Objective function

$$\text{NPV} = \sum_{r=1}^{R} \sum_{\in \text{YEARS}} (1 + d_{r,y})^{\text{REFYR}-y} \cdot \text{ANNCOST(r,y)} \tag{2.1}$$

The objective function in TIMES is to minimize the NPV shown in eq. (2.1) [24, 27]. $R$ is the set of regions and YEARS is the set of years modelled. $d_{r,y}$ is the discount rate and the reference year for annualizing cost is REFYR. ANNCOST(r,y) is the total annual cost in region $r$ and year $y$, and includes a range of cash flows extensively documented in [27]. Main components of the annual costs included in this thesis are capital expenditures (CAPEX), fixed operating and maintenance costs (FOM) and variable operating and maintenance costs (VOM) as well as costs related to import and extraction of energy carriers.

The model minimizes eq. (2.1) while satisfying a number of constraints. An obvious example is that a technology can not produce commodities exceeding its capacity. The constraint driving the model is the commodity balance. The commodity balance ensures that the production of any commodity must be equal or larger (allows for overproduction of energy) than the consumed amount of the commodity in all time-slices. Thus, the end demand described below must be fulfilled at all times, forcing activity in the energy producing units within one period (operation decision) and investment decisions in future periods.

The model chooses freely how to operate within the given restrictions, and the model output consists of technology capacity and commodity flows as well as all related costs.

## 2.3 PRIMES

PRIMES is developed at the National Technical University of Athens and simulate an energy market equilibrium in the EU and its member states. The model consists of modules representing specific energy suppliers or demanders, each maximizing benefit without violating any constraints. Most technologies could be modeled, including for instance renewables and transport technologies. PRIMES is designed to cover the entire energy system and could be used for policy analysis in a range of fields, from for instance taxation and subsidies to security of supply. Perfect foresight is assumed, and all economic decisions are based upon operation of existing equipment and investments in new technologies until 2050. The model is used by the EC in analysis of climate and energy policy in several publications [28, 29]. Detailed documentation about the model is found in [30].

## 2.4 Balmorel

Balmorel is an open source model tool written in GAMS [25]. All code is provided for the user, and also allows modifications according to specific requirements, offering flexibility in the purpose of use. The model offers a flexible time horizon and time-scales, down to each hour of a year. Balmorel was made to analyse long term perspectives of the electricity and combined heat and power sector in large geographical areas in an international perspective [31].

The model makes optimal investment decisions for capacity in a range of electricity and CHP units as well as storage capacities like hydrogen and pumped hydro energy storage [22]. Transmission lines for electricity are modeled in a way that can indicate bottlenecks in the grid. Although developed for the Baltic region, Balmorel has been used in other locations with various purpose. For instance, Balmorel was used to analyse the implementation of large scale heat pumps in Copenhagen [32], the impact of tradable green certificates in Norway and Sweden [33] and the effects of EVs in the power system in Northern Europe [34].

## 2.5 eTransport

eTransport is an optimization model developed by SINTEF Energy Research [23]. The model is divided in an energy system module, minimizing the NPV of all costs in the existing system and an investment module finds the optimal investment plan on a long-term time scale to meet a predefined demand. The user defines investments alternatives consisting of pre-defined technologies and might include scrapping of existing technologies. Seasonal variations are considered by dividing the years, offering hourly resolutions within each season and options to change prices and capacities. eTransport accounts for both energy demand and peak load. Traditionally, eTransport is a deterministic tool, but a stochastic module is included. eTransport is implemented in AMPL [35] and has a visual ”drag-and-drop” interface developed in Microsoft Visio.

Chapter 3

# Method

The working method in this thesis has been centered around developing the model and obtaining relevant input data. Particular information obtained this semester is a production profile for wind power and information about transport sector in Longyearbyen. Costs and efficiency related to energy producing units and operation of vehicles, especially in cold climate was evaluated. Data obtained in the specializing project [3] last semester has been used for deciding upon the energy projections, production profiles for solar PV and modelling of the existing power system. All input data to the model is discussed and presented in chapter 4 and appendix A along with the source of information.

Before developing the model in this thesis, a substantial amount of time was used to review the available ”demo models” with extensive documentation [36, 37] to increase the general knowledge of the TIMES model framework. This documentation was used frequently utilized, especially in the beginning of development when question arose. The ”attribute master” in VEDA FE, providing details about model parameters as also a great help during development.

## 3.1 Developing the model

The model used and developed in this thesis is based on TIMES-Longyearbyen developed by Ringkjøb, Haugan, and Nybø [1] within the data handling tool ANSWER. For the purpose of this thesis, TIMES-Longyearbyen was rebuilt from scratch in the VEDA Front-End data handling tool and further developed.

VEDA Front-End is used to feed the TIMES model framework with data. All input data regarding technologies, commodities, commodity flows as well as scenarios and other factors are imported via tables in Excel-sheets. This input data makes up a reference energy system, which ultimately describes the model of the energy system.

Technologies or processes represent physical devices who transform one commodity to another. These technologies represents for instance steam turbines or solar PV but also demand technologies like electric radiators or cars. The commodities are energy carriers, like electricity or coal, GHG emissions or end-user heat. A technology either consumes or produces a commodity, and the commodity flows represents the links between technologies and commodities.

The model it self was prepared by hand before entered into Excel, connecting all technologies and commodities in a reference energy system, similar to what is shown i for instance fig. 3.4. Having all connections visible and available, the risk of making mistakes during modeling decreased. All parameters in the developed model are deterministic.

### 3.1.1 Model horizon and settings

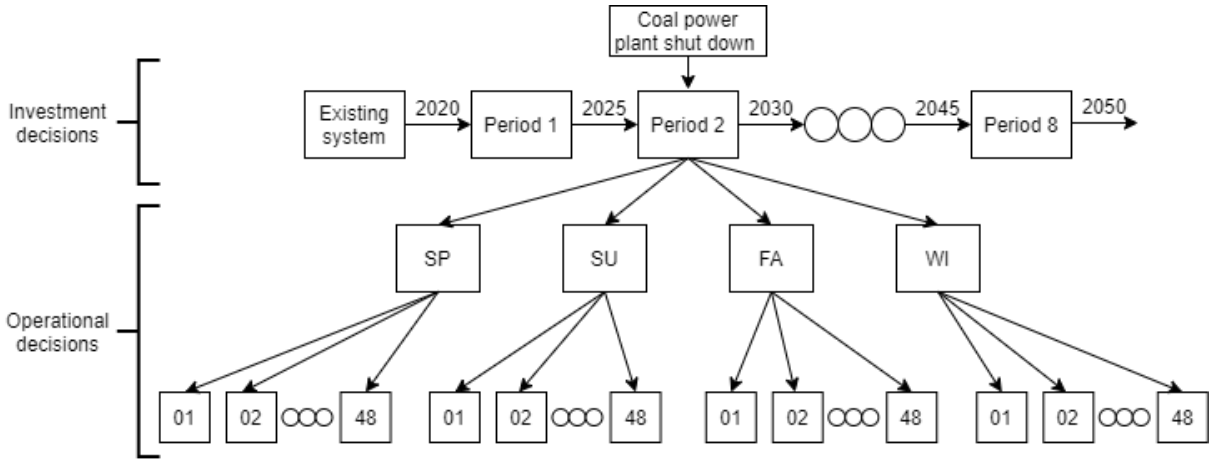


**Figure 3.1:** Overview of the time horizon in the model

Breaking the TIMES model framework down its core, the model seek to fulfill a demand in all defined time steps. The first step in building a model is therefore to decide and define upon the time-slice level and model horizon. The modelling horizon is set from 2020 to 2050, divided in five year intervals where investments can be made. Each year is divided into four seasons with one weekday and one weekend over 24 hours, totalling to 192 time-slices annually. The time horizon is presented graphically in fig. 3.1. The time-slices are denoted like for instance SP01, representing the first hour (00:00-01:00) of the weekday during spring, while SP25 represents the first hour of the weekend. SU, FA and WI are summer, fall and winter. As TIMES is an techno-economical modeling tool, the model also needs a defined discount rate and a base year for discounting. The base year is equal to the beginning of the model horizon, 2020, and the discount rate is set to 4% according to the Ministry of Finance [38].

### 3.1.2 Existing power system

With the time horizon and discount rate defined, the next step is to represent the demand in each period, and the distribution over the time-slices. The approach is explained in detail in chapter 4, but related to the model- the demand is given on the shortest timescale, the hourly time-slices, known as DAYNITE. Next step was to model the energy system, starting with the existing coal fired power plant. The main parts of the power plant is a coal boiler (two, alternating operation) and two turbines. These devices are modeled as individual technologies with commodity flows connecting them. Technologies and commodities are generally on a ”DAYNITE” level, with some exceptions. Production units are modeled by their capacity in MW, while the commodities are given in GWh. This is in line with a real life power plant. The capacity of storage technologies are given in GWh.

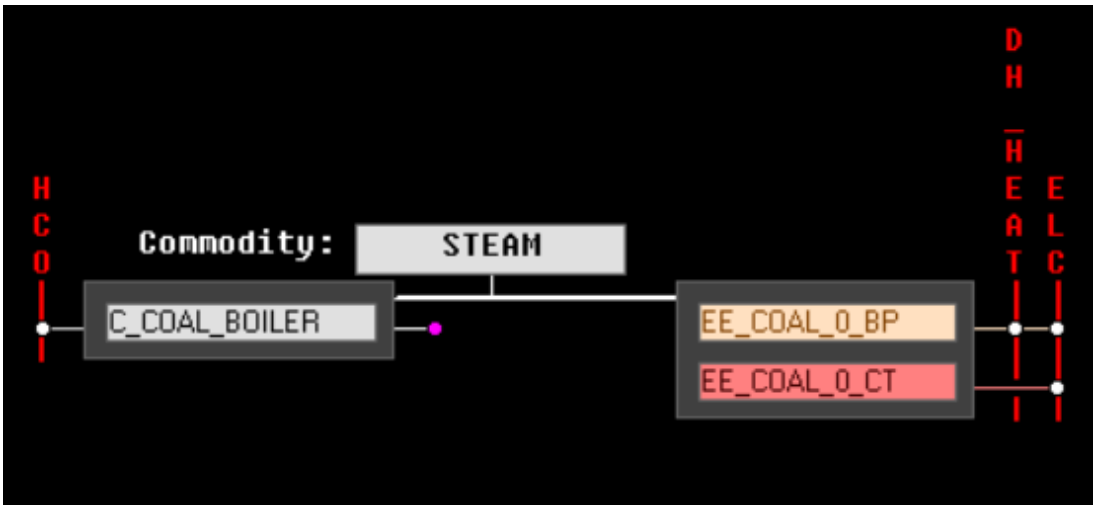


**Figure 3.2:** Coal power plant in the reference energy system from VEDA FE

A part of the reference energy system is shown in fig. 3.2 representing the existing coal fired power plant. High temperature steam (STEAM) connects the coal boiler (C_COAL_BOILER) to the two turbines. Electricity (ELC) is produced in both (white circle is ”connecting point”) while district heating (DH_HEAT) is produced by the back-pressure CHP turbine (EE_COAL_0_BP). Entering the coal boiler, is coal (HCO) and the purple circle leaving the boiler represents $CO_2$ emissions. It is evident from the figure that the coal boiler produces steam by consuming coal, while the turbines consumes steam to produce district heat and electricity. The turbines and their output is ”DAYNITE”, while the boiler and its input and output are ”ANNUAL”. This approach makes STEAM available at all times, ”storing” the produced steam and allowing the turbines to consume it at any given time.

Electricity are at this point only supplied to the demand technology transforming the commodity ELC to the end electricity demand. A transmission efficiency is applied directly to the commodity ELC, representing the loss in the power grid. District heat is supplied to a technology representing the district heating system. This technology is represented with a fixed operating cost and an efficiency, and produces the end heat demand. Together with the technologies and commodities in fig. 3.2, this models a simple energy system.

The installed capacity of the DHS was obtained by running the model without a predefined size and without any costs related to the technology. This way, the model will choose to ”invest” in a system able to meet the heat demand.

The power plant it self consists of the three technologies shown in the figure, with a total of four commodities related to the operation. However, the coal entering the boiler is produced in a mining process not shown in fig. 3.2, crucial to operate the power plant. The technologies in the model has a range of properties defining them, including costs and technological parameters like for instance efficiency. During development of the model, these parameters were based on [1], but some was altered during the process. More details about the used parameters are found in chapter 4 where the input data is described. Once a ”production line” like the coal fired power plant was added, the model was tested to ensure that the processes acted as expected. The same approach was used for the existing diesel generators and boilers. Instead of a mining technology as for coal, the diesel line starts with an import technology of the commodity diesel, which then

are connected to the diesel generator. The import of diesel is ”ANNUAL” as explained over, making sure that diesel is available at all times, not regarding storage capacity for fuel.

As TIMES minimizes costs in operation, adding a new technology with representative technical and economic parameters might not change the optimal solution. This has been the case several times during development of the model, for instance for diesel generators. If the costs related to supplying energy with coal are lower than for diesel, the new technology will not change the solution. To ensure that the new technologies were correctly modeled, a frequent approach during the development has been to change parameters. By for instance lowering the costs of diesel import or increasing efficiency, the diesel generator will increase its competitive ability, and appear in the solution. This ”trial and error” approach has ensured that all processes in the model is working as intended. The parameters was changed back to reasonable values after the tests.

### 3.1.3 Investment decisions

The existing power plant and backup capacity is modeled as a ”past investment” with a given lifetime. At the end of lifetime, the technologies are ”removed” entirely from the model. As this lifetime is shorter than the model horizon as visualized in fig. 3.1, new technologies must be modeled as investment possibilities to fulfil the energy demand throughout the model horizon. The same general approach as for the existing system is followed, adding one ”production line” at the time, starting with the renewable energy sources. New investments are also modeled with a lifetime, and a possibility to reinvest after the lifetime. Technologies assumed to have a potential to change relevant parameters are described with different values in the future, known as vintage. The details are provided in table A.1.

#### Renewable energy sources

The available renewable energy sources (RES) are modeled with two technologies, exemplified by south facing ground mounted PV modules in fig. 3.3. All parameters are applied to the left technology EE_PV_GR_S, which consumes the commodity sun and produces the commodity ELC_PV_G_S according to the PV modules capacity factor based on simulations.

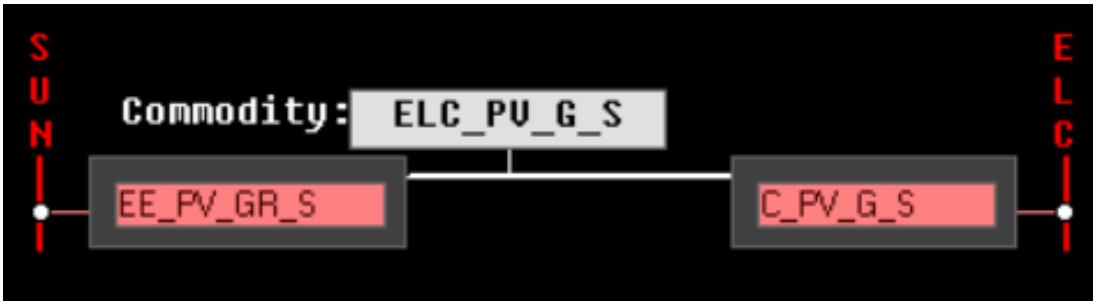


**Figure 3.3:** Solar PV in the reference energy system from VEDA FE

The ELC_PV_G_S commodity are forced to follow a predefined distribution based upon simulated production profiles for PV modules with the given orientation by imposing restrictions in the model. C_PV_G_S is a ”dummy-technology” included to consume the distributed output from the PV module, and produce electricity (ELC) with same distribution. The electricity output from RES are therefore forced by the modeller to follow a given pattern. This differ from the output

from the other technologies like for instance the steam turbines, where the produced energy are free to follow the distribution of the load, representing the operational decisions. Wind power and all orientations of solar PV are modeled similarly, and the distribution is discussed in chapter 4. The commodity SUN (and WIND) are provided by technologies representing the solar irradiance and wind resource, similarly to the mining and import technologies for coal and diesel. Opposed to import and mining, the renewable resources does not have any costs related to them.

Seven various orientations of PV modules are modeled, where two are ground mounted. In addition are five roof mounted orientations modeled with restricted capacity, based on assumptions on available roof area and modules production capacity [3].

### Heating technologies

The renewable, diesel and coal production lines, are all independent, starting from a primary resource, producing district heat or electricity. This far, the only way to produce heat is through fossil energy sources. Therefore, centralized heat pumps and electric boilers are modeled. These technologies consume the already modeled electricity (ELC) and produce district heating (DH_HEAT). In addition, electric radiators are modeled, directly supplying end heat demand from electricity, unrelated to the district heating system.

### Storage

Next, energy storage was modeled for both heat and electricity on a short- and long-term scale. The approach is comparable to the approach for solar and wind, by using ”dummy” technologies and commodities as shown in fig. 3.4. The approach is used as it simplifies reporting of the energy flow related to the storage, and is used for all four storage technologies but explained in detail for the battery.

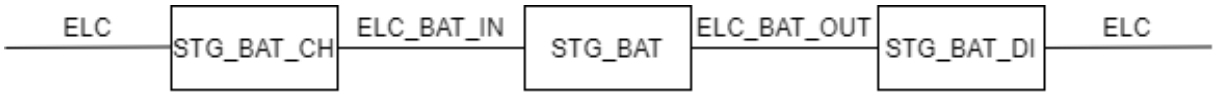


**Figure 3.4:** Battery storage in the reference energy system

STG_BAT represents the physical battery, modeled with a storage efficiency, costs and lifetime. Like the already defined technologies, the the storage technology consumes the incoming commodity (ELC_BAT_IN) and produces the outgoing ELC_BAT_OUT. Unlike the already described technologies, the consumption and production are not necessarily happening simultaneously. The short term units (Battery and Thermos) are limited to store energy within one season, meaning that the sum of ELC_BAT_IN during for instance summer, must be equal to ELC_BAT_OUT adjusted with the storage efficiency. This restriction is imposed because the storage efficiency is constant. Knowing that batteries self-discharge (and hot water cool down) over time [39], limiting the period of time the battery is able to store energy, counteracts the constant storage efficiency.

Long term storage of heat and a hydrogen storage tank is modeled exactly like whats shown in fig. 3.4, but as technology that allows seasonal storage as well as hourly charging/discharging. This allows the sum of input to the storage medium in one season to be larger or smaller than the output, as long as it is in balance on an annual scale.

Although the hydrogen storage tank is modeled like the other storage technologies, there are additional technologies completing the hydrogen production line. Hydrogen could either be produced by a electrolyser, consuming ELC, or imported by a import technology like the one for diesel. Hydrogen is consumed by a fuel cell, producing district heat and electricity.

### Transport

At this point in the development, only the demand for electricity and heat is modeled. The next step was therefore to include the demand for transportation. Three dummy technologies were defined, lossless transforming hydrogen, diesel and electricity to a dummy commodity consumed by the vehicles. Figure 3.5 represents the line for electric vehicles (EV) where TCARELC, is an electric passenger car supplying the demand F_CAR for transport, given as vehicle-kilometres (Vkm). F_SM represents snow mobiles and F_VAN vans. The different demands could all be provided by electricity, diesel (for simplicity diesel and petrol are treated equally) or hydrogen. The vehicles are modeled with fuel efficiency, average driving distance, lifetime and investment and maintenance cost. The line for diesel and hydrogen powered vehicles are ANNUAL, however the EVs are modeled on a DAYNITE level according to an assumed charging profile defined similarly to the production profile for solar and wind. The EVs are not modeled as a storage technology, so this approach ultimately forces the demand to be covered according to the DATYNITE charging profile when supplied by EVs. When supplied by hydrogen or diesel, the demand is ANNUAL. EVs are thus not capable to be used for storing or providing electricity to the grid, so called vehicle-to-grid technology.

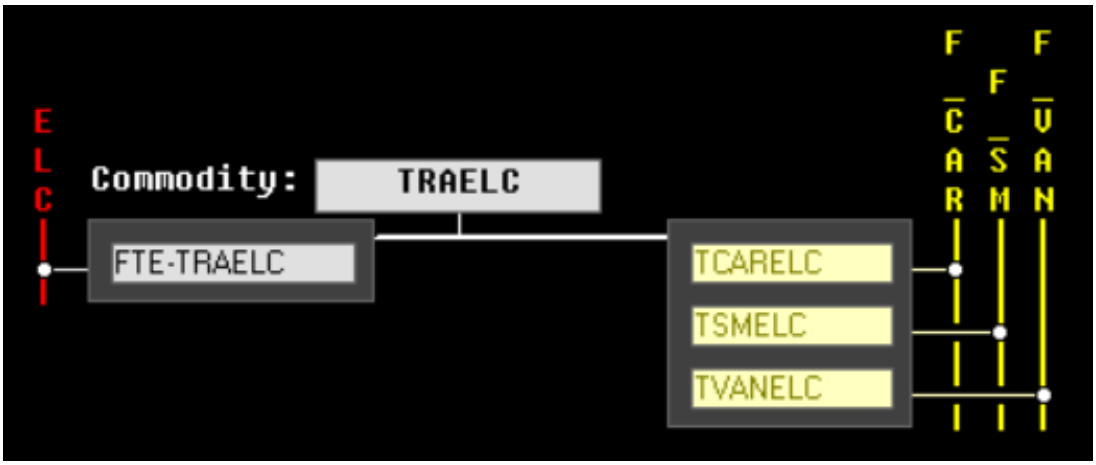


**Figure 3.5:** Electric vehicles in the reference energy system from VEDA FE

The existing stock of vehicles are modeled in a way such that it is decreasing linearly towards zero while being replaced by new cars.

Only land based transport is included in this thesis. In addition to this there is an unknown demand for maritime fuel and an annual demand for jet fuel supplied by Avinor of about 3000 $m^3$ [40]. This fuel covers both flights locally at Svalbard as well as refueling commercial flights from mainland Norway. There are a lot of research into electrifying air traffic, but there are still no available commercial electric planes. Avinor plan to electrify domestic flights within 2040 [41], but it is unknown if this includes Svalbard. Due to the uncertainty of how the energy demand in an electric aircraft will be in the future, the energy demand related to aviation is not

included in this task. However, the energy content of the provided jet fuel is about 40 GWh annually, meaning that if this should be produced locally (as electricity or hydrogen), the chosen energy system is likely to increase its production capacity.

**Energy efficiency matters**

Energy efficient measures meant to reduce heat consumption are model in buildings are included in the model. Four different technologies in both residential and commercial buildings are modeled in the same way, with different restrictions and costs. The technologies produce end heat demand in ANNUAL time-slice, which is similar to distributing the produced end demand evenly over all time-slices. As all other heat producing units acts on a DAYNITE time-slice, the distribution stays the same, but ultimately less heat is produced from for instance electricity.

The different technologies have restrictions related to installed capacity according to the energy savings potential, described in chapter 4. The restrictions are imposed on total capacity, as well as new capacity in each investment period. Technicalities in the modeling, treats the energy efficient measures like other technologies by its capacity in MW. However, as the potential reduction is given in GWh, the installed capacity is scaled accordingly with 1/8.76 (MW/GWh).

### 3.1.4 Early retirement

The district heating and the existing diesel infrastructure is modeled with a possibility of early retirement. This means that the technology can be removed from the solution if it is beneficial to do so, due to reduced operating costs. If parts of the heat demand is covered by electric radiators, the transmission capacity in the district heating system could be reduced. The existing diesel infrastructure has this option as one scenario does not allow import of diesel. Technicalities in the model framework, allows for partly decommissioning of capacity- so that the existing capacity for instance could be halved. The existing diesel infrastructure consists of several units adding up to the capacity shown in table 1.1, making a partly reduction of capacity feasible. The impact on the solutions are discussed in sections 6.1 and 8.5.

### 3.1.5 Techno-economical parameters

During development of the model, all parameters was reused from Ringkjøb, Haugan, and Nybø [1] when available. In completion of the model, some parameters where changed according to different sources and assumptions. All used parameters are found in table A.1 and some assumptions and reasoning is provided in chapter 4.

### 3.1.6 Scenarios and sensitivity

The finalized model was used to investigate different scenarios and to preform a sensitivity analysis. The is done by imposing various restrictions or changes in the model, and are described in detail in chapter 5. The scenarios of interest was created before solving the base scenario, and are not changed. The performed sensitivity analysis however, was slightly altered to address special findings in the scenarios.

Chapter 4

# The developed TIMES model, TIMES-LYR

Input data from several sources has been obtained and evaluated for the purpose of the model developed in this thesis. This chapter accounts for choices and give some calculations regarding efficiencies. Input data not provided in this chapter is found in appendix A.

## 4.1 The existing energy system

Table 4.1 show the techno-economic parameters used to model the existing energy system shown in table 1.1. The PV modules are modeled with a capacity factor, not efficiency, however the model treats the two parameters equally related to energy output. The capacity of the district heating system is based by results from the model as explained in section 3.1. The fixed operating and maintenance costs are based on the actual operating expenditure divided by the installed capacity. The cost of coal is set to 66 kNOK/GWh [4].

**Table 4.1:** Model of the existing energy system

| | Capacity [MW] | Efficiency (el/heat) [%] | FOM [kNOK/MW] | VOM [kNOK/GWh] | Source |
|---|---|---|---|---|---|
| Coal boiler | 25 | 0.8 | - | - | [1] |
| CHP turbine | 5.5 | 0.19/0.63 | 1620 | 12 | [42] |
| Steam turbine | 5.5 | 0.27 | 1620 | 12 | [42] |
| Diesel generator | 8.8 | 0.294 | 291 | 14.6 | [42] |
| Diesel boiler | 15.7 | 0.9 | 194 | 14.6 | [42] |
| PV airport | 0.138 | 0.054 | 85 | - | [40] |
| PV Elvesletta | 0.028 | 0.071 | 85 | - | [43] |
| DHS | 10.3 | 0.841 | 1266 | - | [44] |

## 4.2 Production profiles for renewable energy sources

The nature of RES is fluctuating and varying, and is therefore challenging to capture in a deterministic modelling approach. The chosen data input for solar and wind power should

represent both the daily and seasonal fluctuation, as well as distributing the total production correctly between the seasons.

Hourly production profiles for PV is based on synthetic Metonorm 7.2 (1981-1990) data simulated with a highly efficient PV module, SunPower X-22-360, and was obtained in the specialising project [3] by the software PVsyst [45]. The production data for wind is based on 2018 MERRA-2, solved with a Vestas V150-4200 with hub height at 100 meters in the online application renewables.ninja [46].

The data input in the model is based on the 192 time-slices described in section 3.1.1. Thus, the 8760 data points in the original data sets must be reduced to 48 representative time-slices in each of the four seasons.

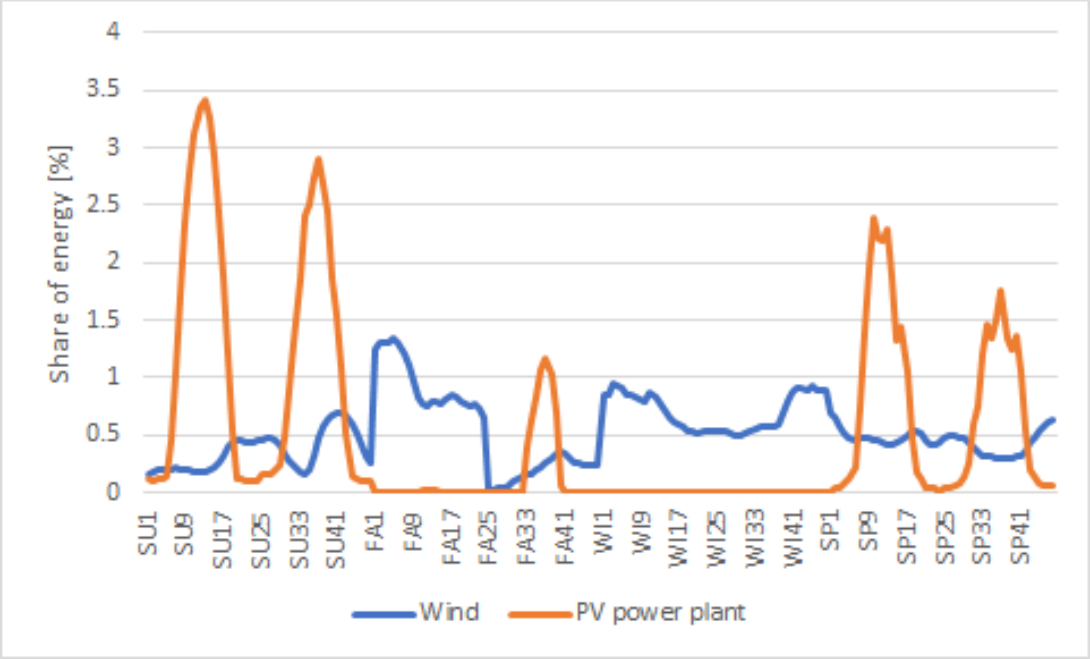


**Figure 4.1:** Production profiles for renewable energy sources

To do so, the production from two successive days (48 hours) from each season was randomly selected from the original data. The 192 chosen values were summed, and each hourly value normalized to investigate how the production was distributed over the seasons. The model distribution (192 data-points) was then compared to the seasonal distribution of the original data set. The 192 data-points were also plotted as seen in fig. 4.1 to investigate the daily distribution. The random selection did not secure a correct seasonal distribution, and a trial and error approach was utilized on different days within each season. This approach was applied to the data for solar PV and wind simultaneously with the same days, to get consistent data.

The final distribution used for solar power was obtained by using the production profile from the 24th and 25th of January. During the other other seasons, 48 successive hours were not found to meet the requirements of the production profile, and the spring profile is the production from the 22th and 24th of April. The summer production is based on the 22th and 24th of July while the fall production is 28th of September and 5th of October. As seen in the utilized production profile in fig. 4.1, the chosen data has different production within each season and the typical peak around noon expected from solar PV. All orientations of PV uses data from the same days

**Table 4.2:** Assumed average heat demand in buildings

| | Area [$m^2$] | Existing buildings [kWh/$m^2$] | Renovated buildings [kWh/$m^2$] |
|---|---|---|---|
| Residential | 99093 | 340 | 238 |
| Commercial | 100772 | 250 | 175 |

without any modifications.

The wind data is based on the same days as for PV during winter and fall. However, as the the production values during the chosen days were to small to represent the seasonal distribution, the data is scaled by a factor of 1.5 Spring and summer data is based on the 2nd and 3rd of April and 23rd and 24th of July. This data is scaled by 0.95 and 0.75 to secure the correct distribution.

An important observation in fig. 4.1 is that there is no production from PV during winter and little during fall. However, the production from wind is at its maximum during these periods. In general, wind and solar irradiance has an opposite cycle [47], as observed in fig. 4.1, and this factor was important in deciding the production profiles. The chosen distribution is discussed in section 8.4

$$CF = \frac{E_{produced}}{8760h \cdot P_{nominal}} \tag{4.1}$$

In the TIMES model, the power production from solar and wind is given by the capacity factor (CF) and installed capacity. CF represents the ratio of produced energy to the potential maximum as shown in eq. (4.1), and is obtained from the used data sets for wind power and each orientation of solar PV. CF is given in table A.1. The already installed PV modules are calculated based on actual production values. RES typically has a small CF due to the intermittent wind and solar resource.

## 4.3 Energy demand

As mentioned in section 1.3 the actual heat demand in Longyearbyen is unknown as the heat consumption is not measured. The base year heat demand in the model is therefore deduced from the production profile shown in fig. 1.2 and assumptions about the average heat demand in buildings.

Table 4.2 lists the area connected to the DHS [2] and the assumed average heat demand. The current residential demand is based on assumptions from Lokalstyre [5] and experience from Statsbygg's older buildings [48] evaluated in the specializing project [3]. As the majority of the district heat is supplied to residential buildings [2], the average demand in commercial buildings are assumed to be 35% lower. With these assumptions, the annual heat demand adds up to 58.9 GWh as seen in fig. 4.2.

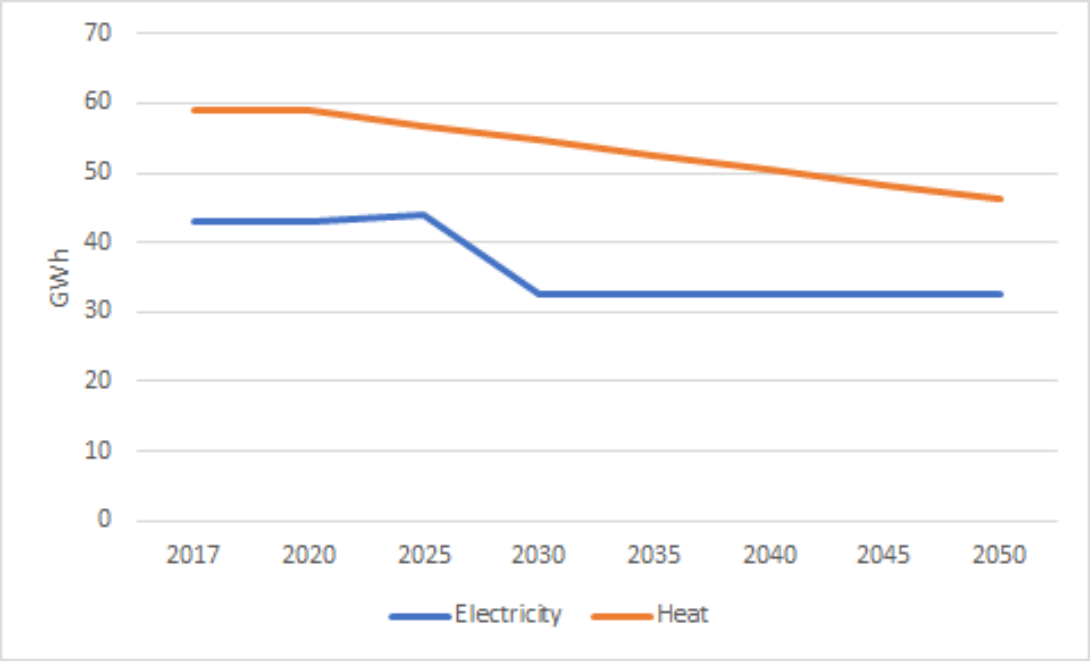


**Figure 4.2:** Base scenario energy demand projection

### 4.3.1 Future energy demand

The future energy demand in Longyearbyen is unknown due to several reasons covered in the specializing project [3]. However, there are some trends and plans that will affect both heat and electricity demand in the future.

Communication with both Statsbygg [48] and SNSK [49] reveal an increased focus on energy efficiency in buildings, and the most recent building projects has been fulfilled in passive house standard. Statsbygg has also installing control units in older buildings and experiences reduction in heat consumption up to 40%. The future renovation rate for both residential and commercial buildings is set to 2% annually and old buildings will be rebuilt with a rate of 0.3% for residential and 5% for commercial buildings according to Rosenberg et al. [50]. As the base scenario populations is assumed to be constant, the total building area will stay remain. Renovated and new building are assumed to have 70% of the heat demand of older buildings. With these assumptions, the heat demand will decrease linearly as shown in fig. 4.2.

The projection in electricity demand used in the base case is shown in fig. 4.2. Gruve 7 and the existing power plant is expected to be shut down in 2030 as the coal reserves are running out reducing the electricity consumption with 30% [4]. KSAT is expecting to increase their consumption with 50% within ten years [2], an increase assumed to happen in two steps in 5 year intervals. After 2030, the electricity demand is assumed to be constant as there are no population growth.

### 4.3.2 Demand profile

The demand profile utilized in the model is obtained similarly to the production profiles for RES from the actual production profiles for heat from the power plant in 2017 and is shown in fig. 4.3. The first day in each season (for instance SU1 to SU24) represent the load during a

normal weekday while second day in each season (SU25 to SU48) represents the load profile during weekends. The heat demand is as expected higher during winter, and notably higher during spring than fall. The electricity demand varies more than the heat demand om a daily base, but the demand similar in the different seasons.

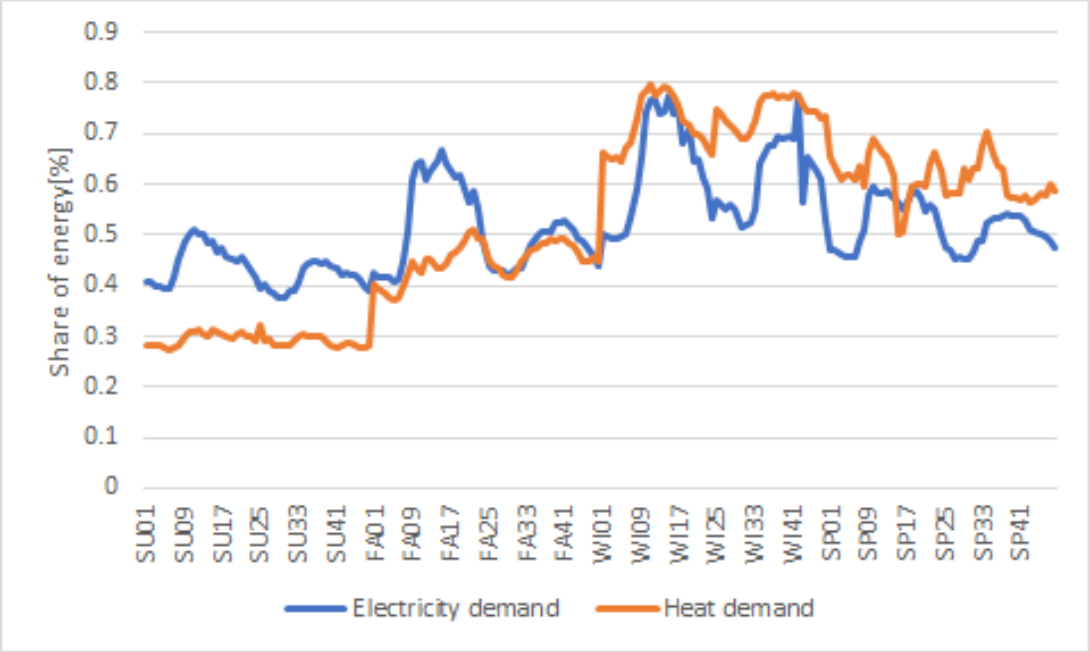


**Figure 4.3:** Demand profiles for end user electricity and heat

The demand profile is obtained by close to the ones used for the production profiles, the 23rd and 28th of January, the 22nd and 24th of April, the 22nd and 24th of July and the 21th and 23rd of October.

## 4.4 Demand technologies and transmission efficiency

The existing DHS is as mentioned currently supplying the entire heat demand in Longyearbyen. This process is related to unknown transmission losses, and is therefore calculated based on the assumptions regarding heat demand presented in table 4.2 and the production profile from the power plant fig. 1.2, producing about 70 GWh heat. If the heat supplied by the diesel boilers and heat curtailed during summer is neglected, the transmission efficiency in the DHS can be calculated by eq. (4.2).

$$\eta = \frac{\text{Useful energy}}{\text{Total energy}} = \frac{58.88 \text{ GWh}}{70 \text{ GWh}} = 0.841 \tag{4.2}$$

An efficiency of 84.1% is significantly lower than the national average of 90% for the last decade [6]. However considering the cold climate in Longyearbyen and that the DHS is operating with high temperature levels this is reasonable as discussed in section 1.3.

The DHS is modeled as a demand technology producing end heat demand by consuming district heat with the given efficiency, kept constant throughout the modeling horizon. District heat is

provided by the existing CHP and centralized heat pumps, electric boilers and fuel cells. The coefficient of performance (COP) of the heat pump is set to 2.5, and is discussed in section 8.3. Electric radiators are modeled to consume electricity and produce end heat demand directly with an efficiency of 100%.

The demand technology for specific electricity demand is modeled with 100% efficiency, however, the constant Norwegian transmission loss of 8% [51] is applied to the commodity ELC to represent loss in the power grid.

## 4.5 Energy efficiency measures

The energy efficiency measures are modeled as technologies providing heat. To ensure that not all heat is provided by this, restrictions upon installed capacity is invoked based on the savings potential and available area. The energy reduction potential, costs and life time presented in table 4.3 are based on Lindberg and Magnussen [52], using numbers related to large energy savings. The potential capacity is calculated by multiplying the potential energy reduction with the given building area presented in table 4.2 and dividing 8.76. The potential capacity is implemented as a restriction on total capacity for all periods as mentioned in section 3.1.3. In addition, is the procedure repeated for all periods with the remaining non-renovated area. This way, only buildings not renovated in the base scenario demand projection is available for additional investments in energy efficiency measures, and available investments in significantly lower in 2050 than 2020.

**Table 4.3:** Parameters for energy efficiency measures [52]

| Measure | Sector | Reduction [kWh/m$^2$] | CAPEX [kNOK/MW] | Life [Years] | Max capacity [MW] |
|---|---|---|---|---|---|
| H1-Energy monitoring | Residential | 10 | 17520 | 10 | 0.1131 |
| | Commercial | 20 | 13140 | 10 | 0.2301 |
| H2-Insulation | Residential | 40 | 219000 | 30 | 0.4525 |
| | Commercial | 10 | 350400 | 30 | 0.1150 |
| H3-Technical equipment | Residential | 30 | 146000 | 15 | 0.3394 |
| | Commercial | 60 | 109500 | 15 | 0.6902 |
| H4-Energy management | Residential | 30 | 73000 | 10 | 0.3394 |
| | Commercial | 70 | 125143 | 10 | 0.8053 |

## 4.6 Land based transport

Table 4.4 shows the number of registered vehicles and their assumed driving distances in 2019 given in vehicle-kilometres (Vkm). Cars with internal combustion engine (ICE) clearly dominate the stock, while the average driving distance is assumed to be equal regardless of the engine type as the cars needs to fulfill the same demand regardless of engine. One of the biggest concerns about EVs is usually the limited range due to the battery size. With roughly 50 km of roads in Longyearbyen [57], this capacity is unlikely to impose a challenge. Considering the short driving distances, the need for fast/super chargers will probably be limited, and hence, the

**Table 4.4:** Number of vehicles and driving distances at Svalbard

| | ICE | EV/PHEV | Average distance [km] | Total distance [MVkm] | Source |
|---|---|---|---|---|---|
| Passenger car | 1106 | 20 | 9471 | 12.86 | [53, 54] |
| Vans | 314 | 2 | 11140 | 7.58 | [53, 54] |
| Snowmobiles | 2192 | - | 3500 | 3.52 | [53, 55] |
| Buses | 20 | - | 5000 | 0.1 | [56] |
| Sum | 3632 | 22 | - | 24.07 | - |

charging pattern is assumed to be similar to the 'home charging'-profile shown in fig. 4.4 [58]. Snowmobiles are assumed to follow the same charging pattern throughout the day.

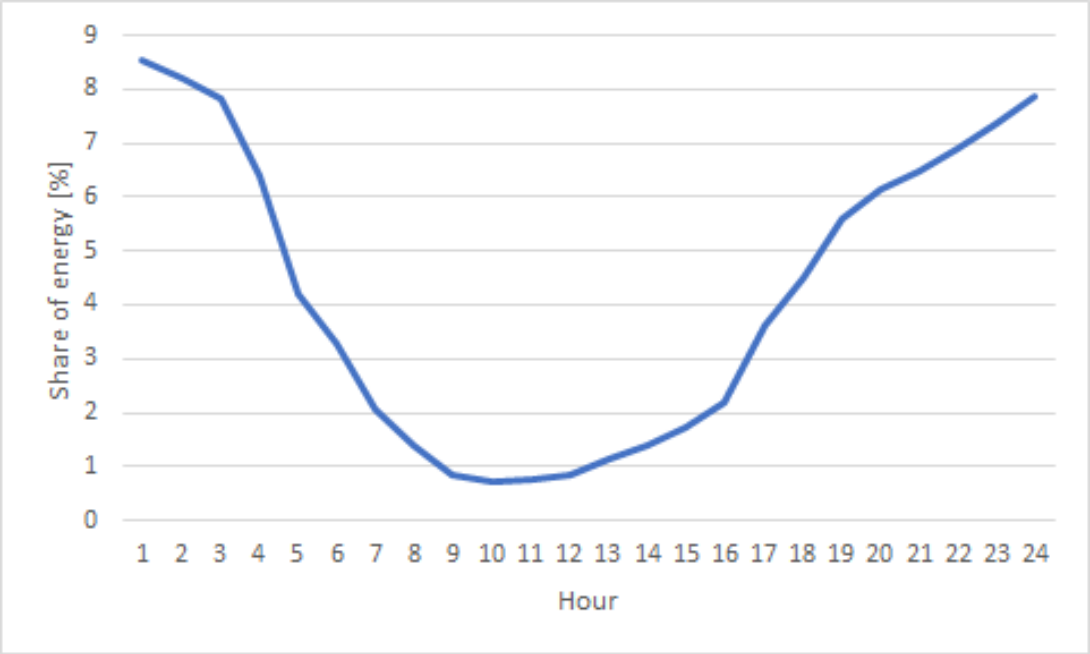


**Figure 4.4:** Assumed charging profile of electric vehicles

**Fuel consumption** Driving pattern and temperature affect fuel consumption of cars. Engines operating outside of their optimal temperature range increase fuel consumption. This is particularly true for short trips, as the engine might not reach optimal temperatures at all. This phenomenon is known as cold start, and is found to increase the fuel consumption up to 25% [59]. Considering the short driving distances and low temperature, this indicates that the fuel consumption of cars in Longyearbyen generally will be higher than what car producers claim. This is also true for EVs, and the consumption of energy is doubled during winter for some cars [58].

Table 4.5 shows the given Worldwide Harmonised Light Vehicle Test Procedure (WLPT) fuel consumption for three similar sized cars powered by different fuel. WLPT is a laboratory test designed to be able to compare different car models [63] and the energy content in the fuel is calculated compare the different fuels. Table 4.5 show that the energy efficiency of the EV and hydrogen car exceeds the ICE whilst the hydrogen powered car is less efficient than EVs.

**Table 4.5:** Combined WLTP consumption for different drivelines

| | Diesel consumption [L/100km] | Hydrogen consumption [kg/100km] | Energy consumption [kWh/100km] | Source |
|---|---|---|---|---|
| E-Golf | - | - | 15.8 | [60] |
| Golf | 6.5 | - | 57.2 | [61] |
| Mirai | - | 0.76 | 25.1 | [62] |

WLPT is preformed at temperatures of 23°C, but as mentioned fuel consumption is expected to increase in cold temperatures. In addition, the carpool in Longyearbyen has a variety of cars, many of them larger vehicles, further increasing fuel consumption. The WLPT consumption is therefore scaled according to the assumptions in table 4.6 before applied in the model. EVs are significantly more efficient than ICE cars, regardless of a larger scaling factor. The efficiency ratio for different drivelines are applied directly to snowmobiles.

Electric buses are frequently used in the mainland, however they are omitted from this thesis due to uncertainties in costs and energy efficiency related to traditional buses. Based on the number of buses and short total driving distance shown in table 4.4, this energy demand is negligible.

**Table 4.6:** Fuel consumption for personal cars

| Fuel | WLPT consumption [kWh/100km] | Scaling factor | Model consumption [kWh/100km] | Efficiency rate vs electricity |
|---|---|---|---|---|
| Electricity | 15.8 | 100% | 31.5 | - |
| Diesel | 57.2 | 50% | 85.8 | 0.37 |
| Hydrogen | 25.1 | 100% | 50.2 | 0.58 |

The energy consumption is kept constant in all seasons and distances for cars assumed to be evenly distributed throughout the seasons. The snowmobiles is assumed to have 60% of its mileage during winter, and 20% in spring and fall. As the base case scenario assumes a constant population, the transport demand is assumed to stay constant throughout the modelling horizon.

## 4.7 Cost

As explained in section 2.2, the TIMES model is a techno-economic modelling tool. Cost projections for the different technologies present in the model is crucial for the solutions presented in section 6.1. The different technologies are presented with CAPEX and operating expenditure (OPEX) and is for some technologies changing in the future. This is particularly true for the renewable technologies and storage in batteries and hydrogen. The average cost of utility scale PV dropped with up to 84% in major markets from 2010 to 2018 and the costs are expected to decrease even further in the future [64]. Costs for onshore wind dropped with an average of 22% in the same period [65], and capacity factors for both technologies is generally increasing, further decreasing Levelized Cost Of Energy (LCOE). It is important to emphasise that the cost projections utilized in the model and found in table A.1 is projections and therefore a matter of insecurity. Costs obtained from sources like National Renewable Energy Laboratory [66] and NVE [42] are not necessarily directly applicable to the conditions in Longyearbyen and might differ from whats used in the model. The uncertainty regarding costs will partly be handled in

the scenarios by preforming a sensitivity analysis.

In the mainland of Norway, incentives like tax reductions and public-transport lanes lead to that 42.4% of the cars sold in 2019 were electrical [67]. As Longyearbyen is a tax-free zone, these measures are not relevant to reduce the share of cars powered by fossil fuels. However, EVs are expected to be cost competitive with conventional cars in 2024 for small cars and 2025 for larger vehicles like SUVs [68]. The maintenance cost related to EVs are smaller than for conventional cars, mainly because of less moving parts. As cost projections for cars are uncertain, investment costs for EVs are set equal to ICE cars throughout the modelling horizon. Hydrogen powered cars are set 33% more expensive as they have a significantly lower market share and are thus more expensive to produce. Maintenance cost for hydrogen cars are assumed to be the average of EVs and conventional vehicles as they are run with electric motors, but also has a hydrogen system on board- increasing complexity. The same rates are applied to snow mobiles for simplicity.

Chapter 5

# Scenarios

A common approach in energy system modelling is to investigate different scenarios to understand the energy system better. The robustness of the solution is investigated by changing key factors like energy demand, costs and technical performance of the renewable energy sources. This thesis will investigate and compare five different scenarios, while the sensitivity analysis is limited to the base scenario to reduce the scope of the thesis.

## 5.1 The base scenario (B)

The base scenario (B) is solved without any restrictions. As there are no limitations to the solution the objective function found in this scenario will be the optimal based on the provided technical and economical data input.

## 5.2 The no wind scenario (NWI)

The no wind scenario (NWI) is included because of the uncertainty regarding a larger wind power development project. The opposition against wind power in the mainland Norway is large, and for instance was the national framework plan for wind power abounded by the government in 2019 due to critical response [69]. 49 of the 56 counties that responded to the plan was clear that they did not want development of wind farms in their area, and ongoing projects like the wind park at Frøya, Trøndelag has experienced vandalism adding up to 15 million NOK [70]. Considering the mainland opposition and the vulnerable nature surrounding Longyearbyen- the political decision to build larger wind turbines might be ”impossible.” Another factor is conflict with KSAT’s satellite station at Platåberget, as this is one of the logic areas to utilize for a wind park. NWI is therefore solved without any wind turbines, but with no further limitations as in B. Regarding the model, a scenario is added to restrict the installed capacity of wind turbines to zero in all periods.

## 5.3 The base scenario with no $CO_2$ (BNC) and no wind scenario with no $CO_2$ (NWC)

As discussed in chapter 1, the average $CO_2$ emission per person is among the highest in the world. This is mainly because of the polluting coal-fired power plant, but also due to a large energy consumption. As the climate change is occurring rapidly in the Arctic due to emission of GHG, it is ironic to allow emissions of $CO_2$ in this vulnerable area. Both the base scenario and the no-wind scenario are therefore investigated are investigated when restricting the $CO_2$-emission to zero from 2030.

## 5.4 The isolated scenario (ISO)

The existing power supply in Longyearbyen is mainly self-sufficient relying on locally mined coal, with a supplement of diesel for heat and electricity production. The advantage of being self sufficient with energy is reduced shipping traffic to Svalbard as well as few uncertainties regarding future energy prices locally. An isolated system without any import will also lead to an emission free energy system, as the energy production will be based entirely on renewable energy sources. In the isolated scenario (ISO), no import of either diesel or hydrogen is allowed the entire modelling horizon, by imposing a restriction in the activity on the import technologies.

## 5.5 Sensitivity analysis

### 5.5.1 The base scenario with population growth (B-G)

All the presented scenarios will be solved with the end-demand projection presented in section 4.3. The demand projection is based on a constant population, ultimately lowering the future energy demand due to energy measures in the building stock. On the other hand, it is likely that the population in Longyearbyen will increase in the future, based on the fact that the population increased with about 30 people annually from 2010 to 2019, an annual increase of about 1.7% [12]. If this growth continues, the population will increase to about 3500 residents in 2050. It is assumed that new residents will have the same need for transport as the existing residents, thus increasing the demand for vehicle-kilometres with 1.7% annually. Population growth must lead to new buildings in Longyearbyen due to the already stressed housing market as discussed in the specialization project [3]. As new buildings are likely to have a significantly lower heat demand as discussed in section 4.3, the heat demand is increased by 0.5% annually according to the base projection. The electricity consumption in Longyearbyen is closely connected to the industry, so it is likely that population growth will not affect the electricity demand linearly. The assumed growth is set to be 1% annually.

**Table 5.1:** Energy demand with population growth

| | 2020 | 2025 | 2030 | 2035 | 2040 | 2045 | 2050 |
|---|---|---|---|---|---|---|---|
| Heat demand [GWh] | 58.88 | 58.21 | 57.47 | 56.64 | 55.75 | 54.77 | 53.70 |
| Electricity demand [GWh] | 42.93 | 46.25 | 35.88 | 37.71 | 39.63 | 41.65 | 43.78 |
| Total transport demand [MVkm] | 24.07 | 26.18 | 28.49 | 30.99 | 33.72 | 36.68 | 39.91 |

Table 5.1 shows how the energy demand will change in B-G. The demand for transport increases with about 65% from the base demand in 2020, while 2050 demand for electricity is about 2% larger than in 2050. This is caused by the large reduction in electricity consumption between 2025 and 2030 as the power plant and coal mine are closed. The total heat demand is reduced by about 10% in 2050 from 2020, due to the renovation of old housing units discussed in section 4.3.1

### 5.5.2 The base scenario with increased costs of wind turbines (B-COST)

As discussed in section 4.7, costs related to RES and storage technologies has fallen drastically the past years. The projected costs for all technologies used in the model has some uncertainty related to it, but especially the ones describing renewable energy sources. On the other hand is diesel generators, a robust and mature technology with small opportunity to reduce cost significantly in the future [42]. In the base scenario with increased costs of wind turbines (B-COST), analysis are preformed with a 20% increase in CAPEX and OPEX for wind power related to the costs presented in table A.1.

### 5.5.3 The base scenario with reduced CF of wind turbines (B-CF)

A key aspect in off-grid energy systems, and especially remote arctic systems like Longyearbyen is to maintain the security of supply [1]. The challenge of relying on RES in a small system like in Longyearbyen is that the energy produced from these sources can vary between years (and days), and therefore not supply a sufficient amount of energy in certain years or periods. The model is therefore investigated with a 15% reduction in CF according to table A.1 for wind turbines to investigate how a year with low wind will affect the installed capacity.

### 5.5.4 The base scenario with bi-facial solar PV modules (B-BiPV)

The production profiles and capacity factors utilized in the presented scenarios are based upon simulations in PVsyst conducted with single sided fixed PV modules. The specific production and therefore the CF could be increased with bi-facial modules. These modules also utilize reflected irradiance on the backside of the modules. Thorud et al. [4] analysed bi-facial modules combined with a tracking device and obtained a specific production of $P_{spec}$ = 1097 kWh/kW$_p$. The south facing described above on the other hand has $P_{spec}$ = 699 kWh/kW$_p$. The alternative with tracker also leads to a changed production profile, and the south facing and tracker are compared in fig. 5.1. The fixed modules has larger peaks, while the tracker solution distributes more of the production over the day. A clear drop in production around noon is visible in the tracked solution.

The bi-facial modules with trackers produces about 50% more energy than the fixed modules used in the scenarios. Costs related to the two different systems are more or less equal, meaning that PV is more likely to be favourable in the base scenario with bi-facial solar PV modules (B-BiPV).

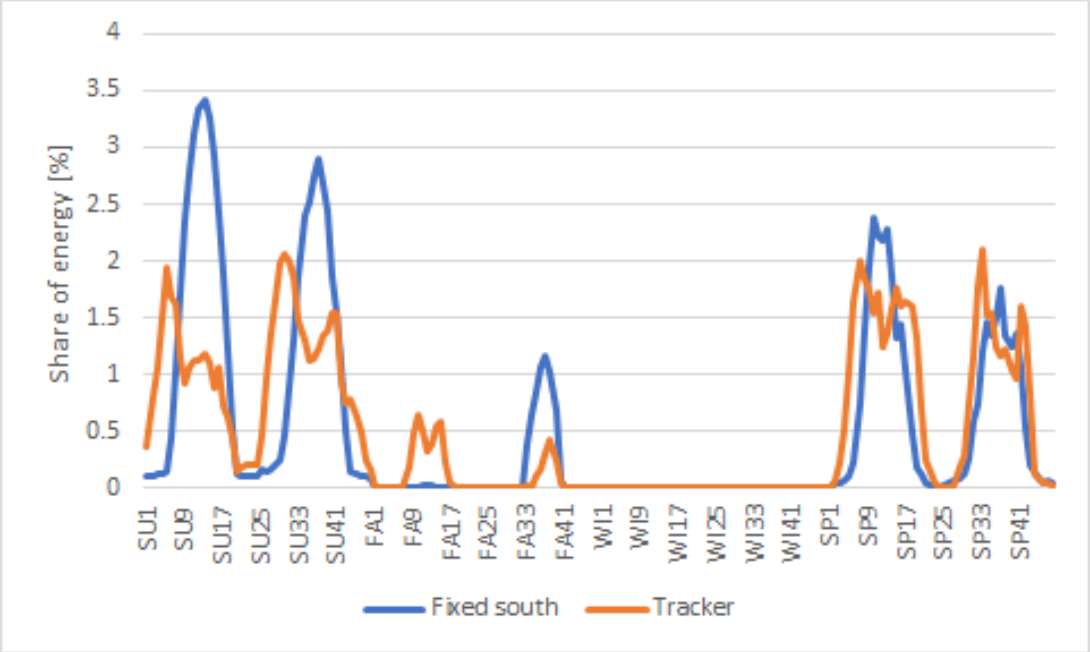


**Figure 5.1:** Comparison of production profile from fixed and tracked PV module

Chapter 6

# Results

## 6.1 General results

All scenarios have at some point installed electric radiators. This is the only technology covering the end heat demand directly, without going through the district heating system. Energy efficiency measures are also implemented in all scenarios, reducing the end heat demand from the demand projection discussed in chapter 4. The end heat demand for all scenarios are shown in fig. 6.1. As described in chapter 4, the DHS is modeled with a fixed operating cost relating to its installed capacity. This capacity is declining in all scenarios, thus reducing operating cost related to the operation of the system. In an actual system, the operation and maintenance costs are related to the length and type of pipes [71]. A reduction of DHS capacity in the model would therefore indicate that buildings should be disconnected from the system, decreasing the total length and thus operating costs. As all buildings in Longyearbyen have a heating demand- disconnected buildings must have electric radiators. This thesis does not cover a plan of how to disconnect buildings, but the results indicate that it would be profitable with the current costs related to the district heating system. It is assumed that the electricity grid is robust enough to handle the increased electricity consumption for direct heating without any additional reinvestment or increased operation and maintenance costs.

All diesel vehicles are replaced with EVs at the end of their lifetime in all scenarios (ISO replaces all vehicles with EVs in 2020 as no diesel is supplied). The EVs consumes 6.63 GWh electricity annually, mostly by charging during night. It is assumed that the charging demand is handled by the existing electricity grid without reinvestment [2].

The model is as explained in section 2.2 minimizing the total discounted costs while supplying an sufficient amount of energy at at all times. Figure 6.2 show the total discounted costs for all scenarios. It is observed that the total costs in B and BNC are about the same. It is also evident from fig. 6.2 that wind is the most economic technology. The isolated case is significantly cheaper than NWI and NWC, but more expensive than B and BNC.

The results from the different scenarios indicate that a system based on renewable energy sources is the optimal solution. Figure 6.2 show the annual $CO_2$ emission from all scenarios. The emissions related to 2020 and 2025 is present in all scenarios, and more than 90% are related to the operation of the coal-fired power plant, while the remaining emissions are from cars with

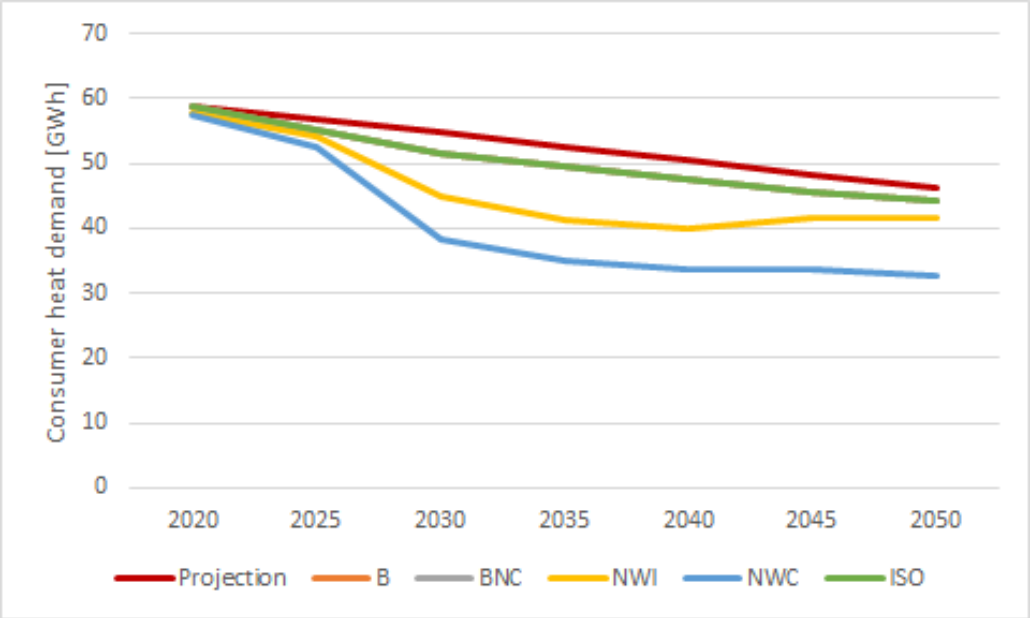


**Figure 6.1:** End consumer heat demand for all scenarios after energy efficient measures.

internal combustion engines. However, the large reduction in emission in B from 2025 to 2030 show that a low emission solution is preferred even without constraints related to the emissions. The only scenario with significant emissions after 2025 is NWI, indicating that wind is crucial to reduce the emissions of $CO_2$ in the most cost-efficient way.

In all scenarios, there are time-slices with an overproduction of electricity that leads to curtailment. This is a known issue of systems including large shares of variable renewable energy sources, as they are uncontrollable. 10 to 20% of the energy produced from wind and solar PV is curtailed annually in the different scenarios. Wind power is curtailed during all seasons except spring. As seen in fig. 4.1, the production from wind is lower during spring and summer, while the heat demand is larger during spring. Spring therefore seems to be the most stressful season in a wind depended system. Most solar energy is curtailed during summer as expected by the production profile, and also some during fall. The annual curtailed energy is specified in Appendix B, and is not visible in the energy flow charts for B, BNC, ISO and NWI. Here, the plotted energy flow is in balance since the plot is of utilized energy from wind and solar PV. The output from the fuel cell in NWC on the other hand represents produced energy- due to a technicality in the modeling approach.

None of the scenarios invests in seasonal storage.

## 6.2 The base scenario (B)

The base scenario shows an increase in installed production capacity for electricity until 2050 as shown in fig. 6.3. In 2030, all electricity capacity is renewable, almost exclusively made up by 27 MW wind power. The small existing amount of PV is still present, and the coal power plant has shut down as discussed in chapter 4. With a lifetime of 20 years for the wind turbines, the capacity in 2050 indicates a reinvestment in the technology. In 2050, 2 MW of south-facing PV is also installed. As the production capacity is solely renewable, it is expected that the total

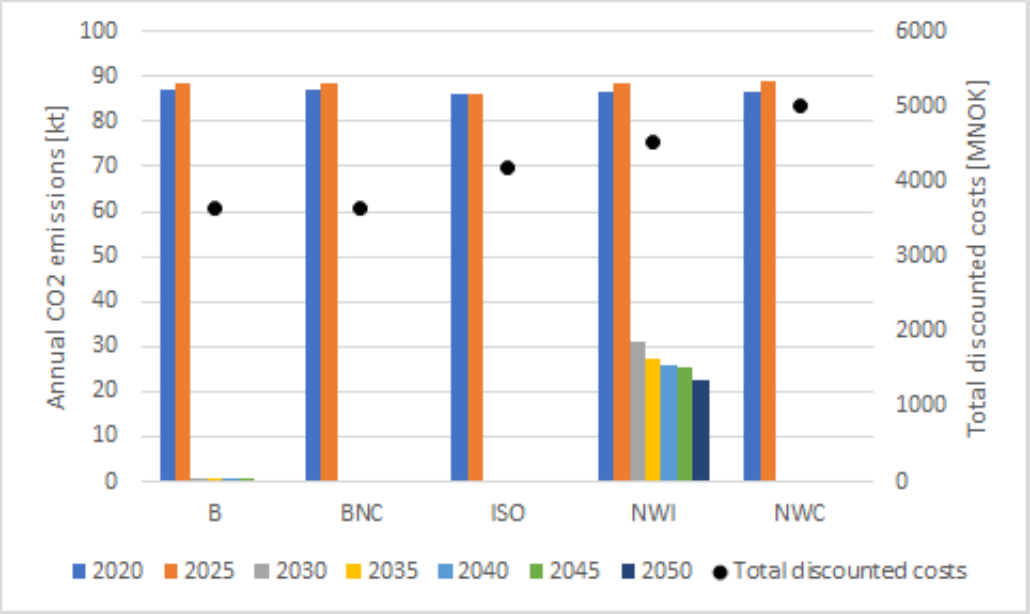


**Figure 6.2:** Annual $CO_2$ emissions and total discounted costs in all scenarios

production capacity is increased because of the low CF of RES.

On the opposite, the production capacity for heat is more than halved to 2050. It is observed that heating capacity is fully electrified in 2050, with roughly 30% share of electric radiators-supplying heat directly in the buildings. The remaining capacity is made up of energy-efficient heat pumps supplying the DHS. In 2030, half of the existing oil boilers (Fyrhus) is present, as well as a 0.8 MW electric boiler.

In addition to the generating units described over, a battery of 8 and 13 MWh is installed in 2030 and 2050 for short term electrical storage and a thermal storage tank, Thermos of 1 MWh in 2030 and 2050. No investments are made in year 2020.

### 6.2.1 Energy flow 2020

The figures presenting the flow of energy in the various scenarios and years in the following sections consists of an area above and beneath the x-axis. The area beneath the x-axis is consumed energy while the are above is delivered energy. The x-axis represents the 192 time-slices of the model described in section 3.1, where FA represents fall, SP spring and so on. The y-axis is the energy input/output for each hourly time-slice, in GWh/h. Note that the power output in these figures are not directly related to the real system, but the energy output is. The power output must be scaled according to the number of time-slices, and is 8760h/192h= 45.625 times lower than stated in the figures. The colors related to each technology is kept constant in all figures, making them easier to compare. The scaling on the y-axis however, is not kept constant due to differences in production profiles. The dark grey area beneath and closes to the x-axis, the actual end demand of electricity and heat after energy efficient measures, based on the assumptions described in chapter 4. The demand is generally lower than produced energy, due to losses in transmission. The results in this chapter are mainly reported in year 2020, 2030 and 2050, while detailed tables with production capacity and produced energy are found for all cases in Appendix B.

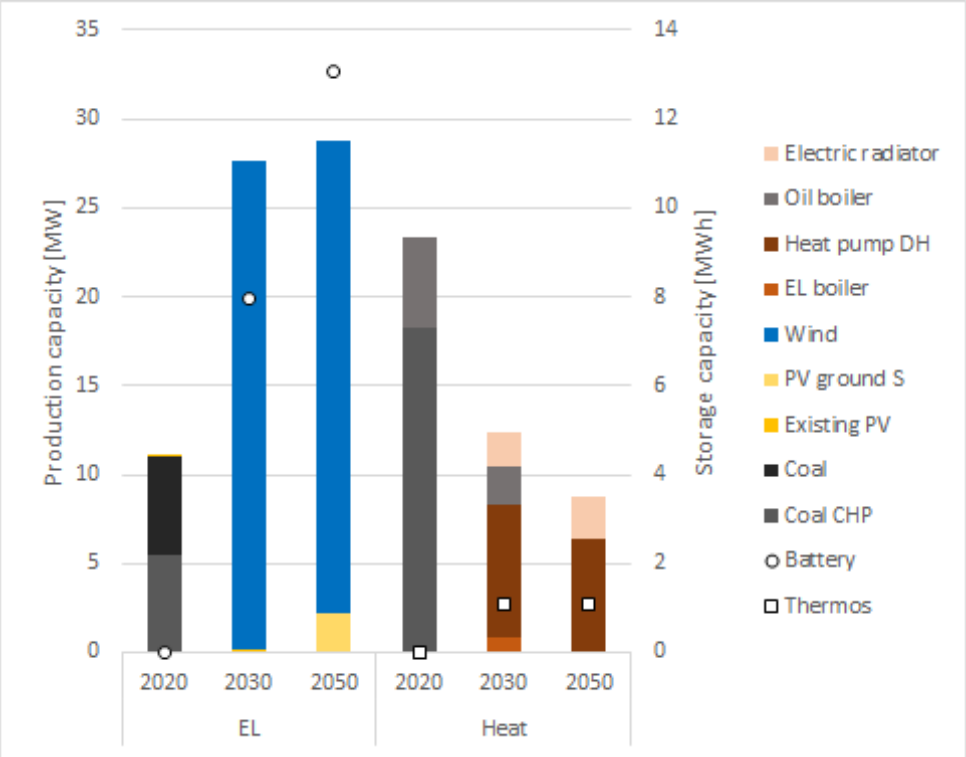


**Figure 6.3:** Installed production capacity (B)

As year 2020 is consisting of the existing power plant described in section 1.3, the production profiles seen in figs. 6.4a and 6.4b is as expected. The coal CHP delivers the entire heat demand by varying the output. The CHP is modeled with a fixed electricity-to-heat-ratio, so the electricity production from the CHP has the same pattern as for heat. Thus, the second coal turbine varies its output to cover the differences in electricity demand. The production from the installed PV is barely visible during daytime in spring and summer with a total of 80 MWh, and the few existing EV consume about 30 MWh, not visible beneath the x-axis. In both figures, it is evident that more energy is produced than consumed, caused by the transmission losses discussed in section 4.3.1. It can be directly observed that loss related to heat transfer is higher than for electricity.

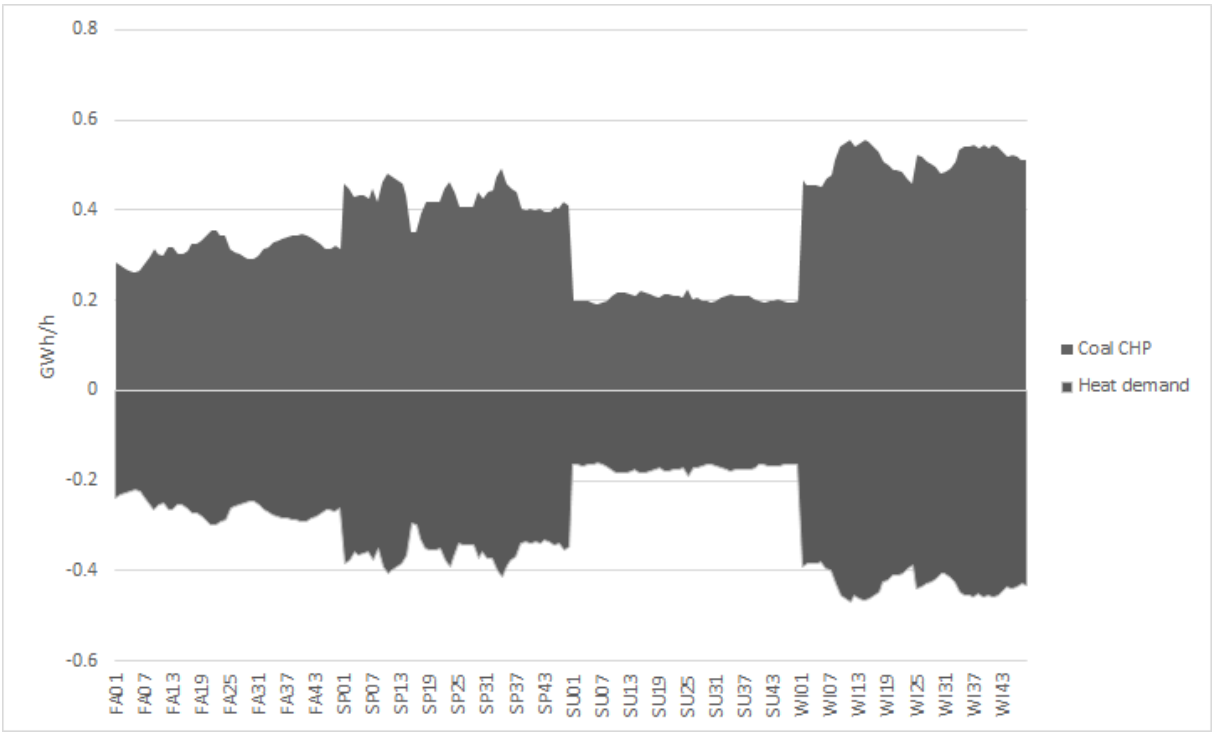


**(a)** Heat flow 2020 (B)

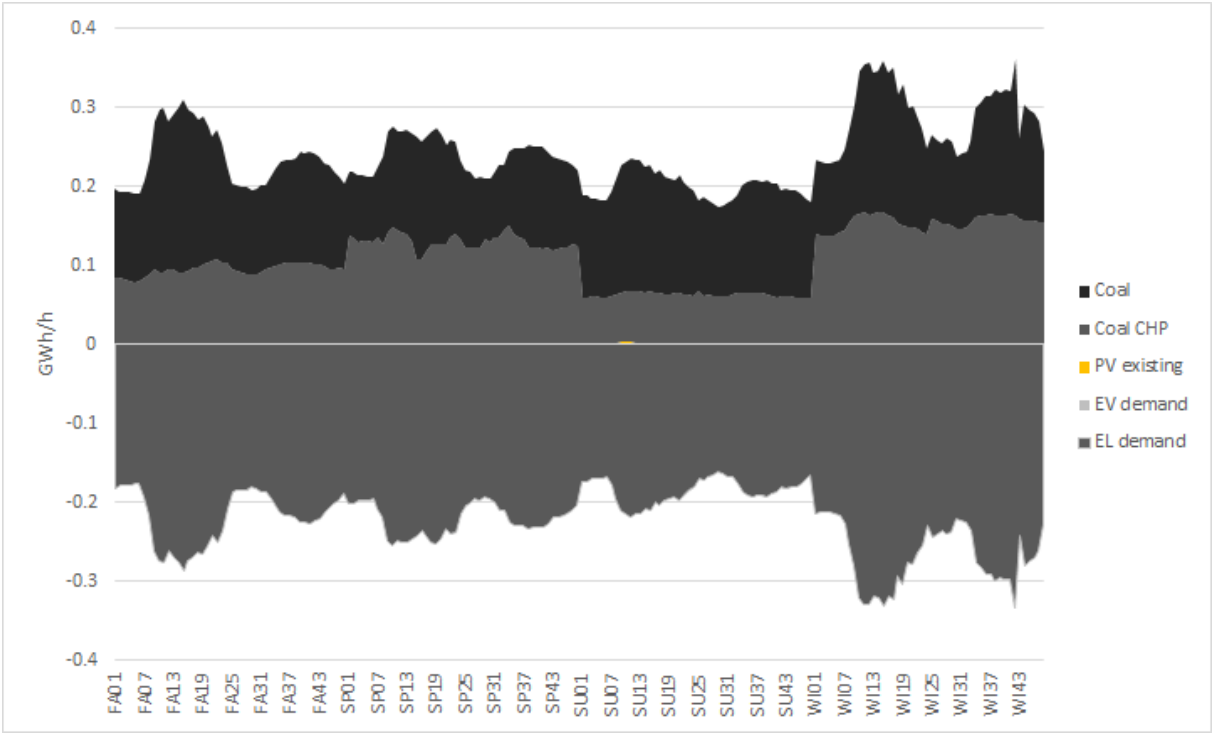


**(b)** Electricity flow 2020 (B)

**Figure 6.4:** Energy flow 2020 (B)

### 6.2.2 Energy flow 2030

By comparing fig. 6.5b to fig. 6.4b it is evident that the energy system has changed. Wind turbines are now, as expected based on the installed production capacity, dominating the electricity production, and more electricity is consumed. The wind turbines are therefore producing significantly more electricity than the coal turbines in 2020. Another evident characteristic, is that the production profile is independent of the load profile, and several large peaks are observed in wind production. These peaks are clearly fed into the battery, having an equal pattern beneath the x-axis. The stored energy is provided in times with low production, clearly shown around hour SU07. Here, the production from the wind turbines are lower than the specific electricity demand, meaning that the load would have been unmet if there was storage technology present.

The charging demand for EVs is visible, following the charging profile shown in fig. 4.4, along with a larger amount of electricity going into heating technologies. The amount of electricity provided for heating is roughly the same during fall and spring, but a larger share of the electricity is supplied to the heat pump during spring.

The two summer days have very different production profiles for wind, while the demand for both heat and electricity is rather stable. It is observed that the electricity is provided to the heat pump during the periods with low wind and to the electric radiators and el boiler during the high production. This is evident when investigating summer hours in fig. 6.5a. While the heat demand is constant, the heat is exclusively provided by the energy-efficient heat pump from SU25 to SU40, which are directly observed as low wind periods in fig. 6.5b. It seems like electric boilers and radiators are used to curtail excess electricity, a known way to increase stability of systems with large shares of wind power [72]. Some thermal energy is stored during peaks from the heat pump (FA 31) and shifted to cover demand in other periods. Oil boilers are used to cover peaks during spring and winter, with a total of 2.6 GWh or about 4.5% of the total heat production. It is also observed that the electric boiler is utilized during the same periods as the electric radiators.

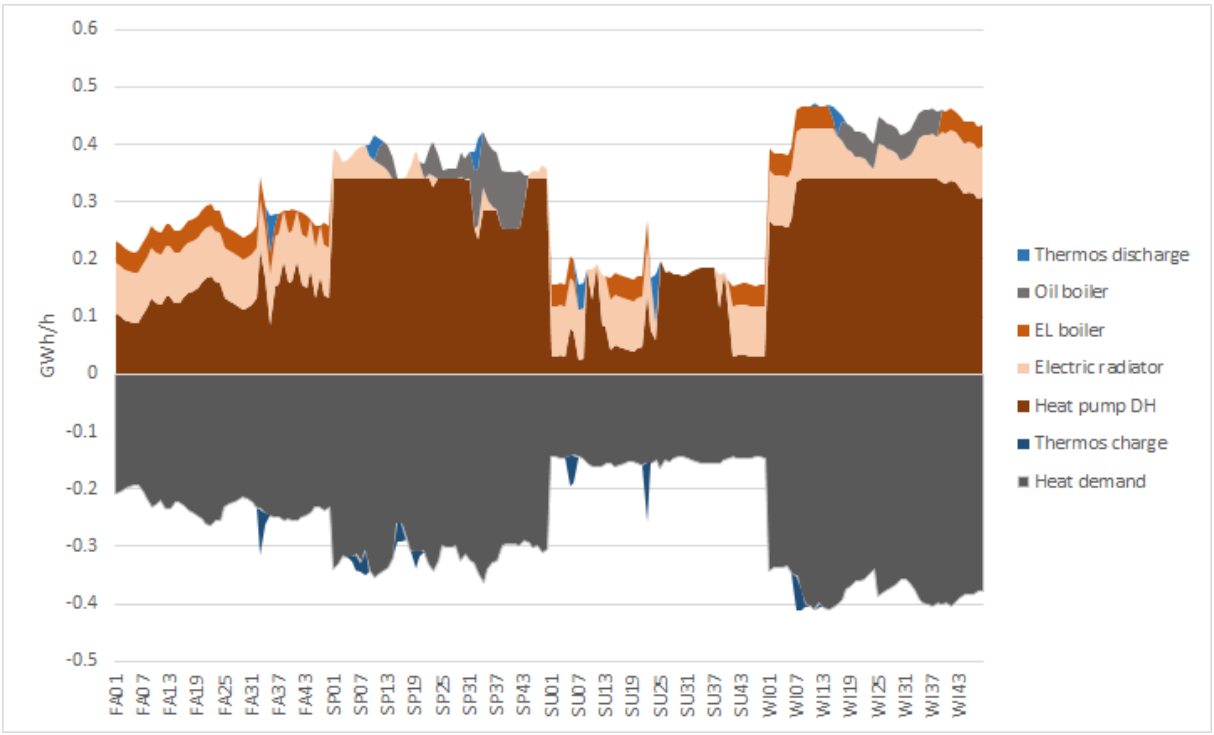


**(a)** Heat flow 2030 (B)

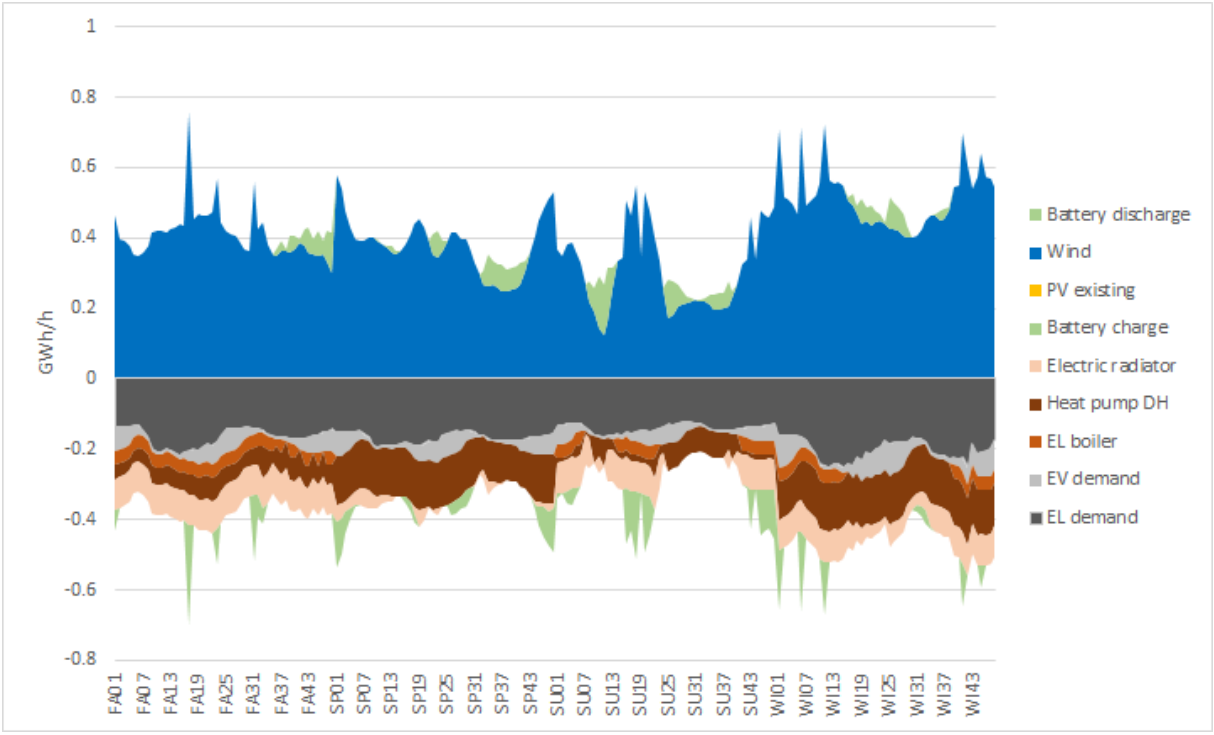


**(b)** Electricity flow 2030 (B)

**Figure 6.5:** Energy flow 2030 (B)

### 6.2.3 Energy flow 2050

The energy flow in 2050 is rather similar to the one in 2030, as expected based on the installed production.. The most evident difference in electricity seen in fig. 6.6a is that south-facing PV is contributing during summer. The peak wind production is still fed into the battery, distributing the energy to times with less production.

Figure 6.6b shows that all heat is now produced by the heat pump and radiators. There is also a smaller difference of how the heat is delivered between the two summer days, with a smaller amount of production in the heat pump. This could indicate that there is a sufficient amount of electricity in the grid. The total heat demand is also lower in 2050 than 2030 based on the baseload projection as well as the extra energy-efficient measures as shown in fig. 6.1.

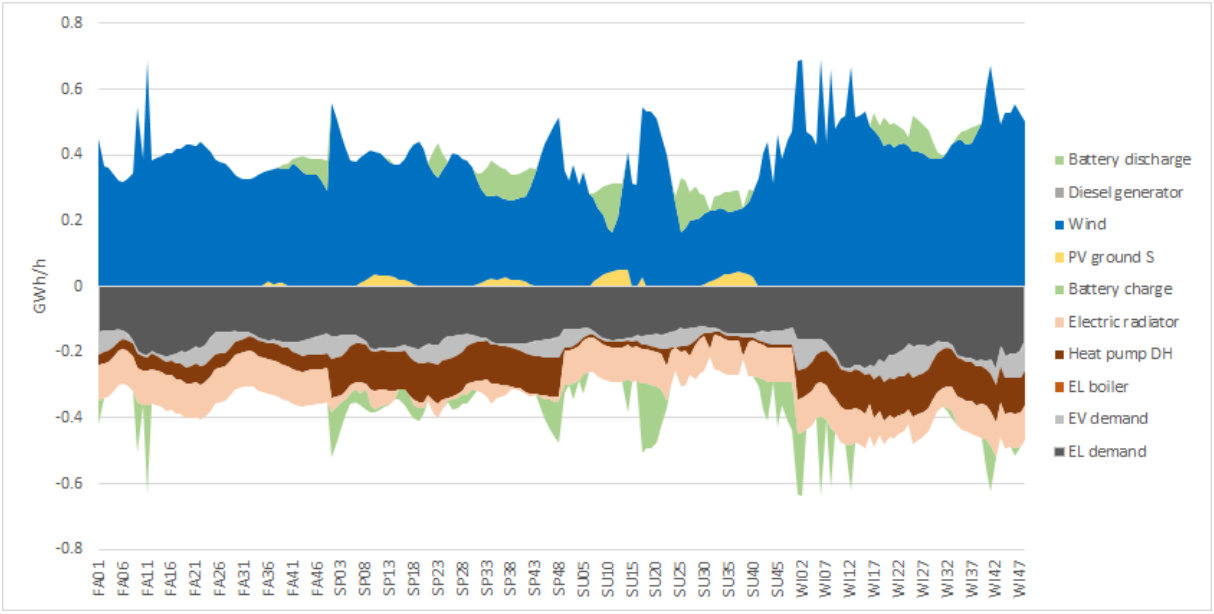


**(a)** Electricity flow 2050 (B)

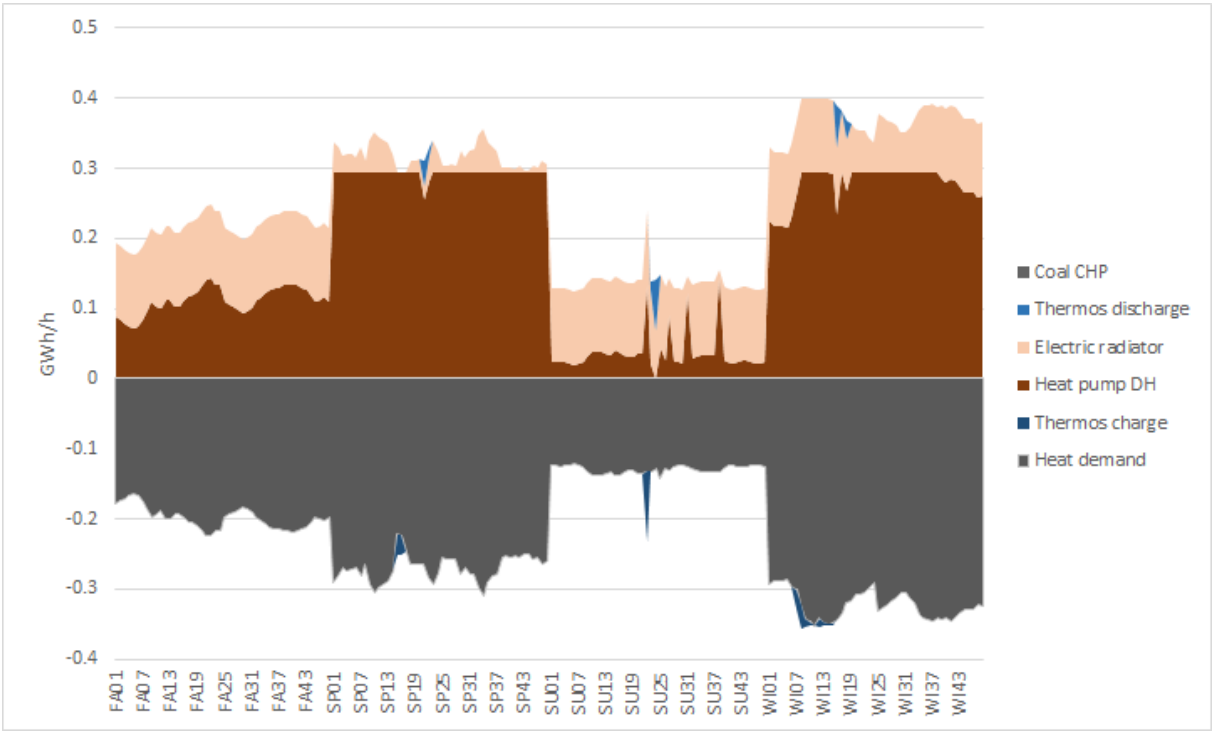


**(b)** Heat flow 2050 (B)

**Figure 6.6:** Energy flow 2050 (B)

## 6.3 The base scenario with no $CO_2$ (BNC)

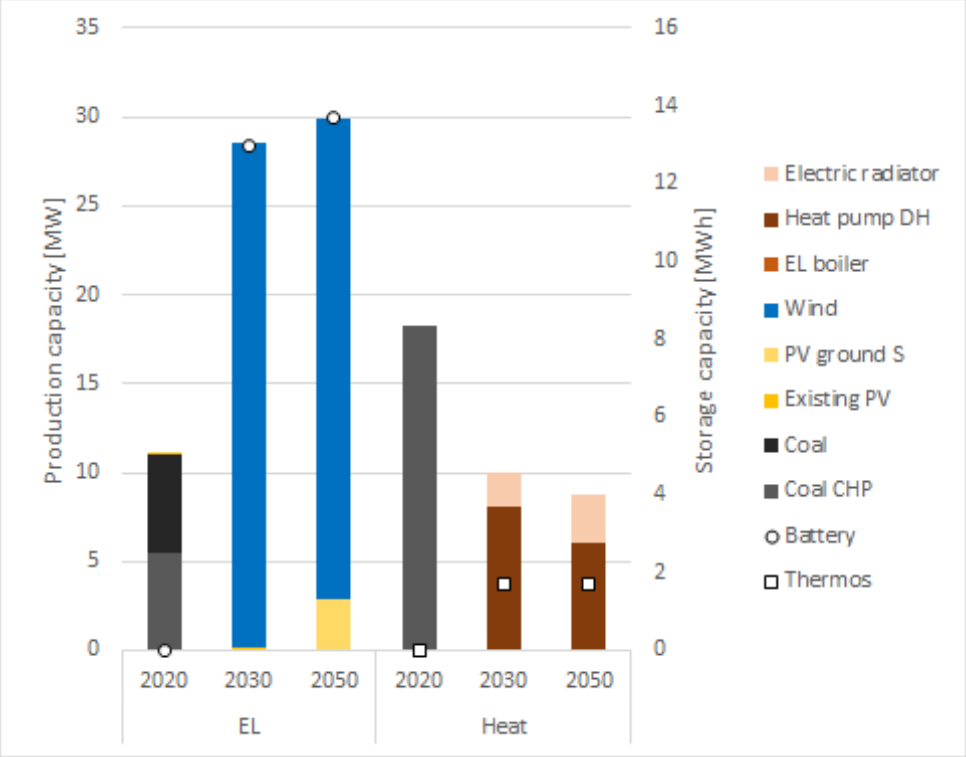


**Figure 6.7:** Installed production capacity (BNC)

The installed production and storage capacity in BNC is shown in fig. 6.7. This scenario has slightly higher installed electricity capacity and storage than B- but the biggest difference is that the oil boiler is not present in 2030 compared with the base scenario shown in fig. 6.3. As $CO_2$ emissions are not allowed after 2025 in this scenario- that is expected. There is no electric boiler installed in 2030, but a small boiler of 59 kW (not visible in the figure) is present in 2050.

### 6.3.1 Energy flow

As the installed production capacity is similar in BNC as in B, the energy flow is expected to follow the same pattern. The energy production is equal to B in 2020 while some changes are evident in heat production in 2030. As there is no oil boiler present, the load covered by this technology is replaced by electric radiators and the slightly larger heat pump as shown in fig. 6.8. The increased use of electricity for heat production is covered by the increased share of wind turbines.

The heat flow in 2050 is shown in fig. 6.9a, and show a reduction of the utilization of heat pump, especially during summer. As discussed in section 6.2, this indicates that there is surplus electricity in the system. The total installed electric production capacity in 2050 is larger than in 2030 (constant electricity demand), emphasizing this trend. The small electric boiler is used for peak load during fall and winter. Electricity flow is more or less equal as in B, but with higher production from wind and solar, and more flow into the electric radiators. The flow is shown in fig. 6.9b.

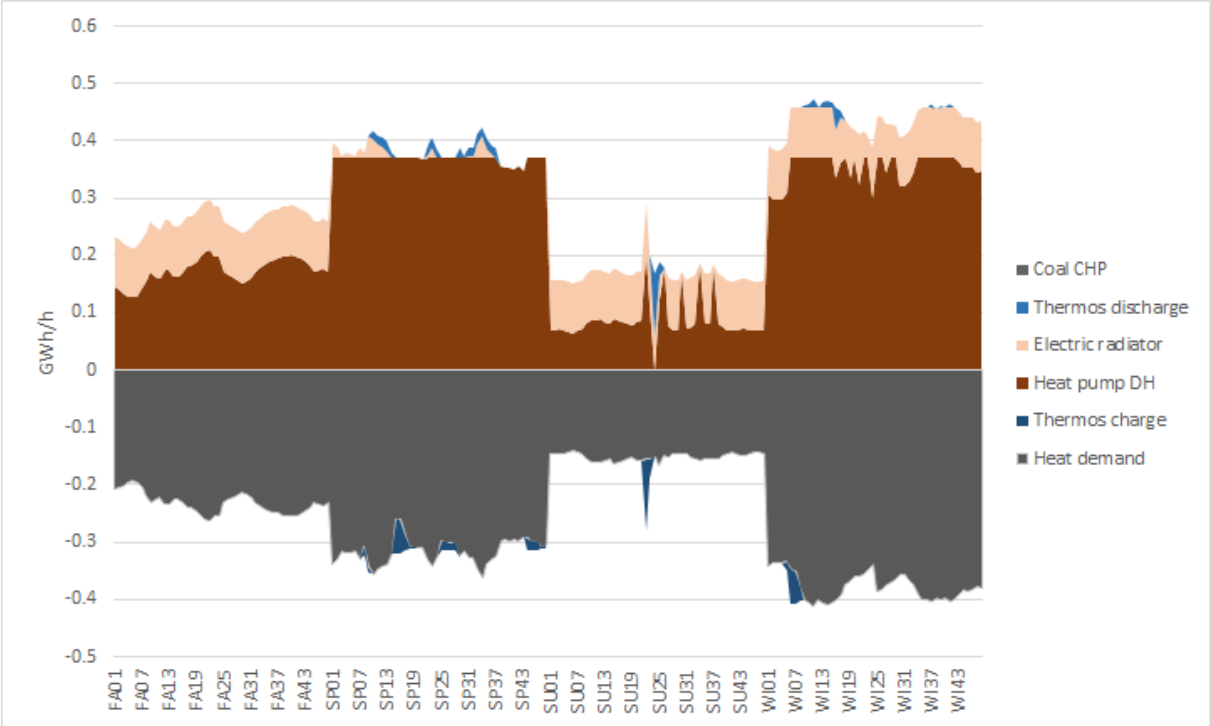


**Figure 6.8:** Heat flow 2030 (BNC)

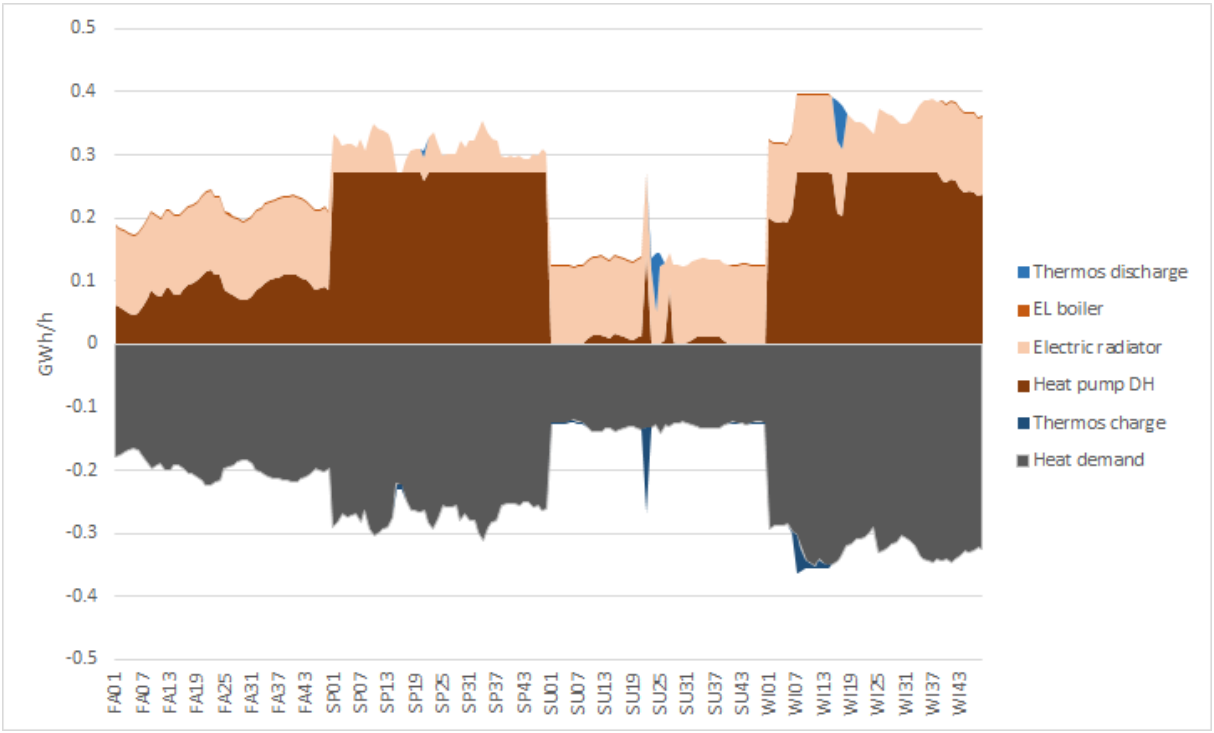


**(a)** Heat flow 2050 (BNC)

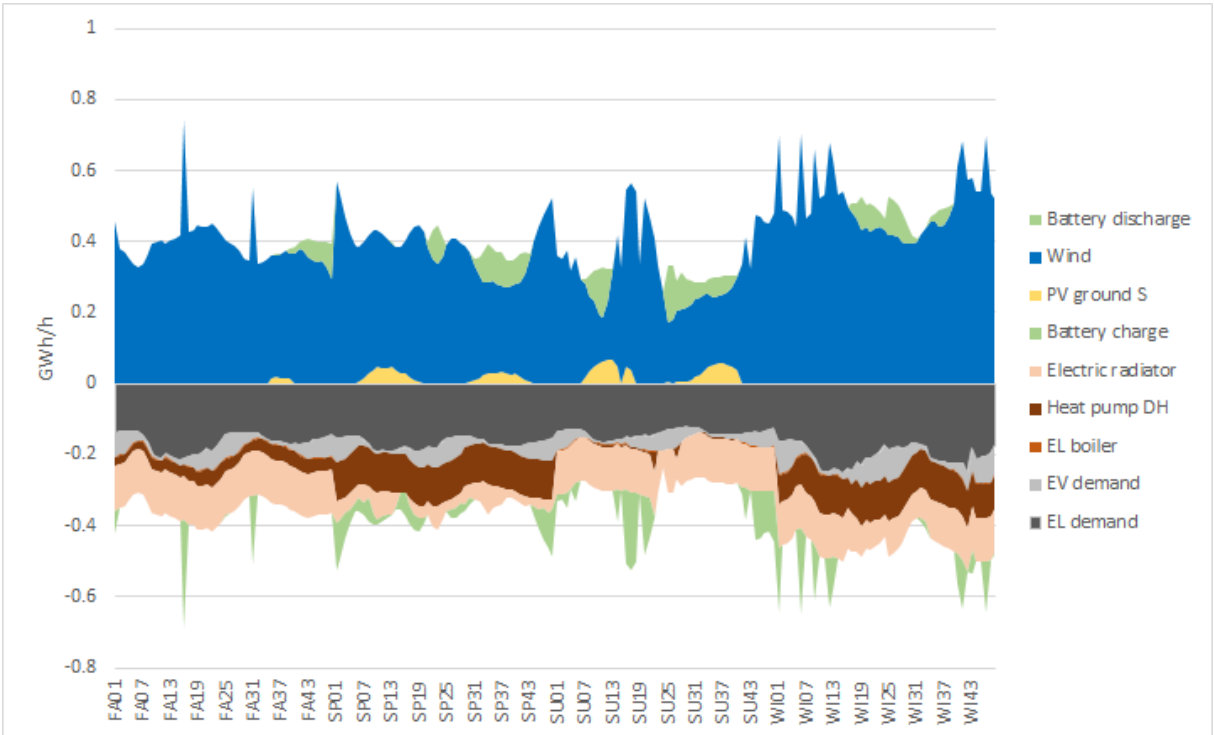


**(b)** Electricity flow 2050 (BNC)

**Figure 6.9:** Energy flow 2050 (BNC)

## 6.4 The isolated scenario (ISO)

The ISO and BNC are almost equal regarding installed capacity, except that there is a 1 MW investment in wind already in 2020 as shown in fig. 6.10. This production capacity is utilized to cover the electric transport demand that is present already in 2020 as diesel import is restricted.

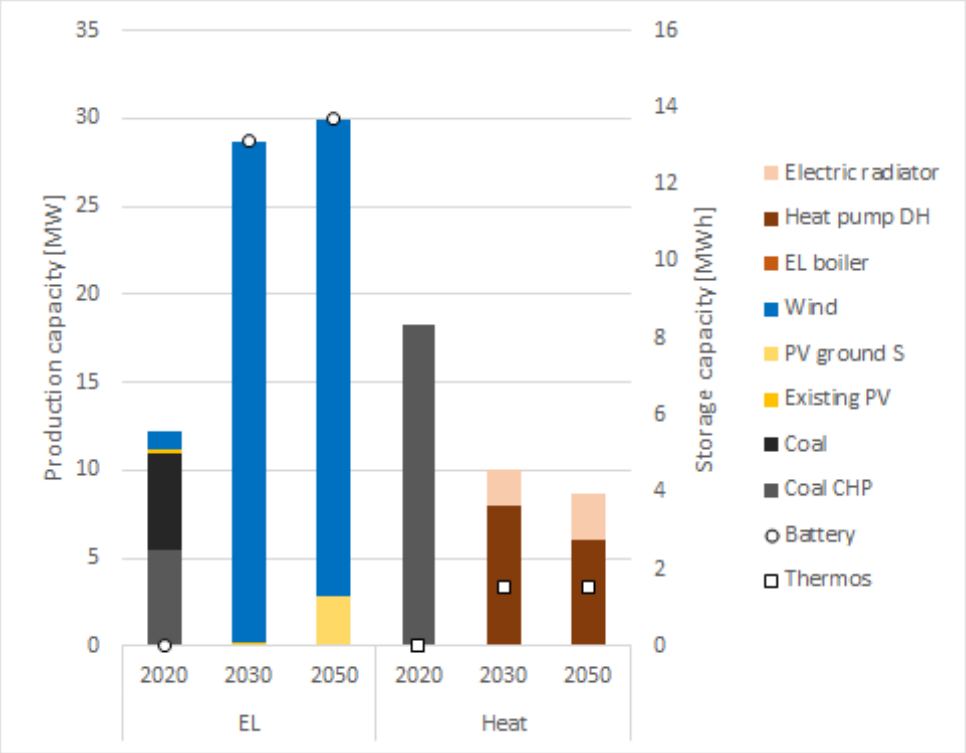


**Figure 6.10:** Installed production capacity (ISO)

The electricity flow in 2020 is therefore different than in B and BNC, and shown in fig. 6.11. The coal turbine is still reacting to the changes in the electricity demand, as well as the variation in EV demand, clearly visible under the y-axis. It is observed that the EV demand increases during winter, and is smaller during summer.

The heat flow for 2020, as well as the electricity and heat production in 2030 and 2050, are more or less equal to BNC and are thus not shown.

## 6.5 Similarities in B, BNC and ISO

The base scenario (B), base scenario with no $CO_2$ (BNC) and isolated scenario (ISO) have more or less identical energy flow from 2030 and to the 2050, all heavily relying on wind power for electricity production and heat pump for heat production as seen in sections 6.2 to 6.4. Investment in energy-efficiency measures are equal in the three scenarios, leading to an equal heat demand as shown in fig. 6.1.

The main difference from B to BNC is that the 4.5% of supplied heat from the oil boilers in 2030 is replaced by the heat pump. To replace the heat produced with fossil fuel, 1 MW additional wind power, along with 0.4 MW increased heat pump is installed. When looking at the total

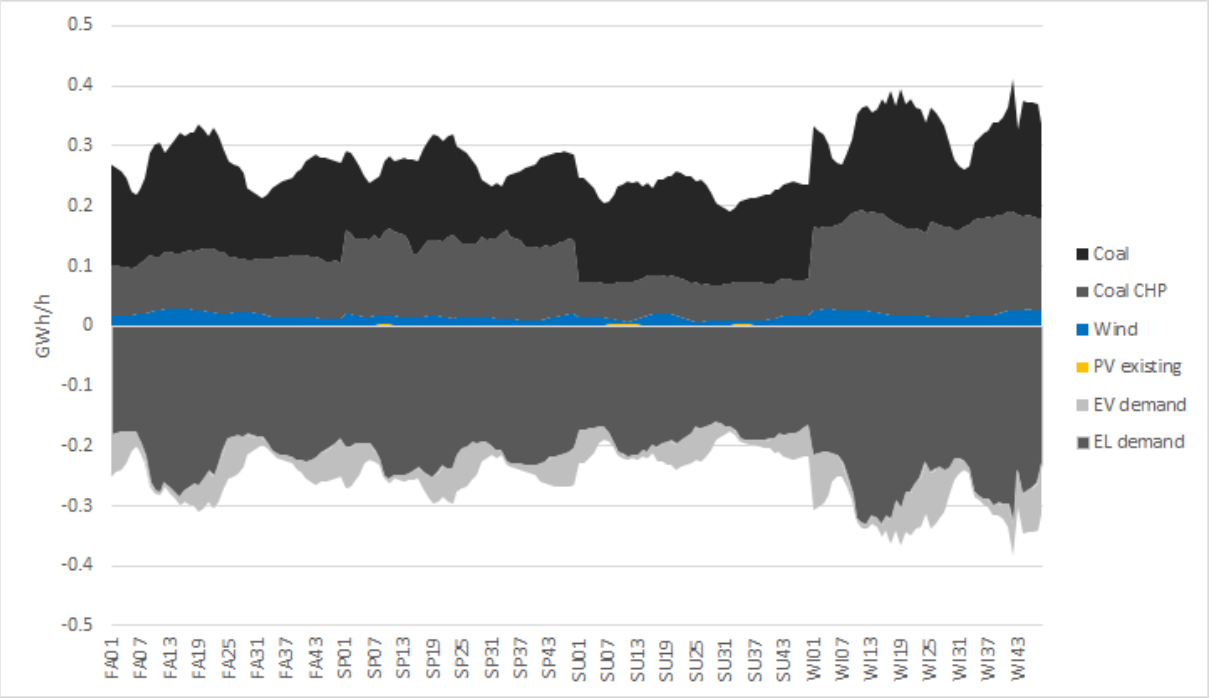


**Figure 6.11:** Electricity flow 2020 (ISO)

discounted costs related to B and BNC from fig. 6.2, the difference between the restricted BNC and the solely optimal based on the input data only 4.4 MNOK or 1%. This is clearly an indication that solutions with low amounts of $CO_2$ emissions are economically feasible after 2030. The energy flow in B, emphasises this by the large electrification of heating, covering only 4.5% of the 2030 heat demand with fossil fuel. The electricity sector is solely based on RES after the existing power plant is closed. The low amount of diesel used for heating represents 0.77 kt $CO_2$ in 2030, rapidly decreasing towards zero in 2050. As clearly shown in fig. 6.2, the emissions from 2030 in B is negligible compared to the emissions from the existing power plant.

ISO differ from B and BNC by an 1 MW investment in wind in 2020. The energy produced from this investment is utilized to cover parts of the demand of EVs which deliver the entire transport demand already in 2020, as import of diesel is restricted to zero. Costs related to this investment, as well as investing in EVs in 2020 explains the increased total costs in ISO towards B and BNC. As shown in table A.1, the CAPEX of wind turbines are expected to decrease in the future, making an investment in 2020 more expensive than in 2025. In addition to this, expenditures that occur early in the modelling horizon has a larger impact to the total discounted cost because of the future value of money is lower than the present, partly explaining the large increase in total discounted costs. The total discounted cost of ISO is about 15% higher than B. If import of diesel is allowed for the existing vehicles, the solution of ISO becomes identical to BNC.

A small amount of ground-mounted solar PV is installed in B, BNC and ISO toward the end of the modelling horizon, partly replacing the early investment in wind turbines who has reached the end of their lifetime. However, the wind turbines provide more than 97% of the utilized electricity in 2050 in all three scenarios, emphasizing the dependency of wind power in the solution.

Wind power is as mentioned curtailed in all seasons except spring. This indicates that the optimal

wind power capacity is of a size that covers the spring load. As production is rather small during spring, and load rather high (easiest observed in figs. 4.1 and 4.3), spring seem to be the stressful season in the system. Sizing the wind turbines for the most stressful season leads to the curtailment of energy in the other seasons - as long as no seasonal storage is installed. The lack of a long-term storage system in these scenarios indicate that it is more cost-efficient to curtail energy than to store it. The curtailment of energy indicates that the size or numbers of wind turbines could be decreased if seasonal storage was implemented.

There are some concerns regarding the solutions including wind. The first and most obvious is that close to 30 MW of wind power close to Longyearbyen will be visible and seem like a huge impact in the Arctic nature. The wind data used in the analysis is from Platåberget, just west of the city centre and is not actual measured data. This means that there is uncertainty regarding the actual production from placing turbines in the area, that could both increase and decrease the energy output on an annual scale, in addition to treating the wind production deterministic as discussed over. Secondly, soil conditions surrounding Longyearbyen is poor [2]. This is likely to have an impact on the CAPEX of wind turbines in particular, needing severe civil work in construction and foundation. Foundation and civil work related to the construction of roads and other infrastructure traditionally make up to 16% of the total CAPEX [73]. Another concern is the transport of the wind turbines to Svalbard, which will be expensive due to the distances involved. Costs related to wind power is according to International Renewable Energy Agency [65] generally very site-specific, and the cost projections utilized in this thesis does not take these factors into account and is therefore likely to be in the lower range of what is expected. Note that these uncertainties also affect all other installations and technology choices, however, it is likely to have a larger impact on wind turbines than for instance solar PV, due to the dimensions of wind turbines. Both an investigation of ground conditions and actual wind measurements in the suggested hub height should be conducted in the area before deciding upon investment. The other mountains surrounding Longyearbyen could also be of interest for establishing a wind park.

## 6.6 The no wind scenario (NWI)

As the name of the scenario indicates, NWI has no installed wind power. The demand is supplied by the existing power plant in 2020 as B, BNC and ISO, however, the 2030 and 2050 installed capacity is very different. A total of 30 and 70 MWp solar PV is ground-mounted in 2030 and 2050 respectively, along with about 6.5 MW diesel generators. The battery capacity is 22 and 47 MWh. Oil boilers make up most of the thermal capacity in both 2030 and 2050, with an increasing share of heat pump and el boiler. Next to no capacity is installed of electric radiators. A small thermal storage of 0.25 MWh and 1.05 MWh is installed in 2030 and 2050. The use of diesel generators and boilers are related to the $CO_2$ emissions shown in fig. 6.2.

### 6.6.1 Energy flow 2030

By investigating figs. 6.13a and 6.13b it is evident that fossil sources are delivering most of the supplied energy in NWI. The diesel generators cover all load during winter, and most during fall and spring. This emphasises the challenge of utilizing solar power in Longyearbyen- the large variation in solar irradiance between summer and winter. The large battery size is related to the amount of installed PV, feeding the peaks around noon into the battery, and discharging

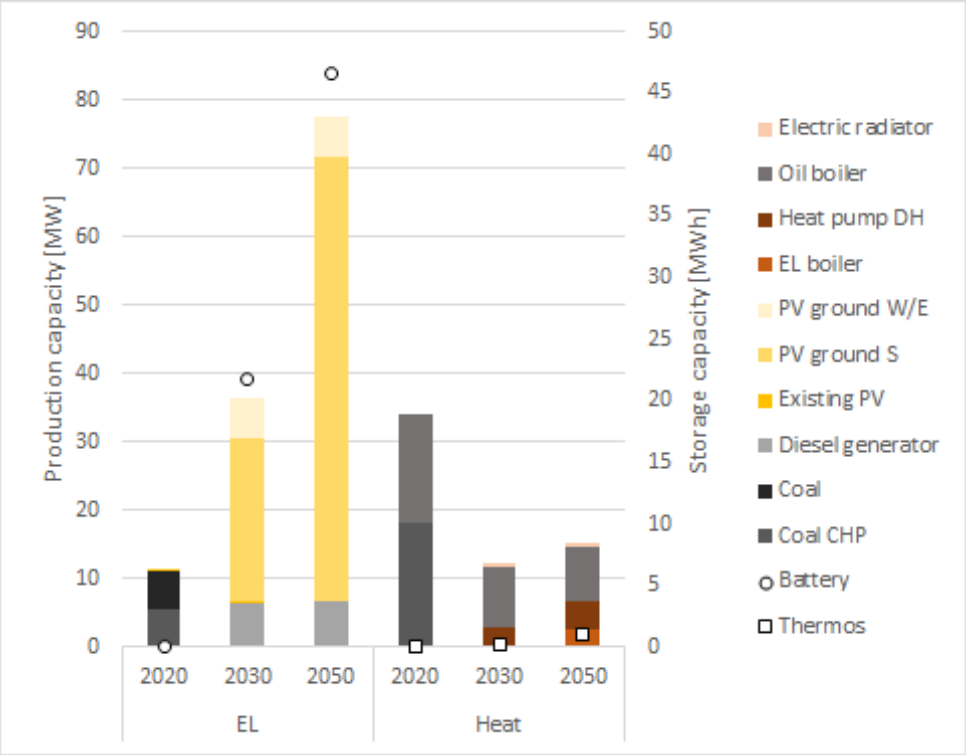


**Figure 6.12:** Installed production capacity (NWI)

during the night. It is also observed that electricity is used for heating in all seasons, practically operating the heat pump with electricity from the diesel generators.

Looking at the heat flow in fig. 6.13b, the heat pump is operating at its maximum capacity almost all year, acting as base production for heat. Summer heat demand is nearly covered by the heat pump, while remaining demand is covered by the oil boiler during the night and electric radiators and El boiler during daytime. The oil boilers cover most heat demand during the other seasons.

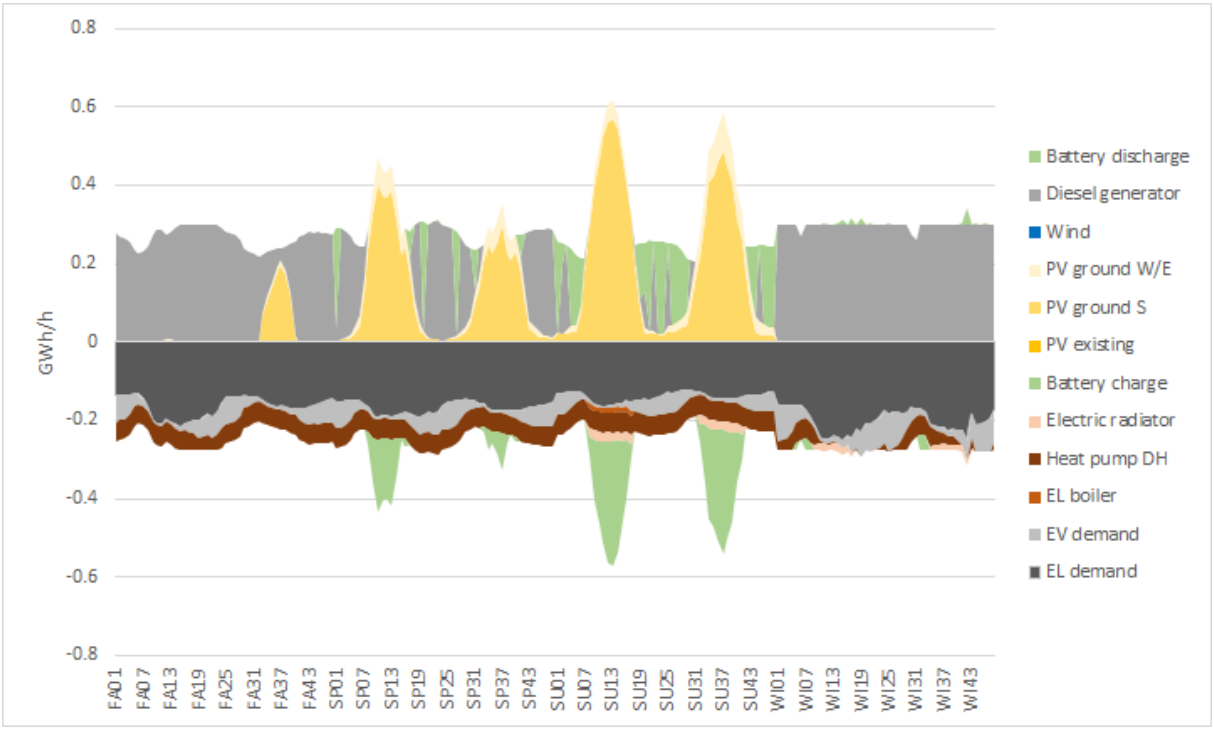


**(a)** Electricity flow 2030 (NWI)

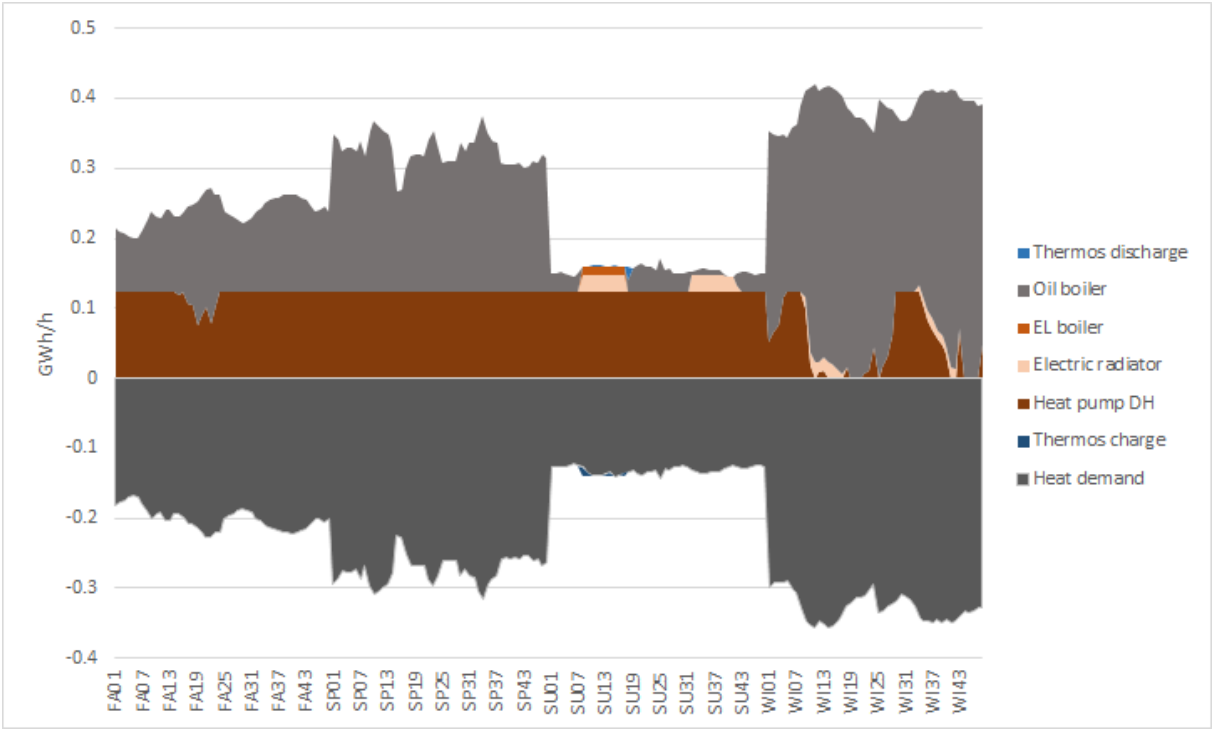


**(b)** Heat flow 2030 (NWI)

**Figure 6.13:** Energy flow 2030 (NWI)

### 6.6.2 Energy flow 2050

The pattern of large solar peaks are even more evident in fig. 6.14a than in fig. 6.13a, and is caused by the large amount of installed PV. Larger peaks of solar production demand a larger battery to handle the fluctuations in production. In 2050, all electricity is produced by solar PV during summer and spring, and shifted to cover the total load by the battery.

Looking at fig. 6.14b, all heat during summer is provided by electric radiators and el boilers, emphasizing the large amount of electricity available in the system during summer. The heat demand is also covered by electric radiators and boilers during daytime the first spring day, utilizing the large amount of electricity from the solar PV. Fall is almost covered by the heat pump, and a small amount of heat is produced in the oil boilers to provide the remaining demand. Most of the winter demand is covered by oil boilers

### 6.6.3 General

Unlike the other scenarios, NWI invests in both south facing and west/east facing modules. The west/east facing modules has lower specific production and thus capacity factor, but a production profile more in line with the load. NWI has by far the largest battery installed of the scenarios, to be able to utilize more of the solar production, produced in large peaks during spring and summer. The solar power is sufficient to completely cover the load during summer and spring in 2050, however, winter operation and large parts of the fall is covered by diesel. In 2030, about 50% of the produced electricity and 60% of heat is covered by diesel. The diesel consumption decreases throughout the time horizon as installed PV capacity increases, and 40% of electricity and 38% of heat is covered by diesel in 2050. 116 GWh and 85 GWh of diesel is imported in 2030 and 2050 respectively. Summer season is completely covered by the PV modules from 2040. As no seasonal storage is implemented, it is impossible to cover the entire load in Longyearbyen only relying on solar PV because of the polar night. However, 18% and 22% of the produced solar power is curtailed during summer in 2045 and 2050 respectively, whilst no electricity is curtailed during spring or fall. This indicates that the PV capacity is dimensioned to cover spring season, similar to the scenarios including wind. If seasonal storage were implemented, this could reduce the diesel consumption by storing the curtailed electricity during summer to other seasons. The absence of seasonal storage indicates that it is beneficial economical to curtail energy, rather than investing in long term storage.

Another challenge related to solar power is that the load is distributed opposite of the solar production. The load is significantly larger during winter (largest variations in heat but also a larger demand for EVs and el demand), when there is no irradiance, and thus no power production from PV. The large investment in PV is therefore not providing energy when the load is at its maximum.

The total discounted costs of NWI is significantly larger than B as shown in fig. 6.2. The total CAPEX and OPEX related to the two scenarios are similar, however the costs related to import of diesel is very different as expected based on the amount. Restricting the capacity for wind turbines to zero increases the total discounted costs with about 24%, and operation is related to an significant increase in $CO_2$ emissions.

NWI has larger investments in energy efficiency measures than B, BNC and ISO, indicating that the cost of heat has increased as more expensive measures are implemented.

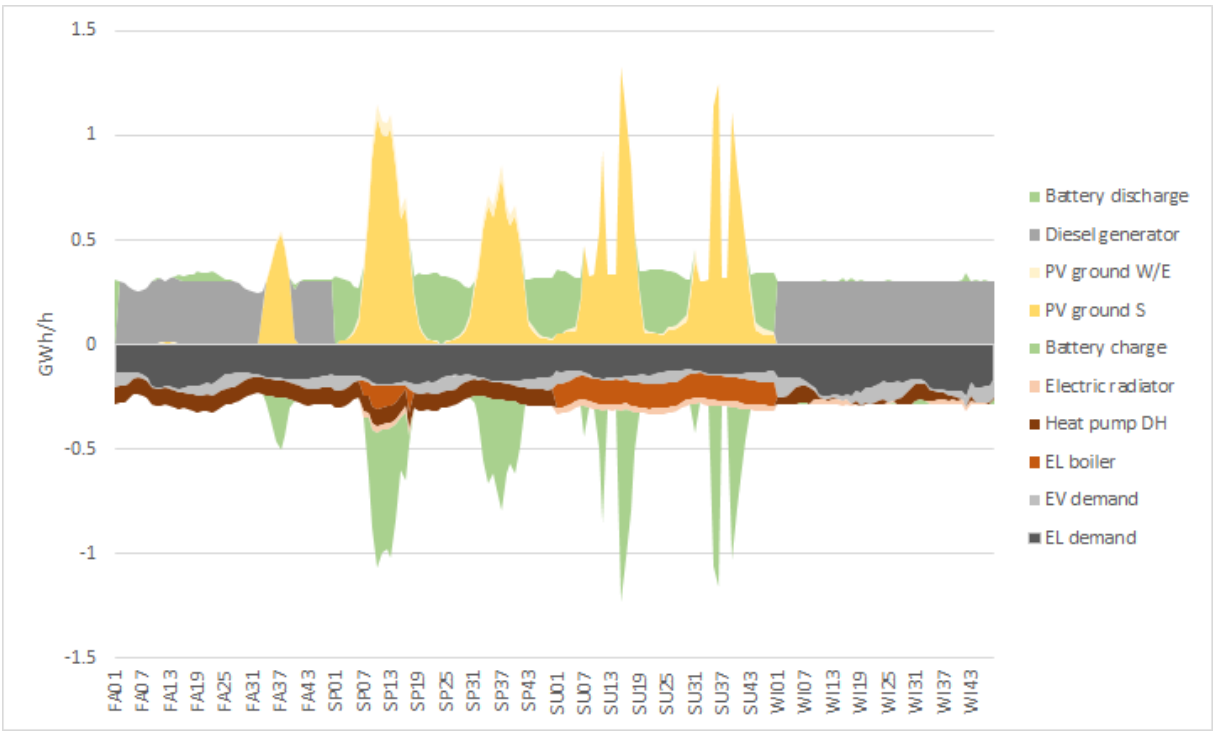


**(a)** Electricity flow 2050 (NWI)

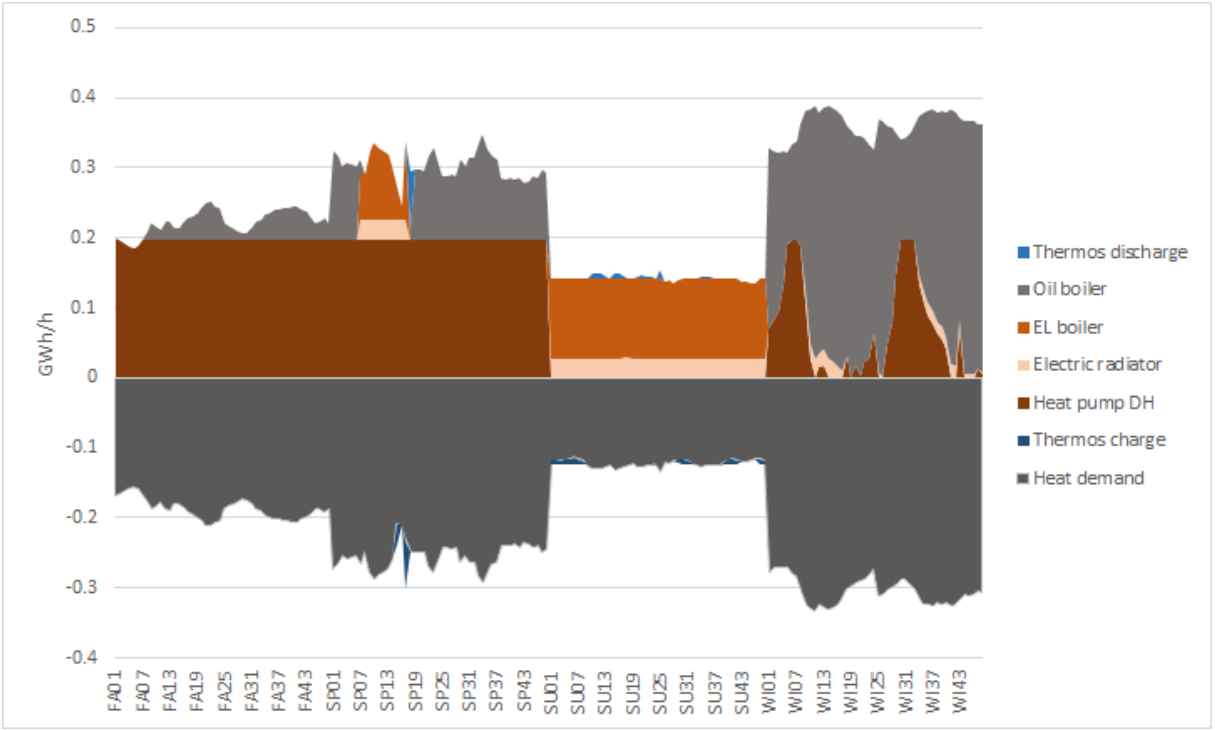


**(b)** Heat flow 2050 (NWI)

**Figure 6.14:** Energy flow 2050 (NWI)

## 6.7 The no wind scenario with no $CO_2$ (NWC)

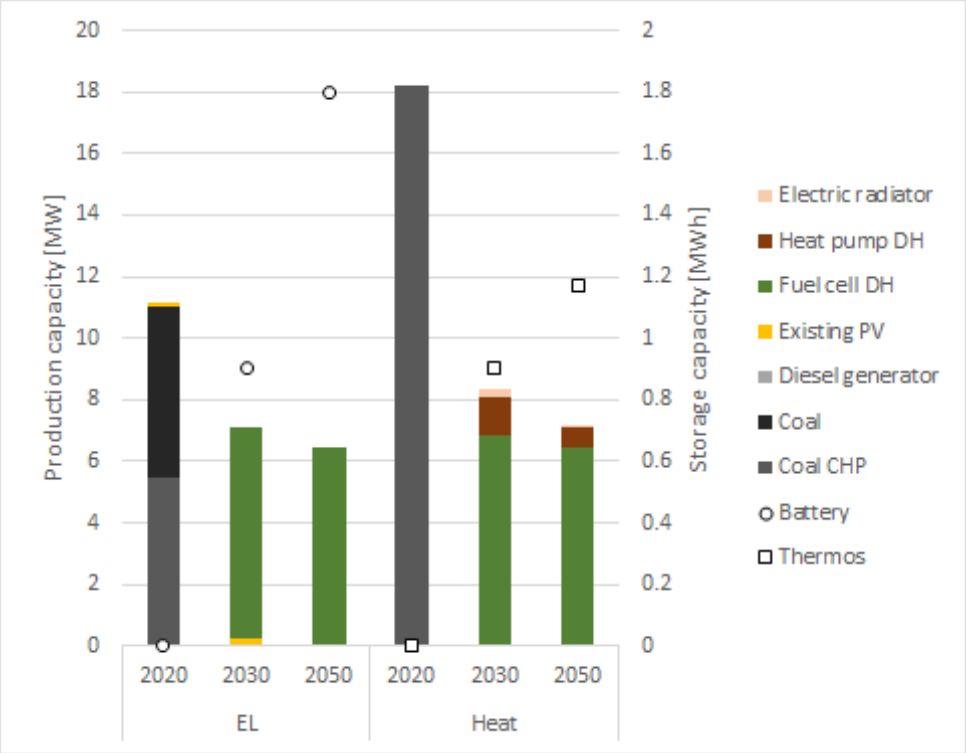


**Figure 6.15:** Installed production capacity (NWC)

When not allowing wind or $CO_2$ emissions, the only way to cover the load in the developed model is to utilize hydrogen. From 2030, NWC is almost exclusively powered by a 7 MW hydrogen fuel cell. There are no investments in new renewable energy sources, meaning that all hydrogen utilized by the fuel cell is imported, rather than investing in electrolysis locally. 123 and 117 GWh of hydrogen are imported in 2030 and 2050 respectively. In addition to the fuel cell providing equal amount of heat and electricity, a small battery and thermal storage tank are installed, and about 1 MW heat pump. The 2020 demand is covered by the existing power plant as shown in fig. 6.15.

The size of the hydrogen tank in NWC is about 6 MWh. Considering the total amount of hydrogen imported, this is obviously not sufficient. For instance, would a monthly delivery of hydrogen require at least 10 GWh storage capacity. A solution with a storage tank with a capacity of about 0.005% of the total hydrogen consumption is infeasible. The small storage tank is likely to be caused by the modelling approach. The hydrogen import is modeled on an ANNUAL timescale. This treats the import as a large ”stored” commodity, available for use at all times. This way, hydrogen is utilized ”directly” in the fuel cell, simply entering and leaving the storage tank simultaneously. This is emphasized by the energy flow in figs. 6.16a and 6.16b, where large curtailments of heat and electricity are observed.

It is observed that the fuel cell is operating at a constant level close to its maximum during large parts of the year, even though the load is changing. The heat output from the fuel cell is equal to the electricity output, and is again observed to be significantly larger than the demand. The results indicate that curtailing energy is cheaper than investing in a larger hydrogen tank. NWC

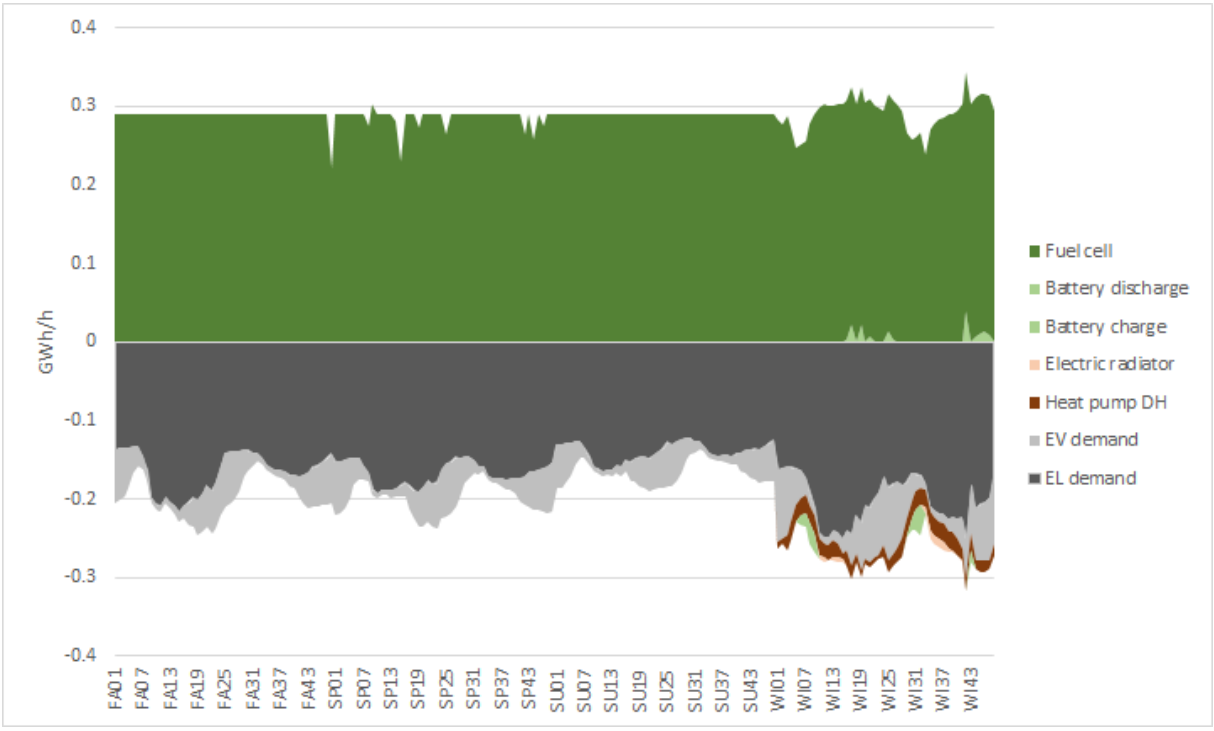


**(a)** Electricity flow 2030 (NWC)

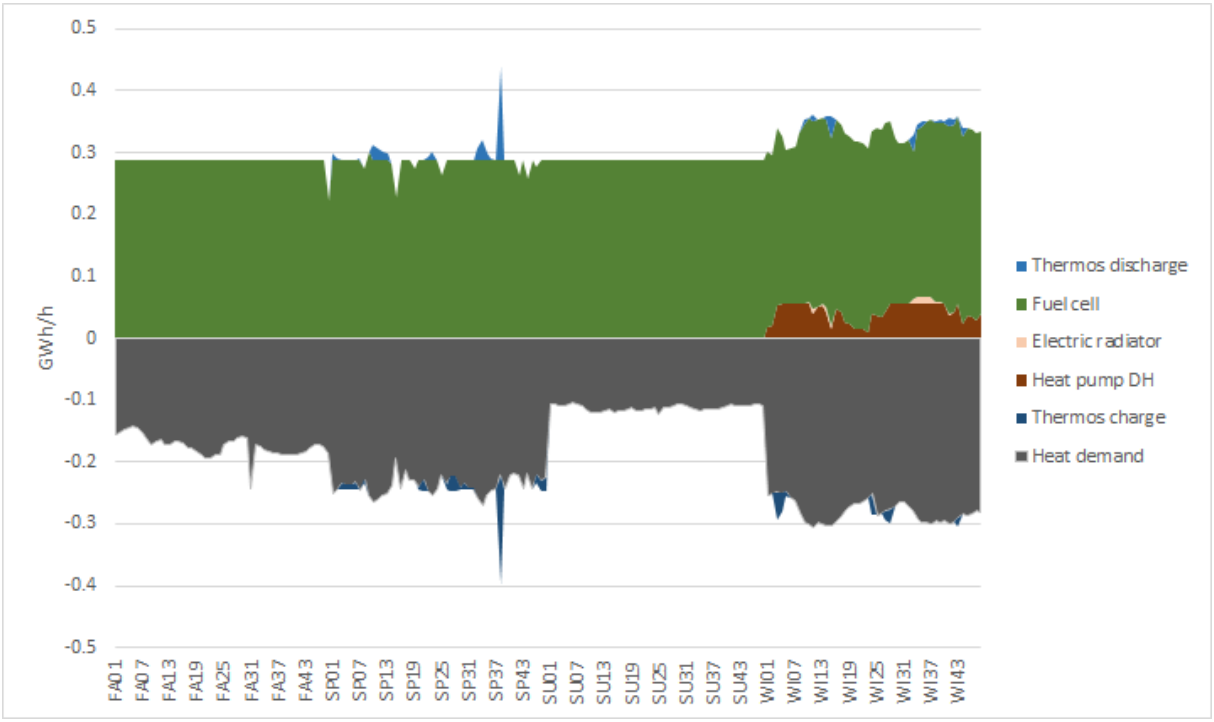


**(b)** Heat flow 2030 (NWC)

**Figure 6.16:** Energy flow 2030 (NWC)

has the largest amount of curtailed energy of all scenarios- which are the opposite of what is expected- as the curtailment in the other scenarios are related to wind and solar production.

Although the result is infeasible, some findings are worth mentioning. First, it is indicated that import of hydrogen is preferred over local electrolysis with the given costs. Secondly, it is observed that the transport demand is electrified although hydrogen is present in the system, utilizing the centralized fuel cell to cover the electricity demand.

Chapter 7

# Sensitivity analysis

Figure 7.2 shows the installed capacities in the different sensitivity analysis. The trend in all scenarios are equal to what was observed in base scenario in section 6.2, with an increasing share of RES dominated by wind power and electrification of heat. All demand is supplied with coal power in 2020 and all production capacity is renewable in 2050. As in B, all vehicles are electrified.

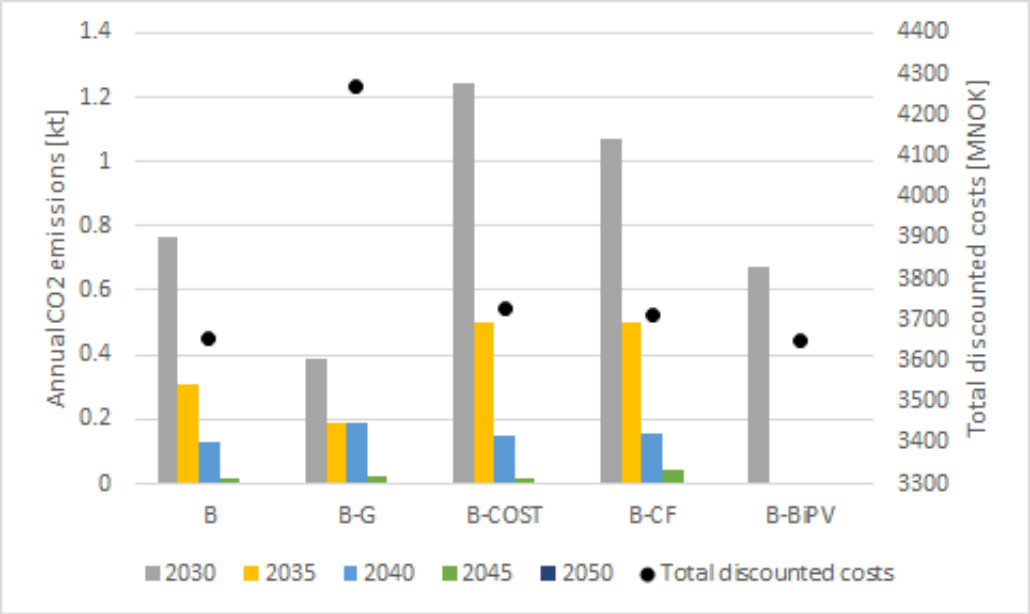


**Figure 7.1:** Annual $CO_2$ emissions and total discounted costs

The energy flow in B-G, B-CF and B-COST are more or less equally distributed as in B and not included. $CO_2$ emissions are equal to B in 2020 and 2025 in the analysis and excluded from fig. 7.1 to increase readability of the emissions from 2030. The total discounted costs are also given in fig. 7.1.

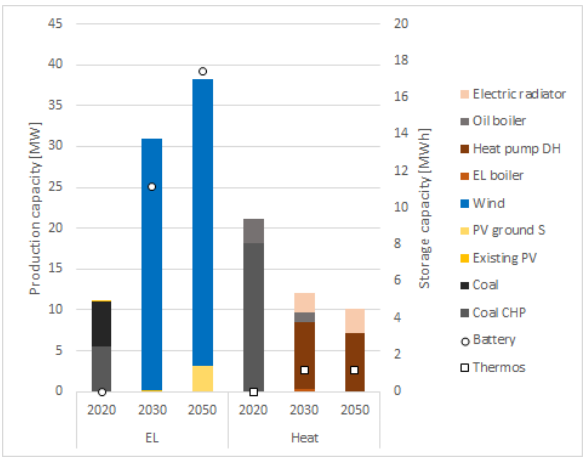


**(a)** Population growth

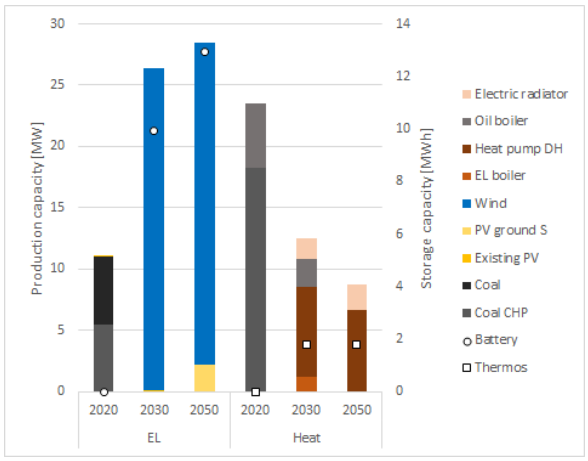


**(b)** Increased cost of wind turbines

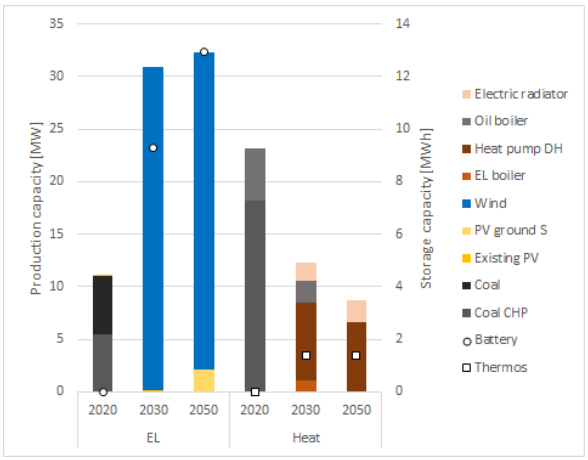


**(c)** Decreased CF of wind turbines

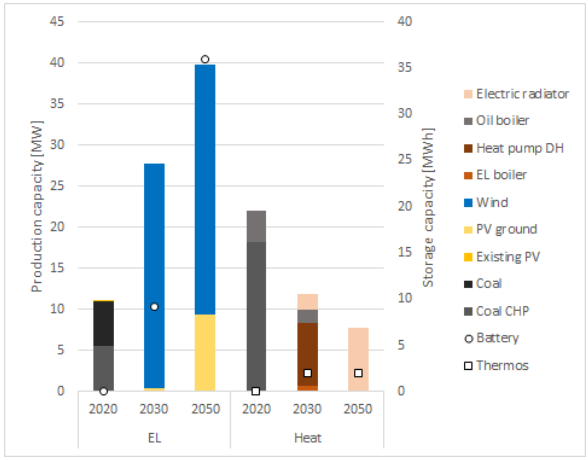


**(d)** Bi-facial PV modules with tracker

**Figure 7.2:** Installed capacities of the sensitivity analysis

## 7.1 B-G

Figure 7.2a shows an increased capacity of wind and solar PV to cover the increased demand. In 2030 roughly 10% additional wind is installed and about 30% in 2050. The PV capacity increases 50% in 2050, while both the heat pump and amount of electric radiators increase about 0.7 MW each. The energy system is entirely based on renewable energy in 2050 as in B, and the energy flow in all years are equally distributed as in B. However, more energy is produced to cover the demand. The battery size increases with 40% and 33% respectively in 2030 and 2050. This is in line with the previous results, were increased share of RES increases the storage capacity. The amount of curtailed energy is also increased.

Regardless of the increased energy demand, the amount of diesel utilized is reduced in 2030 and 2035. As less diesel is consumed, the $CO_2$ emissions is reduced compared to the base scenario as seen in fig. 7.1. The results clearly indicate that wind power is a cost-efficient way to provide energy, choosing to make larger investments early in the time horizon in preference to utilizing fossil fuel. Although the emissions from 2030 already are small compared to 2020, the emissions are halved in B-G compared to the base scenario.

The increased demand leads to larger costs as production capacity is increased. In addition, the total amount of vehicles increases. The total discounted costs increases with 17% due to the population growth.

## 7.2 B-COST

Increasing the costs related to wind power has a rather small impact on the total production capacity as seen in fig. 7.2b. The installed wind capacity is reduced with about 1 MW from 2030 to 2045 while the difference in 2050 is only 0.35 MW. On the other hand, a small increase in PV capacity is observed with 0.2 MW in 2035 and 0.5 MW in 2040.

The reduced production capacity for wind power is replaced by increased use of diesel for heat. In 2030 and 2035 about 50% additional diesel is used for heat, which is directly proportional with the $CO_2$ emissions shown in fig. 7.1. From 2040 the diesel use is about the same as in the base scenario. The reduced amount of available electricity in the system (reduced output from wind) leads to less use of electric radiators, and increased use of the heat pump. These findings are similar to what was observed in the different scenarios, where electric radiators and boilers were utilized in periods with large renewable production. The capacity of the DHS is slightly larger to transmit the increased amount of centralized produced heat.

The amount of curtailed energy is significantly reduced in B-COST compared to B in several periods. A reduction of 50% is observed in 2030 and 2045 and about 15% in 2035 and 2040, thus utilizing more of the produced energy. The battery capacity in 2030 is about 25% larger than in B, and can explain how more energy is utilized.

Although the CAPEX and OPEX of wind turbines is increased with 20%, the total discounted costs only increase with 2%. The overall changes in production capacity are barely noticeable, clearly indicating that wind power is likely to be a part of the solution regardless of uncertainties in costs as discussed in section 6.5.

## 7.3 B-CF

Comparing fig. 7.2c to fig. 6.3 shows an increased capacity of wind turbines in all periods and increased battery size in 2030 but few other changes. The installed capacity of wind increases with about 12%, while the utilized energy from the wind turbines is slightly lower than in B. The amount of curtailed energy is reduced during all periods.

As in B-COST, the heat pump is utilized more as well as an increased diesel consumption to cover the heat demand. The energy flow in B-CF is more or less identical to B-COST, however, slightly more diesel is used in 2030 as observed by investigating the $CO_2$ emissions in fig. 7.1.

The total discounted costs increases compared to B as expected, but only with 1.6%. The result clearly emphasizes the importance of wind in the solution by simply increasing the installed capacity of wind to produce a sufficient amount of electricity. This was also observed in B-G, where the increased demand was covered by increasing the installed capacity of wind.

## 7.4 B-BiPV

Figure 7.2d shows the installed capacity of the base scenario solved with bifacial solar PV module with tracking. Comparing the installed capacity to B, it is more or less identical in 2030, however, 2050 has significantly more PV, wind and battery storage. The PV capacity is almost quintupled in 2050 and wind is increased by 15%. 97% of the heat capacity in 2050 consists of electric radiators, more or less electrifying the entire heat demand.

Looking at fig. 7.1, the $CO_2$ emissions are slightly reduced in 2030 compared to B. However, there are no emissions in the remaining periods, giving an entirely renewable system from 2035. The costs in B-BiPV is reduced by 1% compared to B.

### 7.4.1 Energy flow 2050

Considering the differences in installed capacity in 2050, the energy flow is expected to differ from B. Figure 7.3a shows that the PV modules produce more energy, and has a different shape than before. The production drops around noon, and a larger share of the production is occurring during spring.

The battery is most frequently used during spring and winter, to shift solar and wind energy respectively. It is evident that large parts of the electricity is fed to the electric radiators, which is confirmed by fig. 7.3b. The heat pump is applied during spring and some hours during winter. During winter, the use of the heat pump correlates with charging of the thermos.

The conditions for solar production in this sensitivity analysis is greatly improved. The specific production for the PV modules is increased with about 50%, generating more electricity for the same investment costs. The solution with bifacial modules and tracking device, also changes the production profile, distributing more production to spring (where the load is higher) and changes on a daily basis. The changes are making PV more favorable in the system, and it is therefore as expected that the installed capacity of PV is increased. However, the change in CF for PV leads to additional investments in wind power of about 4 MW. The increased electric production capacity is utilized in electric radiators covering close to 100% of the delivered heat. The increased capacity of electric radiators is in line with the results from the different scenarios,

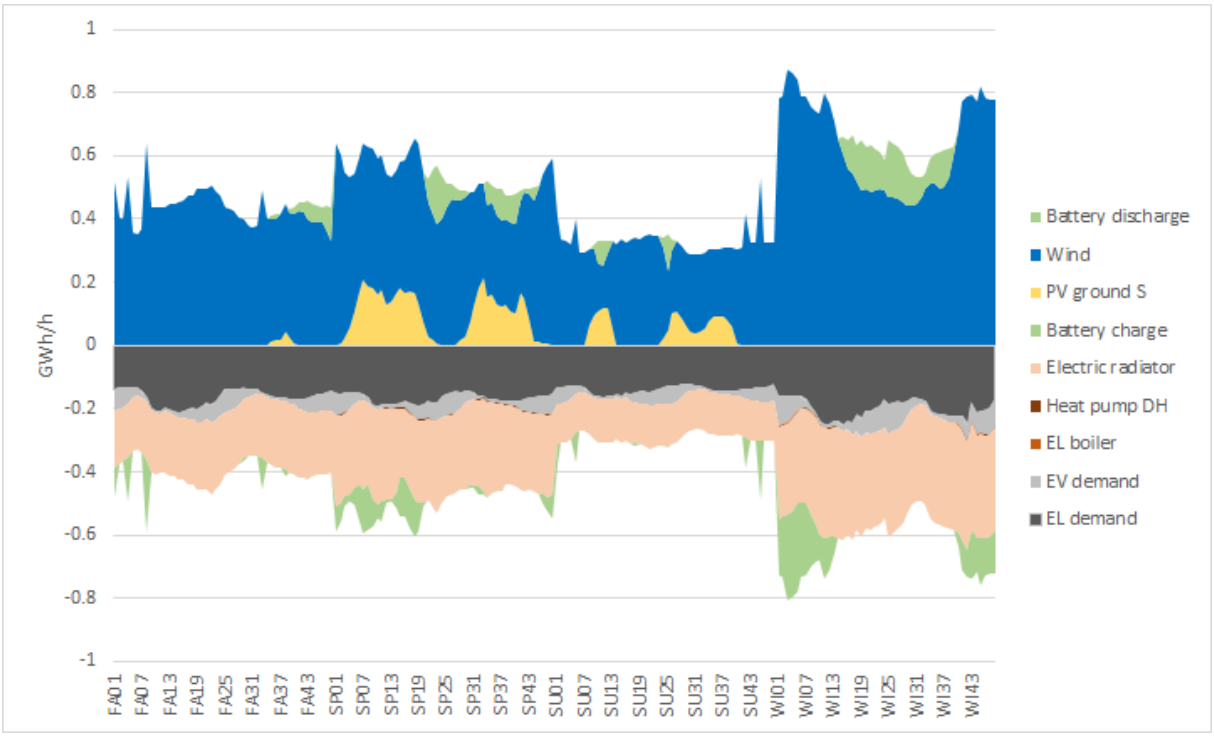


**(a)** Electricity flow 2050 (B-BiPV)

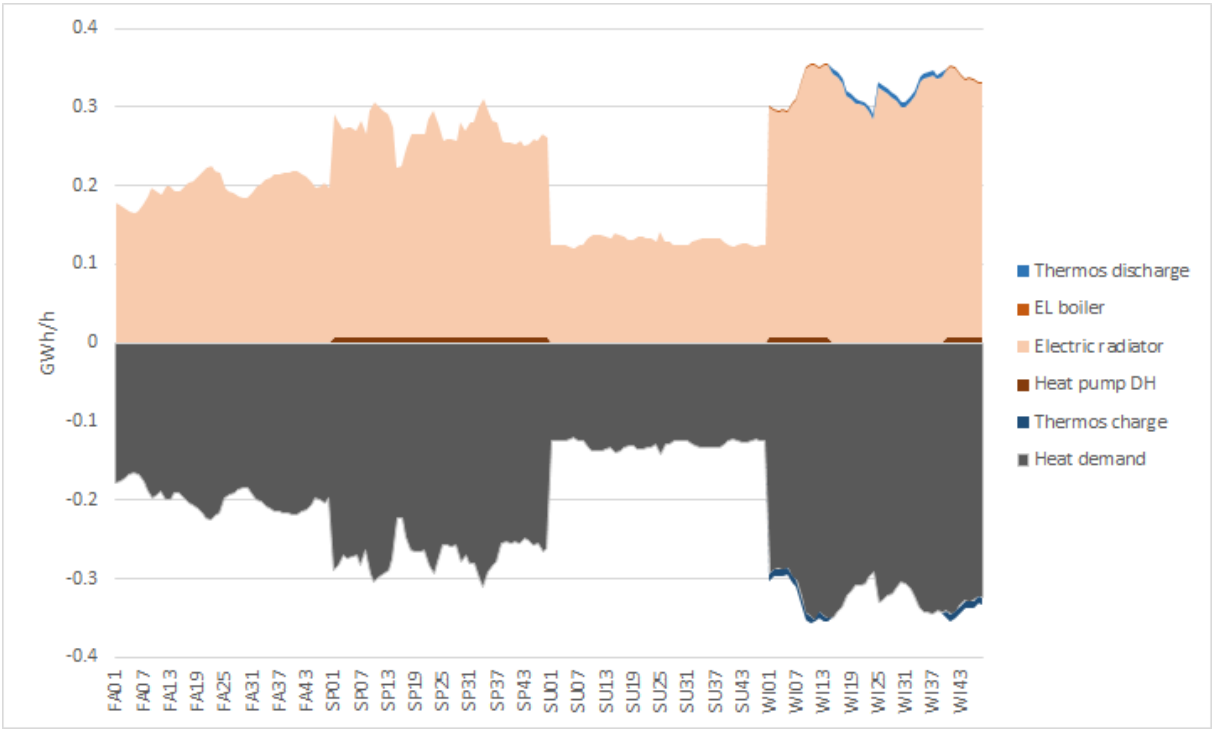


**(b)** Heat flow 2050 (B-BiPV)

**Figure 7.3:** Energy flow 2030 (B-BiPV)

where increased electricity production reduced the utilization of the heat pump. The size of the battery is also increased to handle the varying energy production. As the installed heat pump is about 0.1 MW, it offers less flexibility in the thermal side of the system. This could also increase the size of the battery. A capacity of 0.1 MW is kept of the district heating system, emphasizing the concern about the model approach. A DHS of this size, which corresponds to about 1% of the initial capacity is highly unlikely to be kept, and the total heat demand must be supplied by electric radiators in a real-life application, making the small heat pump and thermal storage redundant. This would increase the costs of the solution slightly, but probably not more than the decreased costs compared to B.

Even with the increased conditions and capacity for solar production, wind power is the main source of energy, providing more than 90% of the utilized electricity. About 38% of the produced solar energy is curtailed in 2050, mostly during summer. No energy is curtailed during spring, once more emphasizing that spring season is the most challenging in the energy system.

Chapter 8

# Discussion

## 8.1 Backup supply

The security of energy supply is crucial in Longyearbyen because of the harsh Arctic climate. The future energy supply is therefore likely to include backup diesel generators able to cover to close to full load [2]. This aspect is not covered by this thesis, and all scenarios expect NWI is optimized without any diesel generators. The investment costs related to backup generators are rather small, and total costs are mostly related to the fuel consumption [74]. The increased CAPEX is therefore unlikely to change the overall costs of the different scenarios in a way worth mentioning- as the diesel consumption will be zero in the other scenarios.

This thesis does not cover questions regarding stability in the system but is merely investigating the energy balance in the system. On a general basis, power systems are reliant on rotating machines to secure stability with frequency response. A battery can provide the same services to ensure stability [4], however, this might increase the battery capacity in all scenarios and thus total costs.

## 8.2 Costs

All costs in this thesis are subject to uncertainty. The utilized costs are provided by various sources, where some are provided in foreign currency. The exchange rate from NOK to USD have changed drastically in 2020, and adds additional insecurity to the future energy system in Longyearbyen. In this thesis an exchange rate of 1USD = 10NOK is used, slightly higher than the average of January -April 2020 [75]. Historically, this is a high exchange rate and a lower rate would decrease the total costs. More interesting is the fact that costs related to the existing system and diesel generators are based on sources operating in NOK, meaning that that RES are beneficial even with expensive foreign currency. The cost projections provided in table A.1 have not been adjusted to consider the local conditions. The harsh Arctic climate might increase costs related to some technologies and things are generally more expensive in Longyearbyen, due to the large distance to the mainland and vulnerable nature. In addition, is the concern related to building in permafrost and the changes because of higher temperatures [3] and soil conditions surrounding the city [2]. These uncertainties apply to all technologies and

investments. Renewable energy sources and storage technologies have a large potential of cost reductions as mentioned in section 4.7, but projecting them towards 2050 is of course related to large uncertainties. The future oil price and price of hydrogen will also affect costs related to scenarios allowing import.

## 8.3 Technical parameters

All technologies are modeled with constant technical parameters, except for the electrolyser and fuel cells who increases efficiency in the future (see table A.1). Like the economical parameters, technical parameters could be improved in the years to come. This is exemplified by the bi-facial modules presented in section 5.5.4, improving CF with about 50%.

Both the diesel generators and steam turbines in the model is modeled with fixed efficiencies. The used efficiencies do not consider rapid changes in load, and the fact that efficiency drops when operated outside their nominal power range [2]. The model approach could therefore underestimate the consumption of fossil fuel and the related $CO_2$ emissions.

The heat pumps are providing heat to the DHS and are modeled with a constant COP of 2.5. The maximum theoretical COP is given by the difference between the hot heat reservoir, $T_H$, and cold reservoir, $TT_C$ as shown in eq. (8.1).

$$\text{COP} = \frac{T_H}{T_H - T_C} \tag{8.1}$$

Using heat pumps for temperature levels over 100°C is generally challenging [76], and the heat pump supplying the city Drammen with district heat at 90°C from 8°C water has a COP of 3 [77]. Considering Isfjorden as the heat source and the high operating temperature of the DHS, it is assumed that the COP in Longyearbyen must be lower, and a COP of 2.5 is chosen. However, this might be too high. Decreasing the COP is likely to shift the heat production to electric boilers and to increase the capacity of renewable energy. The COP could be increased if the operating temperature of the DHS is decreased.

## 8.4 Production profiles and time slices

All scenarios and suggested solutions have insecurities related to them, and especially those with renewable energy sources as a part of the solution. By choosing to represent a full year in 192 time-slices, it is impossible to represent all fluctuations and variations in electricity production from wind and solar and in the demand. The production profiles shown in fig. 4.1 is chosen based on what seems to be the most common hourly profile during each season, simultaneously as it should represent the total share of energy in that season. It should also represent the negative correlation of wind and solar conditions [47], that is known to increase the reliability of a power system when both technologies are present. These factors are rather well covered in the chosen profiles, however, there are periods in each season with small or no production not captured in the chosen time series. Figure 8.1 shows the hourly production profiles for all days in January from the original data-set discussed in section 4.2, and emphasizes how the wind resource is varying. Each day has one color, and output varies from 100% to 0% of installed capacity for some days, with about 12 successive hours with no production. Treating variable renewable

energy sources as deterministic input as in this thesis, tends to overestimate the power production from renewables [1]. By investigating the power output from the wind turbines in for instance fig. 6.5b, it is evident that the chosen wind profile does not capture the successive hours with no contribution.

A production profile with large variations on a short term timescale is likely to increase the need for storage capacity to utilize the produced energy [2]. It is observed that the installed battery capacity increases with the amount of RES in all scenarios.

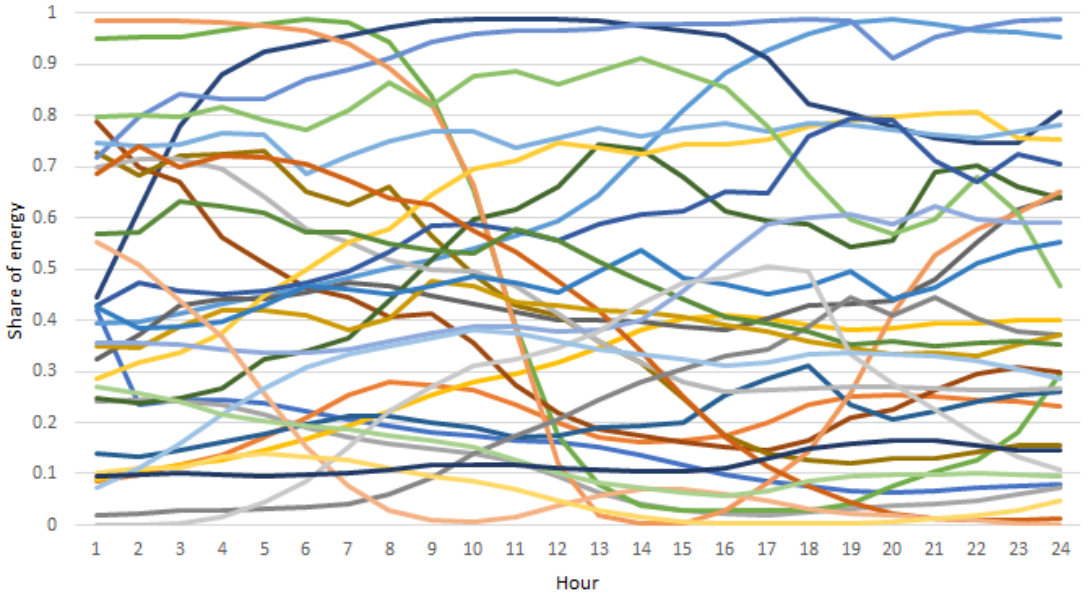


**Figure 8.1:** Hourly wind production profiles for January

The challenge related to the time slices also applies to represent the variation in the load. One of the main challenges related to this task is that the actual load is unknown. The load profile for heat and electricity used in the model is solely based upon the production profile from the existing power plant, as the end consumption is unknown due to lack of measurements. This imposes an uncertainty related to the actual energy demand in the system, as transmission losses, curtailment of heat and use of backup generators and boilers are unknown. The minimum heat output from the existing CHP is 5 MW, and substantial amounts of heat are assumed curtailed during summer [4]. It is therefore likely that the summer heat demand is larger in the model than in reality. The backup diesel generators and boilers are also frequently used, as opposed to the results presented for 2020 in section 6.1. Here, the (except ISO, using wind) total load is supplied by the existing power plant, emphasizing the concern of modeling based on production profiles rather than measured demand. As energy supplied by diesel is more expensive than coal, the costs related to operation in 2020 and 2025 is likely to be underestimated. This might lead to smaller investments in RES early in the modelling horizon.

The data used to obtain the production and demand profiles is given from three different sources. Ideally, the selected 192 data points should represent the same 192 hours of the year. This is not the case in the used data as seen in sections 4.2 and 4.3.2, simply because data from the same hours were not representative. The negative correlation between solar and conditions observed in fig. 4.1 could, therefore, be unnaturally large, as the data was chosen to fit the expected

behaviour. The same applies regarding the temperature, affecting both the heat demand and the solar production [3].

## 8.5 Transmission grids and energy efficiency measures

The installed capacity of the district heating system is decreasing in all scenarios. This is partly caused by a transition to heating with electric radiators, but also by the reduction in the heat demand explained in section 4.3. When the heat demand is reduced, the maximum power transmitted through the DHS is reduced. As costs are related to the installed capacity, it is beneficial to reduce the installed capacity. Operating and maintenance costs of district heating systems are often given as a percentage of the total capital expenditures or of distribution costs [71]. The CAPEX is dominated by the length and size of pipes in the system, and it is not given that reduced heat transfer would decrease the OPEX linearly in the real system as in this model. It might be possible to disconnect some buildings, thus limiting the total pipe length in the system, however, this must be done carefully and planned according to installing other heat sources like electric radiators.

All scenarios have an increase in electricity production and consumption. The cars and snowmobiles are electrified along with some percentage of the heat demand. The increase in electrical load from cars and electric radiators are distributed all over the city. The increased load are assumed to not impose any challenges in the distribution grid. Full electrification of the vehicles will lead to an average load of about 750 kW, where most of the charging will occur during nighttime where the load is lower as seen in, for instance, fig. 6.11, thus utilizing available capacity in the grid. The use of distributed electric radiators, however, might impose challenges in the electrical grid as the heating demand is distributed more like the electrical load. The average power consumption for the electrical radiators is about 1.75 MW in 2050 in scenario B, while the average specific electricity demand is 3.71 MW. This is an increase of close to 50% and could trigger reinvestment costs related to the electricity grid, changing the economics in the solution. However, there are no found to be no limitations in the grid regarding electrification of ships [2], indicating that the increased consumption can be handled by the existing grid. Parts of the grid are said to be old and have a need of replacement, and in this case- upgrading the grid to the new situation are assumed to impose a marginal increase in costs [2].

All scenarios invest in energy efficiency measures to reduce the heat demand in buildings. Taking into account that the heat demand in Longyearbyen is 40% larger than on the mainland [2], it seems like a logical result. B, BNC and ISO make identical investments in energy efficiency as seen in fig. 6.1. All scenarios maximize the potential in energy monitoring in residential and commercial building, which is the cheapest technology but has the least reduction in demand. Additional insulation is only applied for residential buildings in NWC while technical equipment is replaced and control is implemented in NWI and NWC. These findings are interesting to compare with the trends in Longyearbyen. As already mentioned, the majority of buildings in Longyearbyen does not measure heat consumption and the heat is charged per square meter [3]. This leaves no incentives for the resident to reduce consumption. Statsbygg has already installed energy monitoring and control in some buildings and experienced large reductions in consumption. In some buildings, the heat demand was halved by implementing control [48]. As the majority of buildings in Longyearbyen is predating any technical regulations [3], the potential of energy savings might be higher than what is considered in this thesis. As all scenarios invest

in energy efficiency measures it seems clear that this is beneficial. However, as the investments in NWi and NWC are larger than in B, BNC and ISO - it is clear that energy efficiency measures are replaced by cheaper production of heat in some cases.

## 8.6 Installed capacity related to other work

### 8.6.1 B, BNC and ISO

The suggested installed wind capacity of about 27 MW in B, BNC and ISO are similar with the capacity in the ”Pv, wind and battery- scenario” in the report delivered to Ministry of Petroleum and Energy in 2018 [2]. However, in addition to the 25 MW wind power, 25 MWp of solar PV is mounted on roofs in Longyearbyen along with 8.2 MW diesel generators, 15.7 MW diesel boiler and a 42 MWh battery. This analysis shows that about 50% of the load will be covered by diesel when the power production for wind and solar are insufficient to cover the load. The use of diesel is in large contrast to what is observed in B, BNC and ISO and could be caused by various reasons.

First, the chosen time slice level might overestimate the steadiness of the wind power as discussed in section 8.4, eliminating the need for diesel generators to cover periods with no production. This is also likely to reduce the size of the battery, as less energy must be stored to periods without any production. Findings in [2] suggest that doubling the battery capacity would give a small decrease in diesel consumption, as the periods with insufficient renewable production are long. Secondly, the energy demand in [2] is kept constant, ultimately leading to a larger demand than in this thesis because of the projection in fig. 4.2 and additional energy efficiency matters. The supplied heat is reduced with about 20 GWh until 2050 in B, BNC and ISO compared with the 2020 level of 70 GWh which is kept throughout the analysis in [2]. The reduced energy demand leads to smaller relative variations in the load profiles, which could reduce the need for storage for load shifting. Lastly, could different assumptions regarding for instance capacity factor for wind and solar and storage efficiency lead to different results.

### 8.6.2 NWI

Thorud et al. [4] suggests to install 30 MWp of solar PV to fulfill the demand for heat and electricity in Longyearbyen with solar energy during summer (mid-April to mid-August). Comparing the installed capacity in NWI with what’s suggested, the installed solar capacity in 2050 is about doubled in size. However, the installed PV capacity is increasing annually, suggesting only 30 MW in 2030. As already discussed and shown in table A.1, costs of PV is expected to fall drastically in the future. The main investments in PV are done with a substantial lower CAPEX than what’s assumed in [4]. This makes the large over dimensioning of the PV system and the related curtailment ”cheaper,” and could, therefore, be beneficial economically to ensure that the diesel consumption decreases. The curtailment of solar energy increases with the installed capacity up to about 10 GWh in 2050. Another factor likely to affect the installed solar PV capacity is caused by technology choice in the model. In all scenarios, fixed, traditional one-sided PV modules are used to obtain the capacity factor and production profile. The production profiles in [4] is obtained by bi-facial modules with a tracking system, obtaining a higher specific production per module. This is clear by investigating the production details, where the roughly 30 MWp installed in 2030 in NWI produces 20 GWh. Compared with the 30 MWp bi-facial modules

producing 33 GWh in [4].

Chapter 9

# Conclusion

In this thesis, the future energy system of Longyearbyen towards 2050 is analysed using the TIMES modelling tool. The TIMES model minimizes total system costs, including investments and operational costs for all parts of the energy system from production to end-use technologies. Five scenarios are developed describing potential political decisions; the base scenario (B), the base scenario with no $CO_2$ (BNC), the isolated scenario (ISO), the no wind scenario (NWI) and the no wind scenario with no $CO_2$ (NWC).

The results from the solved scenarios clearly indicate that a renewable energy system in Longyearbyen is feasible. Four out of five scenarios make large investments in renewable energy sources, and wind power is preferred as the main source of energy in the B, BNC, and the ISO after decommissioning the coal-fired power plant. The unrestricted base scenario covers more than 95% of its heat demand and the entire electricity demand with renewable energy in all periods and is 100% self-sufficient at the end of the model horizon. The small amount of diesel utilized in B reduces the annual $CO_2$ emissions to less than 1% of 2020 emissions. In 2050, the energy system is 100% renewable and thus no emissions related to the operation. Similar solutions are found in BNC and ISO, only with self-sufficiency already in 2030 and slightly increased total discounted costs. BNC increases the costs with 1% according to B.

The large amounts of electricity produced by wind turbines cover the specific electricity demand and EV demand, electrified in all scenarios. As the power production from wind is not distributed equally as the load, some energy is stored in a battery and shifted to other periods. All scenarios invest in batteries and short term thermal storage in 2030, and the battery size increases with increased renewable capacity in all scenarios. The majority of heat is provided by a centralized heat pump fed with electricity. Electric radiators and boilers are utilized to cover peak heat load and to dump electricity in periods with large production.

When restricting the capacity for wind turbines to zero, a large diesel consumption compliments large investments in solar PV, providing energy during summer and spring in NWI. The diesel is suspect of emissions and large costs, significantly increasing total discounted costs and emissions throughout the modeling horizon. The total discounted costs in NWI is increased with 24% compared to B.

The increased costs are a clear indication that wind power is crucial to keep the costs down. This is related to the large differences in conditions for solar production, needing seasonal storage to

provide energy during winter. Although the increased costs mainly are related to the large diesel consumption, a hydrogen system is found too expensive in no wind scenario. The large costs related to a hydrogen system is confirmed in NWC. Although the proposed solution is infeasible as discussed in section 6.7, the fact that there is no investment in renewable energy sources and all hydrogen is imported indicates that the total cost and efficiency related to local hydrogen production and storage must be improved to be considered economical. The large amounts of imported hydrogen in NWC lead to 37% increased costs compared to B.

The base scenario sensitivity analysis also emphasizes the importance and dependency of wind power. Increased load (B-G) and decreased capacity factor (B-CF) is simply solved by increasing the installed wind capacity, while increased costs of 20% (B-COST) reduced the installed capacity with about 2% from 2035 while utilizing about the same amount of wind energy as in B. Improving the capacity factor of PV increases the installed wind (and PV) capacity, and shifts all heating demand to electric radiators. As the total discounted costs increases with about only 2% and wind power remain the dominating source of energy regardless of the changed technical and economical parameters, wind power seems to be robust against the uncertainties regarding this task.

Electricity is curtailed in all seasons except spring, indicating that the production capacity is dimensioned to cover the spring demand which is the most stressful season in a wind-based system. If seasonal storage were implemented, curtailed electricity from the other seasons could be stored until spring. Seasonal storage is therefore likely to reduce the installed wind capacity in B, BNC and ISO.

Chapter 10

# Further work

The model developed in this thesis could be further improved. First and foremost should the production profiles for solar and wind power be improved to represent the actual production profile with more details. To do so, the number of time-slices are likely to be increased, allowing longer periods to be without renewable production. An increased number of time-slices could also improve the modelling of the energy demand. The most important aspect relating the demand, however, is to obtain measured data of the actual consumption.

The modelling of the hydrogen-chain must be improved to provide insight in a scenario with import of hydrogen. It would also be interesting to perform a sensitivity analysis of costs and technical parameters regarding a hydrogen system, to investigate how seasonal storage might affect the installed capacity of solar and wind.

Land-based transport is included, but modelling could be improved to offer vehicle-to-grid services and fuel consumption and driving distances could be modeled with greater detail. There is also a substantial energy demand related to aviation and sea transport that could be included in the model.

Costs and technical parameters of all technologies could be improved, and site-specific costs would be preferable over generic sources mainly used in this thesis.

# Bibliography


[1] Hans-Kristian Ringkjøb, Peter M. Haugan, and Astrid Nybø. "Transitioning remote Arctic settlements to renewable energy systems – A modelling study of Longyearbyen, Svalbard". In: *Applied Energy* 258 (2020), p. 114079. ISSN: 0306-2619. DOI: https://doi.org/10.1016/j.apenergy.2019.114079. URL: http://www.sciencedirect.com/science/article/pii/S0306261919317660.

[2] Thema and Multiconsult. "Alternativer for framtidig energiforsyning på Svalbard". In: (2018). URL: https://www.regjeringen.no/contentassets/cdaceb5f6b5e4fb1aa4e5e151a87859a/thema-og-multiconsult---energiforsyningen-pa-svalbard.pdf.

[3] Einar Boman Rinde. *Svalbard - 100% renewable energy system*. Specializing project. Department of Electric Power Engineering, NTNU – Norwegian University of Science and Technology, Dec. 2019.

[4] Bjørn Thorud et al. *Feasibility Study for an Energy Storage System for Longyearbyen Energiverk*. 2019.

[5] Rasmus Bøckman. Email. 2019.

[6] SSB. *Fjernvarme og fjernkjøling*. URL: https://www.ssb.no/energi-og-industri/statistikker/fjernvarme (visited on 11/22/2019).

[7] Nguyen Le Truong, Ambrose Dodoo, and Leif Gustavsson. "Final and primary energy use for heating new residential area with varied exploitation levels, building energy performance and district heat temperatures". In: *Energy Procedia* 158 (2019). Innovative Solutions for Energy Transitions, pp. 6544–6550. ISSN: 1876-6102. DOI: https://doi.org/10.1016/j.egypro.2019.01.103. URL: http://www.sciencedirect.com/science/article/pii/S1876610219301134.

[8] SSB. *Svalbard*. URL: https://www.ssb.no/svalbard/faktaside/svalbard (visited on 12/06/2019).

[9] Steinar Johansen. *Samfunns- og næringsanalyse for Svalbard 2017*. 2017.

[10] Syssemannen på Svalbard. *Årsrapport 2018*. Feb. 15, 2019. URL: https://www.sysselmannen.no/contentassets/5ff31149934d418d940510ce19e70ea0/arsrapport-2018-endelig.pdf (visited on 12/06/2019).

[11] Svalbard Folkehøgskole. URL: https://svalbardfolkehogskole.no/om-oss/ (visited on 10/24/2019).

[12] Longyearbyen Lokalstyre. *Boligbehovsutredning 2019*. 2019.

[13] Eirik Hind Sveen. URL: https://www.nrk.no/troms/millioner-til-verdens-nordligste-folkehogskole-pa-svalbard_-_-helt-unikt-1.14216274 (visited on 10/24/2019).
[14] Rolf Stange. *Midnattsol og mørketid*. URL: https://www.spitsbergen-svalbard.no/svalbard-infoside/midnattssol-og-moerketid.html (visited on 11/30/2019).
[15] Ketil Isaksen et al. "Klimascenarioer for Longyearbyen-området Svalbard". In: (2017). URL: https://www.statsbygg.no/Files/samfunnsansvar/fou/klimascenarioerSvalbard-rapport201710.pdf.
[16] Amalie Kvame Holm. *Ferske klimatall viser dramatisk temperaturøkning på Svalbard*. URL: https://www.met.no/nyhetsarkiv/ferske-klimatall-viser-dramatisk-temperaturokning-pa-svalbard (visited on 11/30/2019).
[17] Per Kyrre Reymert. "Fra company town til moderne by". In: (2013). URL: https://www.sysselmannen.no/contentassets/bc51823074cc440f90894ba798f26a82/gamlelongyearbyen_norsk.pdf (visited on 12/07/2019).
[18] Sysselmannen på Svalbard. "Opplev Svalbard på naturens premisser". In: (2006). URL: https://www.sysselmannen.no/contentassets/57a346db960846dcb51b326ef8dd5f09/opplev_svalbard_no_06_zrpnk.pdf (visited on 12/07/2019).
[19] Henrik Rotneberg. In: (Dec. 5, 2018). URL: https://www.regjeringen.no/contentassets/bcb399745aae4162891967198db2213b/sysselmannen-pa-svalbard.pdf?uid=Sysselmannen_p%C3%A5_Svalbard (visited on 12/07/2019).
[20] Bring. *Svalbard*. URL: https://www.bring.no/tjenester/transport-i-norge/svalbard (visited on 12/18/2019).
[21] Hans-Kristian Ringkjøb, Peter M. Haugan, and Ida Marie Solbrekke. "A review of modelling tools for energy and electricity systems with large shares of variable renewables". In: *Renewable and Sustainable Energy Reviews* 96 (2018), pp. 440–459. ISSN: 1364-0321. DOI: https://doi.org/10.1016/j.rser.2018.08.002. URL: http://www.sciencedirect.com/science/article/pii/S1364032118305690.
[22] D. Connolly et al. "A review of computer tools for analysing the integration of renewable energy into various energy systems". In: *Applied Energy* 87.4 (2010), pp. 1059–1082. ISSN: 0306-2619. DOI: https://doi.org/10.1016/j.apenergy.2009.09.026. URL: http://www.sciencedirect.com/science/article/pii/S0306261909004188.
[23] Magne Lorentzen Kolstad et al. *Software tools for local energy system operation and expansion*. 2017.
[24] Richard Loulou et al. In: (). URL: https://iea-etsap.org/docs/Documentation_for_the_TIMES_Model-Part-I_July-2016.pdf (visited on 12/15/2019).
[25] GAMS Software GmbH. *GAMS - Cutting Edge Modeling*. URL: https://www.gams.com/ (visited on 05/31/2020).
[26] ETSAP. *IEA-ETSAP Energy Systems Analysis Tools*. URL: https://iea-etsap.org/index.php/etsap-tools (visited on 05/31/2020).

[27] Richard Loulou et al. *Documentation for the TIMES Model part II*. July 2016. URL: https://iea-etsap.org/docs/Documentation_for_the_TIMES_Model-Part-II_July-2016.pdf (visited on 02/01/2020).

[28] Alessia De Vita, Izabela Kielichowska, and Pavla Mandatowa. *Technology pathways in decarbonisation scenarios*. July 2018. URL: https://ec.europa.eu/energy/sites/ener/files/documents/2018_06_27_technology_pathways_-_finalreportmain2.pdf (visited on 05/31/2020).

[29] P. Capros et al. *EU ENERGY, TRANSPORT AND GHG EMISSIONS TRENDS TO 2050 - REFERENCE SCENARIO 2013*. Dec. 16, 2013. URL: https://ec.europa.eu/clima/sites/clima/files/strategies/2030/docs/eu_trends_2050_en.pdf (visited on 05/31/2020).

[30] National Technical University of Athens. *PRIMES model*. 2014. URL: https://ec.europa.eu/clima/sites/clima/files/strategies/analysis/models/docs/primes_model_2013-2014_en.pdf (visited on 05/25/2020).

[31] The Balmorel Open Source Project. URL: http://www.balmorel.com/ (visited on 05/25/2020).

[32] Bjarne Bach et al. "Integration of large-scale heat pumps in the district heating systems of Greater Copenhagen". In: *Energy* 107 (2016), pp. 321–334. ISSN: 0360-5442. DOI: https://doi.org/10.1016/j.energy.2016.04.029. URL: http://www.sciencedirect.com/science/article/pii/S0360544216304352.

[33] Åsa Grytli Tveten and Torjus Bolkesjø. "Energy system impacts of the Norwegian-Swedish TGC market". In: *International Journal of Energy Sector Management* 10 (Apr. 2016), pp. 69–86. DOI: 10.1108/IJESM-07-2014-0003.

[34] Karsten Hedegaard et al. "Effects of electric vehicles on power systems in Northern Europe". In: *Energy* 48.1 (2012). 6th Dubrovnik Conference on Sustainable Development of Energy Water and Environmental Systems, SDEWES 2011, pp. 356–368. ISSN: 0360-5442. DOI: https://doi.org/10.1016/j.energy.2012.06.012. URL: http://www.sciencedirect.com/science/article/pii/S036054421200463X.

[35] AMPL Optimization Inc. *GAMS -Streamlined modeling for real optimization*. URL: https://www.ampl.com/ (visited on 06/01/2020).

[36] Maurizio Gargiolo. *Getting started with TIMES-VEDA*. May 2009. URL: https://iea-etsap.org/index.php/etsap-demos-models (visited on 02/01/2020).

[37] M. Gargiulo, K. Vailancourt, and R. De Migilio. *Documentation for the TIMES Model part IV*. Oct. 2016. URL: https://iea-etsap.org/index.php/documentation (visited on 02/01/2020).

[38] Ministry of Finance. "Prinsipper og krav ved utarbeidelse av samfunnsøkonomiske analyser mv." In: (Apr. 30, 2014).

[39] A. Lachuriya and R. D. Kulkarni. "Stationary electrical energy storage technology for global energy sustainability: A review". In: *2017 International Conference on Nascent Technologies in Engineering (ICNTE)*. Jan. 2017, pp. 1–6. DOI: 10.1109/ICNTE.2017.7947936.

[40] Carl Einar Ianssen. Email. 2020.

[41] Avinor. *Elektriske fly*. URL: https://avinor.no/konsern/klima/elfly/elektriske-fly (visited on 05/01/2020).

[42] Maria Sidelnikova et al. *Kostnader i energisektoren*. 2015. URL: http://publikasjoner.nve.no/rapport/2015/rapport2015_02a.pdf.

[43] Svalbardsmiljøvernfond. *13/36 Bygningsintegrert solenergianlegg – Etablering i Elvesletta Syd*. Apr. 27, 2015. URL: https://miljovernfondet.sysselmannen.no/globalassets/svalbards-miljovernfond-dokument/prosjekter/rapporter/2015/13-36-sluttrapport-publikumsvennlig---svalbards-miljovernfond.pdf (visited on 12/04/2019).
[44] Rasmus Bøckman. Email. 2020.
[45] PVsyst SA. *PVsyst*. Version 6.85. Nov. 16, 2019. URL: https://www.pvsyst.com.
[46] Iain Staffell and Stefan Pfenninger. "Using bias-corrected reanalysis to simulate current and future wind power output". In: *Energy* 114 (2016), pp. 1224–1239. ISSN: 0360-5442. DOI: https://doi.org/10.1016/j.energy.2016.08.068. URL: renewables.ninja.
[47] Solbakken, Kine, Babar, Bilal, and Boström, Tobias. "Correlation of wind and solar power in high-latitude arctic areas in Northern Norway and Svalbard". In: *Renew. Energy Environ. Sustain.* 1 (2016), p. 42. DOI: 10.1051/rees/2016027. URL: https://doi.org/10.1051/rees/2016027.
[48] William Holberg Engesland. Email. 2019.
[49] Sveinung Lystrup Thesen. Email. 2019.
[50] Eva Rosenberg et al. *CenSES Energy demand projections towards 2050 - Reference path*. 2015. URL: https://www.ntnu.no/documents/7414984/1265644753/Position-paper_Energy-Projections_utenbleed.pdf/b39bc144-cff6-46c3-82d9-37b1f8b2e04f (visited on 01/15/2020).
[51] Stig Haugen et al. *Opprustning av kraftnettet for å redusere energitapet*. Feb. 2004. URL: http://publikasjoner.nve.no/rapport/2004/rapport2004_01.pdf (visited on 04/22/2020).
[52] Karen Byskov Lindberg and Ingrid H. Magnussen. *Tiltak og virkemidler for redusert utslipp av klimagasser fra norske bygninger*. Mar. 24, 2010.
[53] SSB. *Bilparken*. URL: https://www.ssb.no/statbank/table/11823 (visited on 04/20/2020).
[54] SSB. *Kjørelengder*. URL: https://www.ssb.no/statbank/table/12576 (visited on 04/20/2020).
[55] Arne Aalberg. Email. 2020.
[56] Rune Moen. Email. 2020.
[57] SSB. *Dette er Svalbard*. Apr. 2012. URL: https://www.ssb.no/a/histstat/svalbard/dette-er-svalbard2012.pdf (visited on 04/21/2020).
[58] Christer Heen Skotland, Eirik Eggum, and Dag Spilde. *Hva betyr elbiler for strømnettet?* Sept. 2016. URL: http://publikasjoner.nve.no/rapport/2016/rapport2016_74.pdf (visited on 03/01/2020).
[59] Georgios Fontaras, Nikiforos-Georgios Zacharof, and Biagio Ciuffo. "Fuel consumption and CO2 emissions from passenger cars in Europe – Laboratory versus real-world emissions". In: *Progress in Energy and Combustion Science* 60 (2017), pp. 97–131. ISSN: 0360-1285. DOI: https://doi.org/10.1016/j.pecs.2016.12.004. URL: http://www.sciencedirect.com/science/article/pii/S0360128516300442.
[60] Volkswagen. *e-Golf*. URL: https://www.volkswagen.no/no/biler/e-golf.html (visited on 02/07/2020).
[61] Volkswagen. *Golf*. URL: https://www.volkswagen.no/no/biler/golf.html (visited on 02/07/2020).

[62] Toyota. *Mirai*. 2018.
[63] European Automobile Manufacturers' Association. *WHAT IS THE PURPOSE OF THE WLTP LAB TEST?* URL: https://www.wltpfacts.eu/purpose-lab-tests-wltp/ (visited on 04/22/2020).
[64] International Renewable Energy Agency. *Future of Solar Photovoltaic: Deployment, investment, technology, grid integration and socio-economic aspects (A Global Energy Transformation paper)*. Nov. 2019. URL: https://www.irena.org/-/media/Files/IRENA/Agency/Publication/2019/Nov/IRENA_Future_of_Solar_PV_2019.pdf (visited on 04/27/2020).
[65] International Renewable Energy Agency. *Future of wind: Deployment, investment, technology, grid integration and socio-economic aspects (A Global Energy Transformation paper)*. Oct. 2019. URL: https://www.irena.org/-/media/Files/IRENA/Agency/Publication/2019/Oct/IRENA_Future_of_wind_2019.pdf (visited on 04/27/2020).
[66] National Renewable Energy Laboratory. *2019 Annual Technology Baseline*. 2019. URL: https://atb.nrel.gov/electricity/2019/data.html.
[67] Opplysningsrådet for veitrafikken. *Bilsalget i 2019*. URL: https://ofv.no/bilsalget/bilsalget-i-2019 (visited on 05/01/2020).
[68] Nic Lutsey and Michael Nicholas. *Update on electric vehicle costs in the United States through 2030*. Apr. 2, 2019. URL: https://theicct.org/sites/default/files/publications/EV_cost_2020_2030_20190401.pdf (visited on 05/01/2020).
[69] Ministry of Petroleum and Energy. *Skrinlegger nasjonal ramme for vindkraft*. Oct. 17, 2019. URL: https://www.regjeringen.no/no/aktuelt/skrinlegger-nasjonal-ramme-for-vindkraft/id2674311/ (visited on 04/29/2020).
[70] Kirsti Kringstad and Espen Sandmo. *To personer siktet etter skadeverk for 15 millioner kroner i vindkraftanlegg*. URL: https://www.nrk.no/trondelag/to-personer-siktet-etter-skadeverk-for-15-millioner-kroner-i-vindkraftanlegg-pa-froya-i-trondelag-1.14968801 (visited on 04/29/2020).
[71] Erik Ahlgren. *District Heating*. Jan. 2013. URL: https://iea-etsap.org/E-TechDS/PDF/E16_DistrHeat_EA_Final_Jan2013_GSOK.pdf (visited on 04/14/2020).
[72] Da Liu et al. "Optimum Electric Boiler Capacity Configuration in a Regional Power Grid for a Wind Power Accommodation Scenario". In: *Energies* 9 (Mar. 2016), p. 144. DOI: 10.3390/en9030144.
[73] International Renewable Energy Agency. *RENEWABLE ENERGY TECHNOLOGIES: COST ANALYSIS SERIES*. June 2012. URL: https://www.irena.org/documentdownloads/publications/re_technologies_cost_analysis-wind_power.pdf (visited on 05/14/2020).
[74] Steve Völler. *TET4175 Design and Operation of Smart Grid Power Systems - Diesel Generator*. 2019.
[75] Norges Bank. *Valutakurser*. URL: https://www.norges-bank.no/tema/Statistikk/Valutakurser/?tab=currency&id=USD (visited on 05/01/2020).
[76] European heat pump association. *Large scale heat pumps in Europe vol. 2*. URL: https://www.ehpa.org/fileadmin/red/03._Media/Publications/Large_heat_pumps_in_Europe_Vol_2_FINAL.pdf (visited on 03/01/2020).

[77] European heat pump association. *Large scale heat pumps in Europe*. URL: https://www.ehpa.org/fileadmin/red/03._Media/03.02_Studies_and_reports/Large_heat_pumps_in_Europe_MDN_II_final4_small.pdf (visited on 03/01/2020).

[78] Sofia Simoes et al. "Assessing the long-term role of the SET Plan Energy technologies". In: (2013).

[79] Bastian Welsch et al. "Characteristics of medium deep borehole thermal energy storage". In: *International Journal of Energy Research* 40.13 (2016), pp. 1855–1868. DOI: 10.1002/er.3570. eprint: https://onlinelibrary.wiley.com/doi/pdf/10.1002/er.3570. URL: https://onlinelibrary.wiley.com/doi/abs/10.1002/er.3570.

[80] Michael Spielmann et al. *Transport Services*. ecoinvent report No. 14. Dübendorf: Swiss Centre for Life Cycle Inventories, 2007.

Appendix A

# Techno economical values in model

**Table A.1:** Techno economical values for different technologies in the model

| **PV ground south** | **2020** | **2025** | **2030** | **2035** | **2040** | **2045** | **2050** | **ref** |
|---|---|---|---|---|---|---|---|---|
| CAPEX [kNOK/MW] | 9022 | 7334 | 5647 | 4839 | 4226 | 3855 | 3560 | [66] |
| OPEX [kNOK/MW/year] | 107 | 87 | 67 | 57 | 50 | 46 | 42 | [66] |
| CF | 0.0798 | 0.0798 | 0.0798 | 0.0798 | 0.0798 | 0.0798 | 0.0798 | [3] |
| Lifetime [year] | 25 | 25 | 25 | 25 | 25 | 25 | 25 | [66] |
| **PV ground west/east** | **2020** | **2025** | **2030** | **2035** | **2040** | **2045** | **2050** | **ref** |
| CAPEX [kNOK/MW] | 9022 | 7334 | 5647 | 4839 | 4226 | 3855 | 3560 | [66] |
| OPEX [kNOK/MW/year] | 107 | 87 | 67 | 57 | 50 | 46 | 42 | [66] |
| CF | 0.0643 | 0.0643 | 0.0643 | 0.0643 | 0.0643 | 0.0643 | 0.0643 | [3] |
| Lifetime [year] | 25 | 25 | 25 | 25 | 25 | 25 | 25 | [66] |
| **PV saddle roof NW** | **2020** | **2025** | **2030** | **2035** | **2040** | **2045** | **2050** | **ref** |
| CAPEX [kNOK/MW] | 12479 | 9704 | 7798 | 6844 | 5890 | 5431 | 5373 | [66] |
| OPEX [kNOK/MW/year] | 123 | 96 | 77 | 68 | 58 | 54 | 53 | [66] |
| CF | 0.0602 | 0.0602 | 0.0602 | 0.0602 | 0.0602 | 0.0602 | 0.0602 | [3] |
| Lifetime [year] | 25 | 25 | 25 | 25 | 25 | 25 | 25 | [66] |
| **PV saddle roof SE** | **2020** | **2025** | **2030** | **2035** | **2040** | **2045** | **2050** | **ref** |
| CAPEX [kNOK/MW] | 12479 | 9704 | 7798 | 6844 | 5890 | 5431 | 5373 | [66] |
| OPEX [kNOK/MW/year] | 123 | 96 | 77 | 68 | 58 | 54 | 53 | [66] |
| CF | 0.0730 | 0.0730 | 0.0730 | 0.0730 | 0.0730 | 0.0730 | 0.0730 | [3] |
| Lifetime [year] | 25 | 25 | 25 | 25 | 25 | 25 | 25 | [66] |
| **PV saddle roof NE** | **2020** | **2025** | **2030** | **2035** | **2040** | **2045** | **2050** | **ref** |
| CAPEX [kNOK/MW] | 12479 | 9704 | 7798 | 6844 | 5890 | 5431 | 5373 | [66] |
| OPEX [kNOK/MW/year] | 123 | 96 | 77 | 68 | 58 | 54 | 53 | [66] |
| CF | 0.0542 | 0.0542 | 0.0542 | 0.0542 | 0.0542 | 0.0542 | 0.0542 | [3] |
| Lifetime [year] | 25 | 25 | 25 | 25 | 25 | 25 | 25 | [66] |

| **PV saddle roof SW** | **2020** | **2025** | **2030** | **2035** | **2040** | **2045** | **2050** | **ref** |
|---|---|---|---|---|---|---|---|---|
| CAPEX [kNOK/MW] | 12479 | 9704 | 7798 | 6844 | 5890 | 5431 | 5373 | [66] |
| OPEX [kNOK/MW/year] | 123 | 96 | 77 | 68 | 58 | 54 | 53 | [66] |
| CF | 0.0770 | 0.0770 | 0.0770 | 0.0770 | 0.0770 | 0.0770 | 0.0770 | [3] |
| Lifetime [year] | 25 | 25 | 25 | 25 | 25 | 25 | 25 | [66] |
| **PV flat roof SE/NW** | **2020** | **2025** | **2030** | **2035** | **2040** | **2045** | **2050** | **ref** |
| CAPEX [kNOK/MW] | 12479 | 9704 | 7798 | 6844 | 5890 | 5431 | 5373 | [66] |
| OPEX [kNOK/MW/year] | 123 | 96 | 77 | 68 | 58 | 54 | 53 | [66] |
| CF | 0.0643 | 0.0643 | 0.0643 | 0.0643 | 0.0643 | 0.0643 | 0.0643 | [3] |
| Lifetime [year] | 25 | 25 | 25 | 25 | 25 | 25 | 25 | [66] |
| **Onshore wind** | **2020** | **2025** | **2030** | **2035** | **2040** | **2045** | **2050** | **ref** |
| CAPEX [kNOK/MW] | 14980 | 13113 | 11245 | 10488 | 9717 | 8933 | 8134 | [66] |
| OPEX [kNOK/MW/year] | 414 | 379 | 344 | 318 | 292 | 266 | 241 | [66] |
| CF | 0.359 | 0.359 | 0.359 | 0.359 | 0.359 | 0.359 | 0.359 | [46] |
| Lifetime [year] | 20 | 20 | 20 | 20 | 20 | 20 | 20 | [66] |
| **Battery storage** | **2020** | **2025** | **2030** | **2035** | **2040** | **2045** | **2050** | **ref** |
| CAPEX [kNOK/GWh] | 2904545 | 1795537 | 1214628 | 1095806 | 976983 | 858161 | 739339 | [66] |
| OPEX [kNOK/GWh/year] | 72613.620 | 44888.420 | 30365.696 | 27395.139 | 24424.581 | 21454.024 | 18483.467 | [66] |
| Roundtrip efficiency | 0.85 | 0.85 | 0.85 | 0.85 | 0.85 | 0.85 | 0.85 | [66] |
| Lifetime [year] | 15 | 15 | 15 | 15 | 15 | 15 | 15 | [66] |
| **Hydrogen storage tank** | **2020** | **2025** | **2030** | **2035** | **2040** | **2045** | **2050** | **ref** |
| CAPEX [kNOK/GWh] | 92116 | 74984 | 56655 | 42807 | 42807 | 42807 | 42807 | [1] |
| OPEX [kNOK/GWh/year] | 2303 | 1874 | 1416 | 1070 | 1070 | 1070 | 1070 | [1] |
| Storage efficiency [%] | 95 | 95 | 95 | 95 | 95 | 95 | 95 | Assump |
| Lifetime [year] | 20 | 20 | 20 | 20 | 20 | 20 | 20 | [1] |
| Import cost [kNOK/GWh] | 1050 | 1050 | 1050 | 1050 | 1050 | 1050 | 1050 | [1] |

| **PEM electrolyser** | **2020** | **2025** | **2030** | **2035** | **2040** | **2045** | **2050** | **ref** |
|---|---|---|---|---|---|---|---|---|
| CAPEX [kNOK/MW] | 11280.78 | 10922.66 | 10385.48 | 9848.3 | 9848.3 | 9848.3 | 9848.3 | [1] |
| OPEX [kNOK/MW/year] | 379.0103 | 319.3237 | 259.637 | 259.637 | 259.637 | 259.637 | 259.637 | [1] |
| Efficiency [%] | 0.64 | 0.65 | 0.66 | 0.67 | 0.68 | 0.69 | 0.7 | [1] |
| Lifetime [year] | 10 | 10 | 10 | 10 | 10 | 10 | 10 | [1] |
| **Alkine electrolyser** | **2020** | **2025** | **2030** | **2035** | **2040** | **2045** | **2050** | **ref** |
| CAPEX [kNOK/MW] | 17906 | 15578.22 | 11997.02 | 11997.02 | 11997.02 | 11997.02 | 11997.02 | [1] |
| OPEX [kNOK/MW/year] | 282.0167 | 259.6333 | 237.25 | 237.25 | 237.25 | 237.25 | 237.25 | [1] |
| Efficiency [%] | 0.68 | 0.69 | 0.71 | 0.71 | 0.71 | 0.71 | 0.71 | [1] |
| Lifetime [year] | 9 | 9 | 9 | 9 | 9 | 9 | 9 | [1] |
| **PEMFC** | **2020** | **2025** | **2030** | **2035** | **2040** | **2045** | **2050** | **ref** |
| CAPEX [kNOK/MW] | 20294 | 13642 | 6989 | 6989 | 6989 | 6989 | 6989 | [1] |
| OPEX [kNOK/MW/year] | 1015 | 682 | 349 | 349 | 349 | 349 | 349 | [1] |
| Efficiency [%] | 0.4 | 0.43 | 0.45 | 0.45 | 0.45 | 0.45 | 0.45 | [1] |
| Heat to power ratio | 1.25 | 1.11 | 1 | 1 | 1 | 1 | 1 | [1] |
| Lifetime [year] | 8 | 8 | 9 | 9 | 9 | 9 | 9 | [1] |
| **Thermos thermal storage** | **2020** | **2025** | **2030** | **2035** | **2040** | **2045** | **2050** | **ref** |
| CAPEX [kNOK/GWh] | 1000000 | 1000000 | 1000000 | 1000000 | 1000000 | 1000000 | 1000000 | [4] |
| OPEX [kNOK/GWh/year] | 5000 | 5000 | 5000 | 5000 | 5000 | 5000 | 5000 | [4] |
| Roundtrip efficiency | 0.85 | 0.85 | 0.85 | 0.85 | 0.85 | 0.85 | 0.85 | [4] |
| Lifetime [year] | 40 | 40 | 40 | 40 | 40 | 40 | 40 | [4] |
| **UTES** | **2020** | **2025** | **2030** | **2035** | **2040** | **2045** | **2050** | **ref** |
| CAPEX [kNOK/GWh] | 2500000 | 2500000 | 2500000 | 2500000 | 2500000 | 2500000 | 2500000 | [78] assump |
| OPEX [kNOK/GWh/year] | 50000 | 50000 | 50000 | 50000 | 50000 | 50000 | 50000 | [78] assump |
| Roundtrip efficiency | 0.85 | 0.85 | 0.85 | 0.85 | 0.85 | 0.85 | 0.85 | [79] |
| Lifetime [year] | 20 | 20 | 20 | 20 | 20 | 20 | 20 | [1] |

| **Heat pump sea water** | **2020** | **2025** | **2030** | **2035** | **2040** | **2045** | **2050** | **ref** |
|---|---|---|---|---|---|---|---|---|
| CAPEX [kNOK/MW] | 6475 | 6135 | 5794 | 5453 | 5453 | 5453 | 5453 | [1] |
| OPEX [kNOK/MW/year] | 28 | 26.00 | 25 | 23 | 23 | 23 | 23 | [1] |
| Variable OPEX | 12 | 12 | 12 | 12 | 12 | 12 | 12 | [1] |
| COP | 2.50 | 2.50 | 2.50 | 2.50 | 2.50 | 2.50 | 2.50 | [77] assump |
| Lifetime [year] | 12 | 12 | 12 | 12 | 12 | 12 | 12 | [1] |
| **Heat pump geothermal** | **2020** | **2025** | **2030** | **2035** | **2040** | **2045** | **2050** | **ref** |
| CAPEX [kNOK/MW] | 12752 | 12081 | 11409 | 10738 | 10738 | 10738 | 10738 | [1] |
| OPEX [kNOK/MW/year] | 22 | 21 | 20 | 19 | 19 | 19 | 19 | [1] |
| Variable OPEX [kNOK/GWh] | 12 | 12 | 12 | 12 | 12 | 12 | 12 | [1] |
| COP | 2.50 | 2.50 | 2.50 | 2.50 | 2.50 | 2.50 | 2.50 | [77] assump |
| Lifetime [year] | 20 | 20 | 20 | 20 | 20 | 20 | 20 | [1] |
| **Electric radiator** | **2020** | **2025** | **2030** | **2035** | **2040** | **2045** | **2050** | **ref** |
| CAPEX [kNOK/MW] | 2000 | 2000 | 2000 | 2000 | 2000 | 2000 | 2000 | [78] |
| Efficiency [%] | 100 | 100 | 100 | 100 | 100 | 100 | 100 | [1] |
| Lifetime [year] | 15 | 15 | 15 | 15 | 15 | 15 | 15 | [1] |
| **Diesel generator** | **2020** | **2025** | **2030** | **2035** | **2040** | **2045** | **2050** | **ref** |
| CAPEX [kNOK/MW] | 3136 | 3136 | 3136 | 3136 | 3136 | 3136 | 3136 | [1] |
| OPEX [kNOK/MW/year] | 562.7 | 562.7 | 562.7 | 562.7 | 562.7 | 562.7 | 562.7 | [1] |
| Variable OPEX [kNOK/GWh] | 4.8 | 4.8 | 4.8 | 4.8 | 4.8 | 4.8 | 4.8 | [1] |
| Efficiency [%] | 41 | 41 | 41 | 41 | 41 | 41 | 41 | [1] |
| Lifetime [year] | 25 | 25 | 25 | 25 | 25 | 25 | 25 | [1] |
| Fuel cost [kNOK/GWh] | 752 | 752 | 752 | 752 | 752 | 752 | 752 | [4] |
| Emission [ktCO2/GWh$_{diesel}$] | 265 | 265 | 265 | 265 | 265 | 265 | 265 | [80] |

Appendix B

# Detailed numbers from all cases

## B.1 Capacity

**Table B.1:** Installed capacities B

| | 2020 | 2025 | 2030 | 2035 | 2040 | 2045 | 2050 |
|---|---|---|---|---|---|---|---|
| Coal boiler [MW] | 25.00 | 25.00 | | | | | |
| DHS [MW] | 10.27 | 8.19 | 7.09 | 6.48 | 6.05 | 5.48 | 5.41 |
| Coal CHP [MW] | 5.50 | 5.50 | | | | | |
| Coal turbine [MW] | 5.50 | 5.50 | | | | | |
| PV airport [MWp] | 0.14 | 0.14 | 0.14 | 0.14 | 0.06 | | |
| PV Elvesletta [MWp] | 0.03 | 0.03 | 0.03 | 0.03 | 0.01 | | |
| PV ground S [MWp] | | | | | | 2.18 | 2.18 |
| Wind [MW] | | 0.85 | 27.53 | 27.53 | 27.53 | 27.13 | 26.59 |
| El boiler [MW] | | | 0.82 | 0.82 | 0.82 | 0.82 | |
| DH heat pump [MW] | | | 7.47 | 7.47 | 7.47 | 6.44 | 6.44 |
| Oil boiler [MW] | 5.12 | 5.12 | 2.17 | 0.71 | 0.58 | 0.06 | |
| El radiator [MW] | | 1.46 | 1.92 | 2.16 | 2.23 | 2.48 | 2.31 |
| H1-RES [MW] | | 0.05 | 0.11 | 0.11 | 0.11 | 0.11 | 0.08 |
| H1-COM [MW] | | 0.12 | 0.23 | 0.23 | 0.23 | 0.20 | 0.14 |
| Battery [MWh] | | | 7.96 | 11.81 | 11.81 | 13.15 | 13.07 |
| Thermos [MWh] | | | 1.10 | 1.10 | 1.10 | 1.10 | 1.10 |
| ICE car | 1350 | 675 | | | | | |
| Electric car | 8 | 683 | 1358 | 1358 | 1358 | 1358 | 1358 |
| ICE snow mobile | 2167 | | | | | | |
| Electric snow mobile | | 2167 | 2167 | 2167 | 2167 | 2167 | 2167 |
| ICE van | 314 | 157 | | | | | |
| Electric van | 2 | 159 | 316 | 316 | 316 | 316 | 316 |

**Table B.2:** Installed capacities BNC

| | 2020 | 2025 | 2030 | 2035 | 2040 | 2045 | 2050 |
|---|---|---|---|---|---|---|---|
| Coal boiler [MW] | 25.00 | 25.00 | | | | | |
| DHS [MW] | 10.27 | 8.19 | 7.11 | 6.27 | 5.73 | 5.12 | 5.02 |
| Coal CHP [MW] | 5.50 | 5.50 | | | | | |
| Coal turbine [MW] | 5.50 | 5.50 | | | | | |
| PV airport [MWp] | 0.14 | 0.14 | 0.14 | 0.14 | 0.06 | | |
| PV Elvesletta [MWp] | 0.03 | 0.03 | 0.03 | 0.03 | 0.01 | | |
| PV ground S [MWp] | | | | | | 2.78 | 2.91 |
| Wind [MW] | | 0.85 | 28.40 | 28.40 | 28.40 | 27.74 | 27.03 |
| El boiler [MW] | | | | | | 0.06 | 0.06 |
| DH heat pump [MW] | | | 8.11 | 8.11 | 8.11 | 5.97 | 5.97 |
| El radiator [MW] | | 1.46 | 1.90 | 2.37 | 2.55 | 2.84 | 2.70 |
| H1-RES [MW] | | 0.05 | 0.11 | 0.11 | 0.11 | 0.11 | 0.08 |
| H1-COM [MW] | | 0.12 | 0.23 | 0.23 | 0.23 | 0.20 | 0.14 |
| Battery [MWh] | | | 12.98 | 13.17 | 13.24 | 12.73 | 13.71 |
| Thermos [MWh] | | | 1.71 | 1.71 | 1.71 | 1.71 | 1.71 |
| ICE car | 1350 | 675 | | | | | |
| Electric car | 8 | 683 | 1358 | 1358 | 1358 | 1358 | 1358 |
| ICE snow mobile | 2167 | | | | | | |
| Electric snow mobile | | 2167 | 2167 | 2167 | 2167 | 2167 | 2167 |
| ICE van | 314 | 157 | | | | | |
| Electric van | 2 | 159 | 316 | 316 | 316 | 316 | 316 |

**Table B.3:** Installed capacities ISO

| | 2020 | 2025 | 2030 | 2035 | 2040 | 2045 | 2050 |
|---|---|---|---|---|---|---|---|
| Coal boiler [MW] | 25.00 | 25.00 | | | | | |
| DHS [MW] | 10.27 | 8.19 | 6.99 | 6.24 | 6.12 | 5.11 | 5.02 |
| Coal CHP [MW] | 5.50 | 5.50 | | | | | |
| Coal turbine [MW] | 5.50 | 5.50 | | | | | |
| PV airport [MWp] | 0.14 | 0.14 | 0.14 | 0.14 | 0.06 | | |
| PV Elvesletta [MWp] | 0.03 | 0.03 | 0.03 | 0.03 | 0.01 | | |
| PV ground S [MWp] | | | | | 0.65 | 2.77 | 2.86 |
| Wind [MW] | 1.02 | 1.71 | 28.50 | 28.50 | 27.48 | 27.74 | 27.04 |
| El boiler [MW] | | | | | | 0.05 | 0.05 |
| DH heat pump [MW] | | | 8.03 | 8.03 | 8.03 | 5.97 | 5.97 |
| El radiator [MW] | | 1.46 | 2.02 | 2.41 | 2.16 | 2.85 | 2.70 |
| H1-RES [MW] | | 0.05 | 0.11 | 0.11 | 0.11 | 0.11 | 0.08 |
| H1-COM [MW] | | 0.12 | 0.23 | 0.23 | 0.23 | 0.20 | 0.14 |
| Battery [MWh] | | | 13.13 | 13.13 | 13.13 | 12.89 | 13.71 |
| Thermos [MWh] | | | 1.52 | 1.52 | 1.52 | 1.52 | 1.52 |
| ICE car | 1350 | 675 | | | | | |
| Electric car | 1358 | 1358 | 1358 | 1358 | 1358 | 1358 | 1358 |
| ICE snow mobile | 2167 | | | | | | |
| Electric snow mobile | 2167 | 2167 | 2167 | 2167 | 2167 | 2167 | 2167 |
| ICE van | 314 | 157 | | | | | |
| Electric van | 316 | 316 | 316 | 316 | 316 | 316 | 316 |

**Table B.4:** Installed capacities NWI

| | 2020 | 2025 | 2030 | 2035 | 2040 | 2045 | 2050 |
|---|---|---|---|---|---|---|---|
| Coal boiler [MW] | 25.00 | 25.00 | | | | | |
| DHS [MW] | 10.27 | 8.95 | 7.30 | 6.72 | 6.67 | 6.67 | 6.67 |
| Coal CHP [MW] | 5.50 | 5.50 | | | | | |
| Coal turbine [MW] | 5.50 | 5.50 | | | | | |
| New diesel generator [MW] | | | 6.53 | 6.53 | 6.53 | 6.58 | 6.70 |
| PV airport [MWp] | 0.14 | 0.14 | 0.14 | 0.14 | 0.06 | | |
| PV Elvesletta [MWp] | 0.03 | 0.03 | 0.03 | 0.03 | 0.01 | | |
| PV ground S [MWp] | | 1.64 | 23.94 | 32.45 | 38.10 | 49.31 | 64.95 |
| PV ground W/E [MWp] | | | 5.78 | 5.78 | 5.78 | 5.78 | 5.78 |
| El boiler [MW] | | | 0.25 | 0.25 | 0.25 | 2.74 | 2.49 |
| DH heat pump [MW] | | | 2.73 | 2.73 | 2.73 | 3.06 | 4.33 |
| Oil boiler [MW] | 15.70 | 15.70 | 8.68 | 7.75 | 7.75 | 7.94 | 7.94 |
| El radiator [MW] | | 0.53 | 0.53 | 0.53 | 0.29 | 0.60 | 0.60 |
| H1-RES [MW] | | 0.05 | 0.11 | 0.11 | 0.11 | 0.11 | 0.08 |
| H1-COM [MW] | 0.12 | 0.23 | 0.23 | 0.23 | 0.23 | 0.20 | 0.14 |
| H3-COM [MW] | | | 0.52 | 0.60 | 0.60 | 0.12 | 0.04 |
| H4-RES [MW] | | | 0.26 | 0.34 | 0.26 | 0.33 | 0.25 |
| Battery [MWh] | | | 21.70 | 27.71 | 27.71 | 24.96 | 46.66 |
| Thermos [MWh] | | | 0.25 | 1.05 | 1.05 | 1.05 | 1.05 |
| ICE car | 1350 | 675 | | | | | |
| Electric car | 8 | 683 | 1358 | 1358 | 1358 | 1358 | 1358 |
| ICE snow mobile | 2167 | | | | | | |
| Electric snow mobile | | 2167 | 2167 | 2167 | 2167 | 2167 | 2167 |
| ICE van | 314 | 157 | | | | | |
| Electric van | 2 | 159 | 316 | 316 | 316 | 316 | 316 |

**Table B.5:** Installed capacities NWC

| | 2020 | 2025 | 2030 | 2035 | 2040 | 2045 | 2050 |
|---|---|---|---|---|---|---|---|
| Coal boiler [MW] | 25.00 | 25.00 | | | | | |
| DHS [MW] | 10.27 | 8.93 | 6.51 | 6.01 | 5.77 | 5.77 | 5.57 |
| Coal CHP [MW] | 5.50 | 5.50 | | | | | |
| Coal turbine [MW] | 5.50 | 5.50 | | | | | |
| New diesel generator [MW] | | 0.08 | 0.08 | 0.08 | 0.08 | 0.08 | |
| PV airport [MWp] | 0.14 | 0.14 | 0.14 | 0.14 | 0.06 | | |
| PV Elvesletta [MWp] | 0.03 | 0.03 | 0.03 | 0.03 | 0.01 | | |
| DH heat pump [MW] | | | 1.22 | 1.22 | 1.22 | 0.64 | 0.64 |
| El radiator [MW] | | 0.25 | 0.25 | 0.25 | 0.12 | 0.12 | 0.12 |
| H1-RES [MW] | 0.06 | 0.11 | 0.11 | 0.11 | 0.11 | 0.11 | 0.08 |
| H1-COM [MW] | 0.12 | 0.23 | 0.23 | 0.23 | 0.23 | 0.20 | 0.14 |
| H2-RES [MW] | | | 0.35 | 0.35 | 0.35 | 0.45 | 0.45 |
| H3-RES [MW] | | | 0.26 | 0.26 | 0.26 | 0.14 | 0.14 |
| H3-COM [MW] | | 0.05 | 0.57 | 0.69 | 0.69 | 0.43 | 0.48 |
| H4-RES [MW] | | 0.08 | 0.34 | 0.34 | 0.26 | 0.33 | 0.25 |
| Battery [MWh] | | | 0.90 | 0.90 | 0.90 | 1.58 | 1.80 |
| Hydrogen tank [MWh] | | | 6.00 | 6.00 | 6.28 | 06.28 | 4.69 |
| Fuel cell [MW] | | | 6.85 | 6.66 | 6.60 | 6.56 | 6.44 |
| Thermos [MWh] | | | 0.91 | 0.91 | 0.91 | 1.17 | 1.17 |
| ICE car | 1350 | 675 | | | | | |
| Electric car | 8 | 683 | 1358 | 1358 | 1358 | 1358 | 1358 |
| ICE snow mobile | 2167 | | | | | | |
| Electric snow mobile | | 2167 | 2167 | 2167 | 2167 | 2167 | 2167 |
| ICE van | 314 | 157 | | | | | |
| Electric van | 2 | 159 | 316 | 316 | 316 | 316 | 316 |

**Table B.6:** Installed capacities B-G

| | 2020 | 2025 | 2030 | 2035 | 2040 | 2045 | 2050 |
|---|---|---|---|---|---|---|---|
| Coal boiler [MW] | 25.00 | 25.00 | | | | | |
| DHS [MW] | 10.27 | 8.39 | 7.15 | 6.86 | 6.81 | 6.08 | 6.01 |
| Coal CHP [MW] | 5.50 | 5.50 | | | | | |
| Coal turbine [MW] | 5.50 | 5.50 | | | | | |
| PV airport [MWp] | 0.14 | 0.14 | 0.14 | 0.14 | 0.06 | | |
| PV Elvesletta [MWp] | 0.03 | 0.03 | 0.03 | 0.03 | 0.01 | | |
| PV ground S [MWp] | | | | | 0.02 | 2.88 | 3.21 |
| Wind [MW] | | 1.90 | 30.74 | 31.78 | 32.59 | 34.02 | 35.09 |
| El boiler [MW] | | | 0.39 | 0.39 | 0.39 | 0.39 | |
| DH heat pump [MW] | | | 8.07 | 8.07 | 8.07 | 7.14 | 7.14 |
| Oil boiler [MW] | 2.96 | 2.96 | 1.25 | 0.71 | 0.71 | 0.06 | |
| El radiator [MW] | | 1.51 | 2.35 | 2.50 | 2.39 | 3.00 | 3.02 |
| H1-RES [MW] | | 0.05 | 0.11 | 0.11 | 0.11 | 0.11 | 0.08 |
| H1-COM [MW] | | 0.12 | 0.23 | 0.23 | 0.23 | 0.20 | 0.14 |
| Battery [MWh] | | | 11.16 | 13.66 | 13.66 | 16.57 | 17.45 |
| Thermos [MWh] | | | 1.17 | 1.17 | 1.17 | 1.17 | 1.17 |
| ICE car | 1350 | 675 | | | | | |
| Electric car | 8 | 802 | 1607 | 1749 | 1902 | 2070 | 2252 |
| ICE snow mobile | 2167 | | | | | | |
| Electric snow mobile | | 2358 | 2565 | 2790 | 3036 | 3303 | 3593 |
| ICE van | 314 | 157 | | | | | |
| Electric van | 2 | 187 | 374 | 407 | 443 | 482 | 524 |

**Table B.7:** Installed capacities B-COST

| | 2020 | 2025 | 2030 | 2035 | 2040 | 2045 | 2050 |
|---|---|---|---|---|---|---|---|
| Coal boiler [MW] | 25 | 25 | | | | | |
| DHS [MW] | 10.27 | 8.46 | 7.32 | 6.81 | 6.43 | 5.79 | 5.61 |
| Coal CHP [MW] | 5.50 | 5.50 | | | | | |
| Coal turbine [MW] | 5.50 | 5.50 | | | | | |
| PV airport [MWp] | 0.14 | 0.14 | 0.14 | 0.14 | 0.06 | | |
| PV Elvesletta [MWp] | 0.03 | 0.03 | 0.03 | 0.03 | 0.01 | | |
| PV ground S [MWp] | | | | 0.20 | 0.46 | 2.12 | 2.21 |
| Wind [MW] | | 0.68 | 26.22 | 26.87 | 26.87 | 26.58 | 26.24 |
| El boiler [MW] | | | 1.24 | 1.24 | 1.24 | 1.24 | |
| DH heat pump [MW] | | | 7.33 | 7.52 | 7.52 | 6.81 | 6.63 |
| Oil boiler [MW] | 5.26 | 5.26 | 2.23 | 0.85 | 0.64 | 0.02 | |
| El radiator [MW] | | 1.19 | 1.69 | 1.84 | 1.85 | 2.17 | 2.11 |
| H1-RES [MW] | | 0.05 | 0.11 | 0.11 | 0.11 | 0.11 | 0.08 |
| H1-COM [MW] | | 0.12 | 0.23 | 0.23 | 0.23 | 0.20 | 0.14 |
| Battery [MWh] | | | 9.93 | 11.14 | 11.14 | 13.11 | 12.92 |
| Thermos [MWh] | | | 1.78 | 1.78 | 1.78 | 1.78 | 1.78 |
| ICE car | 1350 | 675 | | | | | |
| Electric car | 8 | 683 | 1358 | 1358 | 1358 | 1358 | 1358 |
| ICE snow mobile | 2167 | | | | | | |
| Electric snow mobile | | 2167 | 2167 | 2167 | 2167 | 2167 | 2167 |
| ICE van | 314 | 157 | | | | | |
| Electric van | 2 | 159 | 316 | 316 | 316 | 316 | 316 |

**Table B.8:** Installed capacities B-CF

| | 2020 | 2025 | 2030 | 2035 | 2040 | 2045 | 2050 |
|---|---|---|---|---|---|---|---|
| Coal boiler [MW] | 25 | 25 | | | | | |
| DHS [MW] | 10.27 | 8.39 | 7.22 | 6.71 | 6.34 | 5.74 | 5.61 |
| Coal CHP [MW] | 5.50 | 5.50 | | | | | |
| Coal turbine [MW] | 5.50 | 5.50 | | | | | |
| PV airport [MWp] | 0.14 | 0.14 | 0.14 | 0.14 | 0.06 | | |
| PV Elvesletta [MWp] | 0.03 | 0.03 | 0.03 | 0.03 | 0.01 | | |
| PV ground S [MWp] | | | | | 0.28 | 1.86 | 2.12 |
| Wind [MW] | | 0.83 | 30.71 | 31.06 | 31.06 | 30.70 | 30.22 |
| El boiler [MW] | | | 1.09 | 1.09 | 1.09 | 1.09 | |
| DH heat pump [MW] | | | 7.35 | 7.45 | 7.45 | 6.73 | 6.63 |
| Oil boiler [MW] | 4.96 | 4.96 | 2.10 | 0.92 | 0.67 | 0.07 | |
| El radiator [MW] | | 1.26 | 1.79 | 1.93 | 1.94 | 2.22 | 2.11 |
| H1-RES [MW] | | 0.05 | 0.11 | 0.11 | 0.11 | 0.11 | 0.08 |
| H1-COM [MW] | | 0.12 | 0.23 | 0.23 | 0.23 | 0.20 | 0.14 |
| Battery [MWh] | | | 9.30 | 11.31 | 11.31 | 13.12 | 12.92 |
| Thermos [MWh] | | | 1.37 | 1.37 | 1.37 | 1.37 | 1.37 |
| ICE car | 1350 | 675 | | | | | |
| Electric car | 8 | 683 | 1358 | 1358 | 1358 | 1358 | 1358 |
| ICE snow mobile | 2167 | | | | | | |
| Electric snow mobile | | 2167 | 2167 | 2167 | 2167 | 2167 | 2167 |
| ICE van | 314 | 157 | | | | | |
| Electric van | 2 | 159 | 316 | 316 | 316 | 316 | 316 |

**Table B.9:** Installed capacities B-BiPV

| | 2020 | 2025 | 2030 | 2035 | 2040 | 2045 | 2050 |
|---|---|---|---|---|---|---|---|
| Coal boiler [MW] | 25.00 | 25.00 | | | | | |
| DHS [MW] | 10.27 | 8.19 | 7.15 | 6.51 | 5.87 | 0.12 | 0.11 |
| Coal CHP [MW] | 5.50 | 5.50 | | | | | |
| Coal turbine [MW] | 5.50 | 5.50 | | | | | |
| PV airport [MWp] | 0.14 | 0.14 | 0.14 | 0.14 | 0.06 | | |
| PV Elvesletta [MWp] | 0.03 | 0.03 | 0.03 | 0.03 | 0.01 | | |
| PV ground tracker [MWp] | | | 0.32 | 1.17 | 1.17 | 7.53 | 9.41 |
| Wind [MW] | | 0.85 | 27.22 | 27.22 | 27.22 | 32.50 | 30.44 |
| El boiler [MW] | | | 0.76 | 0.76 | 0.76 | 0.76 | 0.05 |
| DH heat pump [MW] | | | 7.60 | 7.60 | 7.60 | 0.14 | 0.14 |
| Oil boiler [MW] | 3.76 | 3.76 | 1.59 | | | | |
| El radiator [MW] | | 1.46 | 1.86 | 2.13 | 2.41 | 7.84 | 7.61 |
| H1-RES [MW] | | 0.05 | 0.11 | 0.11 | 0.11 | 0.11 | 0.08 |
| H1-COM [MW] | | 0.12 | 0.23 | 0.23 | 0.23 | 0.20 | 0.14 |
| Battery [MWh] | | | 9.25 | 13.55 | 13.55 | 28.47 | 35.91 |
| Thermos [MWh] | | | 2.00 | 2.00 | 2.00 | 2.00 | 2.00 |
| ICE car | 1350 | 675 | | | | | |
| Electric car | 8 | 683 | 1358 | 1358 | 1358 | 1358 | 1358 |
| ICE snow mobile | 2167 | | | | | | |
| Electric snow mobile | 0 | 2167 | 2167 | 2167 | 2167 | 2167 | 2167 |
| ICE van | 314 | 157 | | | | | |
| Electric van | 2 | 159 | 316 | 316 | 316 | 316 | 316 |

## B.2 Detailed commodity flows

**Table B.10:** Commodity flow [GWh] in different technologies B

| | 2020 | 2025 | 2030 | 2035 | 2040 | 2045 | 2050 |
|---|---|---|---|---|---|---|---|
| El demand | 42.9 | 44.0 | 32.5 | 32.5 | 32.5 | 32.5 | 32.5 |
| Heat demand | 58.9 | 55.3 | 51.7 | 49.6 | 47.5 | 45.6 | 44.3 |
| EV demand | 0.0 | 4.1 | 6.6 | 6.6 | 6.6 | 6.6 | 6.6 |
| Coal CHP (el/heat) | 21.1/70.0 | 19.6/65.0 | | | | | |
| Coal turbine | 25.2 | 31.3 | | | | | |
| Existing PV | 0.1 | 0.1 | 0.1 | 0.1 | 0.0 | | |
| PV ground S | | | | | | 1.3 | 1.3 |
| Wind | | 2.7 | 77.1 | 78.3 | 77.9 | 77.4 | 73.5 |
| El boiler | | | 3.4 | 3.6 | 3.6 | 3.5 | |
| DH heat pump | | | 42.4 | 38.8 | 35.9 | 30.8 | 34.4 |
| Oil boiler | | | 2.6 | 1.0 | 0.4 | 0.1 | |
| El radiator | | 1.6 | 11.0 | 13.1 | 13.9 | 16.7 | 15.3 |
| Battery (in/out) | | | 4.0/3.4 | 5.5/4.6 | 5.3/4.5 | 5.5/4.7 | 4.9/4.2 |
| Thermos (in/out) | | | 0.6/0.5 | 0.4/0.3 | 0.5/0.4 | 0.2/0.2 | 0.3/0.2 |
| Curtailed energy | | 1.1 | 9.5 | 8.3 | 8.6 | 8.1 | 10.3 |
| Import diesel | 24.0 | 9.3 | 2.9 | 1.2 | 0.5 | 0.1 | |
| Mining coal | 255.6 | 273.8 | | | | | |
| CO2 [kt] | 86.9 | 88.7 | 0.8 | 0.3 | 0.1 | 0.0 | |

**Table B.11:** Commodity flow [GWh] in different technologies BNC

| | 2020 | 2025 | 2030 | 2035 | 2040 | 2045 | 2050 |
|---|---|---|---|---|---|---|---|
| El demand | 42.9 | 44.0 | 32.5 | 32.5 | 32.5 | 32.5 | 32.5 |
| Heat demand | 58.9 | 55.3 | 51.7 | 49.6 | 47.5 | 45.6 | 44.3 |
| EV demand | 0.0 | 4.1 | 6.6 | 6.6 | 6.6 | 6.6 | 6.6 |
| Coal CHP (el/heat) | 21.1/70.0 | 19.6/65.0 | | | | | |
| Coal turbine | 25.2 | 31.3 | | | | | |
| Existing PV | 0.1 | 0.1 | 0.1 | 0.1 | 0.0 | | |
| PV ground S | | | | | | 1.6 | 1.8 |
| Wind | | 2.7 | 76.8 | 77.6 | 77.6 | 76.7 | 75.3 |
| El boiler | | | | | | 0.3 | 0.3 |
| DH heat pump | | | 47.0 | 40.7 | 36.0 | 30.3 | 29.9 |
| El radiator | | 1.6 | 12.2 | 15.5 | 17.3 | 20.0 | 18.9 |
| Battery (in/out) | | | 5.0/4.2 | 5.2/4.4 | 5.2/4.4 | 4.9/4.1 | 5.1/4.3 |
| Thermos (in/out) | | | 0.6/0.5 | 0.8/0.7 | 0.8/0.7 | 0.5/0.4 | 0.3/0.3 |
| Curtailed energy | | 1.1 | 12.5 | 11.7 | 11.7 | 10.9 | 10.0 |
| Import diesel | 24.0 | 9.3 | | | | | |
| Mining coal | 255.6 | 273.8 | | | | | |
| CO2 [kt] | 86.9 | 88.7 | | | | | |

**Table B.12:** Commodity flow [GWh] in different technologies ISO

| | 2020 | 2025 | 2030 | 2035 | 2040 | 2045 | 2050 |
|---|---|---|---|---|---|---|---|
| El demand | 42.9 | 44.0 | 32.5 | 32.5 | 32.5 | 32.5 | 32.5 |
| Heat demand | 58.9 | 55.3 | 51.7 | 49.6 | 47.5 | 45.6 | 44.3 |
| EV demand | 6.6 | 6.6 | 6.6 | 6.6 | 6.6 | 6.6 | 6.6 |
| Coal CHP | 21.1/70.0 | 19.5/64.6 | | | | | |
| Coal turbine | 29.1 | 31.4 | | | | | |
| Existing PV | 0.1 | 0.1 | 0.1 | 0.1 | 0.0 | | |
| PV ground S | | | | | 0.4 | 1.7 | 1.7 |
| Wind | 3.2 | 5.4 | 77.3 | 77.8 | 75.3 | 76.6 | 75.3 |
| El boiler | | | | | | 0.2 | 0.2 |
| DH heat pump | | | 46.1 | 40.2 | 39.9 | 30.3 | 30.0 |
| El radiator | | 1.6 | 13.0 | 15.8 | 14.0 | 20.0 | 18.8 |
| Battery (in/out) | | | 5.1/4.3 | 5.2/4.4 | 5.0/4.2 | 4.9/4.2 | 5.1/4.3 |
| Thermos (in/out) | | | 0.5/0.5 | 0.6/0.5 | 0.7/0.6 | 0.4/0.4 | 0.3/0.3 |
| Curtailed energy | | 0.7 | 12.4 | 11.8 | 11.2 | 10.9 | 10.1 |
| Mining coal | 273.8 | 273.8 | | | | | |
| CO2 [kt] | 86.2 | 86.2 | | | | | |

**Table B.13:** Commodity flow [GWh] in different technologies NWI

| | 2020 | 2025 | 2030 | 2035 | 2040 | 2045 | 2050 |
|---|---|---|---|---|---|---|---|
| El demand | 42.9 | 44.0 | 32.5 | 32.5 | 32.5 | 32.5 | 32.5 |
| Heat demand | 57.9 | 54.3 | 44.8 | 41.4 | 39.9 | 41.7 | 41.7 |
| EV demand | 0.0 | 4.1 | 6.6 | 6.6 | 6.6 | 6.6 | 6.6 |
| Coal CHP (el/heat) | 20.8/68.8 | 19.4/64.4 | | | | | |
| Coal turbine | 25.6 | 31.5 | | | | | |
| Diesel generator | | | 33.1 | 29.7 | 28.4 | 27.9 | 26.5 |
| Existing PV | 0.1 | 0.1 | 0.1 | 0.0 | 0.0 | | |
| PV ground S | | 1.1 | 16.7 | 22.0 | 23.6 | 29.0 | 36.0 |
| PV ground W/E | | | 3.2 | 2.2 | 2.2 | 2.0 | 2.0 |
| El boiler | | | 0.1 | 0.3 | 0.3 | 4.2 | 6.3 |
| DH heat pump | | | 20.1 | 20.0 | 20.4 | 19.2 | 22.1 |
| Oil boiler | | | 32.2 | 28.0 | 26.0 | 24.7 | 18.8 |
| El radiator | | 0.2 | 0.8 | 0.9 | 0.7 | 1.4 | 2.0 |
| Battery (in/out) | | | 5.3/4.5 | 8.0/6.8 | 9.2/7.8 | 9.7/8.2 | 15.2/12.9 |
| Thermos (in/out) | | | 0.0/0.0 | 0.3/0.3 | 0.2/0.2 | 0.3/0.2 | 0.2/0.2 |
| Curtailed energy | | 0.1 | 0.0 | 1.8 | 4.1 | 6.8 | 10.7 |
| Import diesel | 24.0 | 9.3 | 116.4 | 103.6 | 98.2 | 95.4 | 85.4 |
| Mining coal | 254.9 | 273.8 | | | | | |
| CO2 [kt] | 86.6 | 88.7 | 30.9 | 27.5 | 26.0 | 25.3 | 22.6 |

**Table B.14:** Commodity flow [GWh] in different technologies NWC

| | 2020 | 2025 | 2030 | 2035 | 2040 | 2045 | 2050 |
|---|---|---|---|---|---|---|---|
| El demand | 42.9 | 44.0 | 32.5 | 32.5 | 32.5 | 32.5 | 32.5 |
| Heat demand | 57.3 | 52.6 | 38.6 | 35.5 | 34.2 | 34.4 | 33.0 |
| EV demand | 0.0 | 4.1 | 6.6 | 6.6 | 6.6 | 6.6 | 6.6 |
| Coal CHP (el/heat) | 20.6/68.2 | 18.9/62.5 | | | | | |
| Coal turbine | 25.8 | 32.3 | | | | | |
| Diesel generator | | 0.7 | | | | | |
| Existing PV | 0.1 | 0.1 | | | | | |
| DH heat pump | | | 2.1 | 1.2 | 0.8 | 0.8 | 0.5 |
| Fuel cell (el+heat) | | | 55.3 | 51.4 | 51.4 | 48.1 | 47.5 |
| El radiator | | 0.0 | 0.1 | 0.0 | 0.0 | 0.0 | 0.0 |
| Battery (in/out) | | | 0.2/0.2 | 0.1/0.1 | 0.2/0.1 | 0.2/0.2 | 0.3/0.2 |
| Thermos (in/out) | | | 0.5/0.4 | 0.5/0.5 | 0.3/0.2 | 0.2/0.2 | 1.3/1.1 |
| Curtailed energy | | 0.0 | 22.6 | 18.2 | 19.5 | 12.6 | 13.0 |
| Import hydrogen | | | 123.4 | 119.5 | 117.9 | 118.1 | 116.8 |
| Import diesel | 24.0 | 11.0 | | | | | |
| Mining coal | 254.5 | 273.8 | | | | | |
| CO2 [kt] | 86.5 | 89.2 | | | | | |

**Table B.15:** Commodity flow [GWh] in different technologies B-G

| | 2020 | 2025 | 2030 | 2035 | 2040 | 2045 | 2050 |
|---|---|---|---|---|---|---|---|
| El demand | 42.9 | 46.3 | 35.9 | 37.7 | 39.6 | 41.7 | 43.8 |
| Heat demand | 58.9 | 56.8 | 54.5 | 53.6 | 52.7 | 52.1 | 51.7 |
| EV demand | 0.0 | 4.6 | 7.8 | 8.5 | 9.3 | 10.1 | 11.0 |
| Coal CHP (el/heat) | 21.1/70.0 | 20.1/66.5 | | | | | |
| Coal turbine | 25.2 | 30.6 | | | | | |
| Existing PV | 0.1 | 0.1 | 0.1 | 0.1 | 0.0 | | |
| PV ground S | | | | | 0.0 | 1.8 | 1.9 |
| Wind | | 6.0 | 85.0 | 88.5 | 90.5 | 95.2 | 97.1 |
| El boiler | | | 1.8 | 1.8 | 1.8 | 1.8 | |
| DH heat pump | | | 44.8 | 43.1 | 43.0 | 35.6 | 36.9 |
| Oil boiler | | | 1.3 | 0.6 | 0.6 | 0.1 | |
| El radiator | | 1.6 | 14.3 | 15.4 | 14.5 | 20.6 | 20.7 |
| Battery (in/out) | | | 5.2/4.4 | 6.0/5.1 | 6.0/5.1 | 6.5/5.5 | 6.5/5.5 |
| Thermos (in/out) | | | 0.5/0.5 | 0.3/0.3 | 0.4/0.4 | 0.2/0.2 | 0.2/0.2 |
| Curtailed energy | | 0.9 | 11.6 | 11.5 | 12.0 | 12.0 | 13.6 |
| Import diesel | 24.0 | 9.3 | 1.5 | 0.7 | 0.7 | 0.1 | |
| Mining coal | 255.6 | 273.8 | | | | | |
| CO2 [kt] | 86.9 | 88.7 | 0.4 | 0.2 | 0.2 | 0.0 | |

**Table B.16:** Commodity flow [GWh] in different technologies B-COST

| | 2020 | 2025 | 2030 | 2035 | 2040 | 2045 | 2050 |
|---|---|---|---|---|---|---|---|
| El demand | 42.9 | 44.0 | 32.5 | 32.5 | 32.5 | 32.5 | 32.5 |
| Heat demand | 58.9 | 55.3 | 51.7 | 49.6 | 47.5 | 45.6 | 44.3 |
| EV demand | 0.0 | 4.1 | 6.6 | 6.6 | 6.6 | 6.6 | 6.6 |
| Coal CHP (el/heat) | 21.1/70.0 | 19.6/65.1 | | | | | |
| Coal turbine | 25.2 | 31.2 | | | | | |
| Existing PV | 0.1 | 0.1 | 0.1 | 0.1 | 0.0 | | |
| PV ground S | | | | 0.1 | 0.3 | 1.5 | 1.3 |
| Wind | | 2.1 | 76.2 | 77.5 | 77.1 | 77.0 | 72.6 |
| El boiler | | | 4.4 | 5.1 | 5.4 | 5.3 | |
| DH heat pump | | | 41.9 | 39.5 | 37.6 | 32.2 | 36.3 |
| Oil boiler | | | 4.2 | 1.7 | 0.5 | 0.0 | |
| El radiator | | 1.1 | 9.2 | 10.8 | 11.0 | 14.1 | 13.8 |
| Battery (in/out) | | | 4.8/4.1 | 5.2/4.4 | 5.2/4.4 | 5.5/4.7 | 4.8/4.1 |
| Thermos (in/out) | | | 0.6/0.5 | 0.8/0.7 | 0.7/0.6 | 0.5/0.4 | 0.4/0.4 |
| Curtailed energy | | 0.6 | 6.3 | 7.0 | 7.4 | 6.6 | 10.2 |
| Import diesel | 24.0 | 9.3 | 4.7 | 1.9 | 0.6 | 0.1 | |
| Mining coal | 204.5 | 219 | | | | | |
| CO2 [kt] | 86.9 | 88.7 | 1.2 | 0.5 | 0.1 | 0.0 | |

**Table B.17:** Commodity flow [GWh] in different technologies B-CF

| | 2020 | 2025 | 2030 | 2035 | 2040 | 2045 | 2050 |
|---|---|---|---|---|---|---|---|
| El demand | 42.9 | 44.0 | 32.5 | 32.5 | 32.5 | 32.5 | 32.5 |
| Heat demand | 58.9 | 55.3 | 51.7 | 49.6 | 47.5 | 45.6 | 44.3 |
| EV demand | 0.0 | 4.1 | 6.6 | 6.6 | 6.6 | 6.6 | 6.6 |
| Coal CHP (el/heat) | 21.1/70.0 | 19.6/65.1 | | | | | |
| Coal turbine | 25.2 | 31.2 | | | | | |
| Existing PV | 0.1 | 0.1 | 0.1 | 0.1 | 0.0 | | |
| PV ground S | | | | | 0.2 | 1.3 | 1.2 |
| Wind | | 2.3 | 76.7 | 77.6 | 77.2 | 77.0 | 72.7 |
| El boiler | | | 4.2 | 4.5 | 4.8 | 4.7 | |
| DH heat pump | | | 41.8 | 39.3 | 37.4 | 32.3 | 36.3 |
| Oil boiler | | | 3.6 | 1.7 | 0.5 | 0.1 | |
| El radiator | | 1.2 | 10.0 | 11.4 | 11.6 | 14.4 | 13.7 |
| Battery (in/out) | | | 4.5/3.9 | 5.3/4.5 | 5.2/4.5 | 5.6/4.7 | 4.9/4.1 |
| Thermos (in/out) | | | 0.6/0.5 | 0.6/0.6 | 0.5/0.4 | 0.4/0.4 | 0.3/0.3 |
| Curtailed energy | | 0.7 | 7.3 | 7.3 | 7.8 | 7.0 | 10.2 |
| Import diesel | 24.0 | 9.3 | 4.1 | 1.9 | 0.6 | 0.2 | |
| Mining coal | 204.5 | 219 | | | | | |
| CO2 [kt] | 86.9 | 88.7 | 1.1 | 0.5 | 0.2 | 0.0 | |

**Table B.18:** Commodity flow [GWh] in different technologies B-BiPV

| | 2020 | 2025 | 2030 | 2035 | 2040 | 2045 | 2050 |
|---|---|---|---|---|---|---|---|
| El demand | 42.9 | 44.0 | 32.5 | 32.5 | 32.5 | 32.5 | 32.5 |
| Heat demand | 58.9 | 55.3 | 51.7 | 49.6 | 47.5 | 45.6 | 44.3 |
| EV demand | 0.0 | 4.1 | 6.6 | 6.6 | 6.6 | 6.6 | 6.6 |
| Coal CHP (el/heat) | 21.1/70.0 | 19.6/65.0 | | | | | |
| Coal turbine | 25.2 | 31.3 | | | | | |
| Existing PV | 0.1 | 0.1 | 0.1 | 0.1 | 0.0 | | |
| PV ground S | | | 0.3 | 1.2 | 1.2 | 5.1 | 6.4 |
| Wind | | 2.7 | 77.0 | 77.8 | 77.9 | 87.5 | 84.8 |
| El boiler | | | 3.4 | 3.5 | 3.3 | 0.2 | 0.1 |
| DH heat pump | | | 42.9 | 39.4 | 34.4 | 0.3 | 0.4 |
| Oil boiler | | | 2.3 | | | | |
| El radiator | | 1.6 | 10.9 | 13.6 | 15.9 | 45.2 | 43.9 |
| Battery (in/out) | | | 4.5/3.8 | 5.8/5.0 | 5.6/4.7 | 5.2/4.4 | 6.0/5.1 |
| Thermos (in/out) | | | 0.8/0.7 | 0.6/0.5 | 0.9/0.8 | 0.2/0.2 | 0.2/0.2 |
| Curtailed energy | | 1.1 | 8.7 | 7.9 | 7.8 | 17.8 | 14.8 |
| Import diesel | 24.0 | 9.3 | 2.5 | | | | |
| Mining coal | 255.6 | 273.8 | | | | | |
| CO2 [kt] | 86.9 | 88.7 | 0.7 | | | | |

Einar Boman Rinde

# TIMES-LYR – the future energy system in Longyearbyen

NTNU
Kunnskap for en bedre verden